nagra.

Arbeitsbericht NAB 22-04

TBO Bachs-1-1: Data Report

Dossier IV Microfacies, Bio- and Chemo-stratigraphic Analysis

August 2023

S. Wohlwend, H.R. Bläsi, S. Feist-Burkhardt,
B. Hostettler, U. Menkveld-Gfeller,
V. Dietze & G. Deplazes

National Cooperative
for the Disposal of
Radioactive Waste

Hardstrasse 73
P.O. Box
5430 Wettingen
Switzerland
Tel. +41 56 437 11 11

nagra.ch

nagra.

Arbeitsbericht NAB 22-04

TBO Bachs-1-1: Data Report

Dossier IV Microfacies, Bio- and Chemo-stratigraphic Analysis

August 2023

S. Wohlwend[1], H.R. Bläsi[2], S. Feist-Burkhardt[3,4], B. Hostettler[5], U. Menkveld-Gfeller[5], V. Dietze[6] & G. Deplazes[7]

[1] Geological Institute, ETH Zurich
[2] Geo-Consulting, Wünnewil, Switzerland
[3] SFB Geological Consulting & Services, Ober-Ramstadt, Germany
[4] Département des Sciences de la Terre, Université de Genève
[5] Natural History Museum Bern
[6] Nördlingen, Germany
[7] Nagra

Keywords:
BAC1-1, Nördlich Lägern, TBO, deep drilling campaign, microfacies, lithostratigraphy, biostratigraphy, ammonite stratigraphy, palynostratigraphy, chemostratigraphy, dinoflagellate cysts, stable carbon isotopes

National Cooperative for the Disposal of Radioactive Waste

Hardstrasse 73
P.O. Box
5430 Wettingen
Switzerland
Tel. +41 56 437 11 11

nagra.ch

Nagra Arbeitsberichte ("Working Reports") present the results of work in progress that have not necessarily been subject to a comprehensive review. They are intended to provide rapid dissemination of current information.

This NAB aims at reporting drilling results at an early stage. Additional borehole-specific data will be published elsewhere.

In the event of inconsistencies between dossiers of this NAB, the dossier addressing the specific topic takes priority. In the event of discrepancies between Nagra reports, the chronologically later report is generally considered to be correct. Data sets and interpretations laid out in this NAB may be revised in subsequent reports. The reasoning leading to these revisions will be detailed there.

This Dossier was prepared by a project team consisting of:
S. Wohlwend (sampling, chemostratigraphy, conceptualisation and compilation)
H.R. Bläsi (microfacies)
S. Feist-Burkhardt (palynostratigraphy)
B. Hostettler, U. Menkveld-Gfeller, V. Dietze (ammonite stratigraphy)
G. Deplazes (project management and conceptualisation)

Editorial work: P. Blaser and M. Unger

The Dossier has greatly benefitted from technical discussions with, and reviews by, external and internal experts. Their input and work are very much appreciated.

Table of Contents

List of Tables

List of Figures

List of Appendices

1 Introduction

1.1 Context

To provide input for site selection and the safety case for deep geological repositories for radioactive waste, Nagra has drilled a series of deep boreholes ("Tiefbohrungen", TBO) in Northern Switzerland. The aim of the drilling campaign is to characterise the deep underground of the three remaining siting regions located at the edge of the Northern Alpine Molasse Basin (Fig. 1-1).

In this report, we present the results from the Bachs-1-1 borehole.

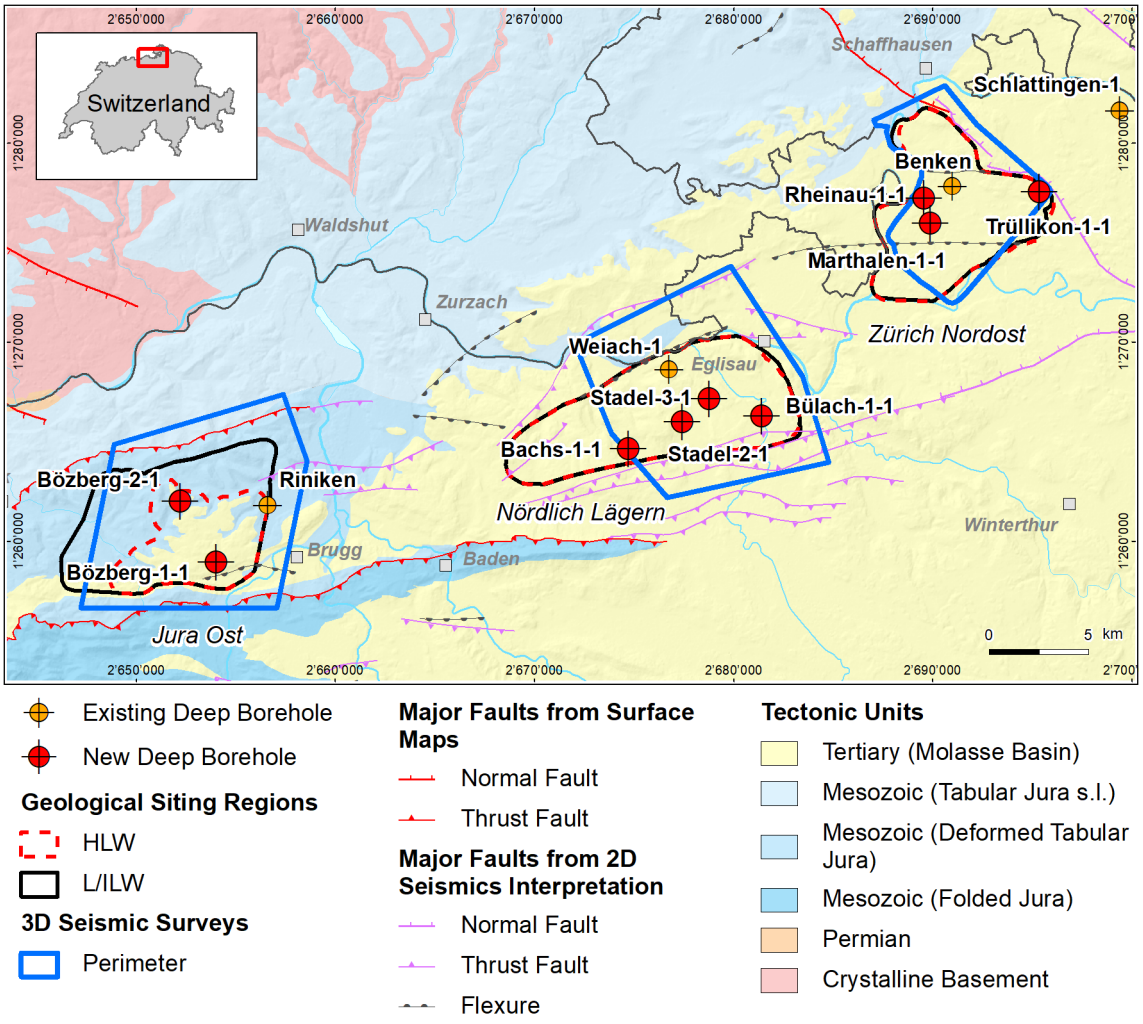

Fig. 1-1: Tectonic overview map with the three siting regions under investigation

1.2 Location and specifications of the borehole

The Bachs-1-1 (BAC1-1) exploratory borehole is the ninth (and last) borehole drilled within the framework of the TBO project. The drill site is located in the western part of the Nördlich Lägern siting region (Fig. 1-2). The vertical borehole reached a final depth of 1'306.26 m (MD)[1]. The borehole specifications are provided in Tab. 1-1.

Due to a loss of a measurement tool (dilatometer), the borehole was cemented up to 500 m MD and a sidetrack was initiated with a kickoff point (KOP) at about 600 m MD. This sidetrack was labelled Bachs-1-1B (BAC1-1B). BAC1-1B reached a final depth of 952 m MD but was abandoned during borehole reaming operations due to entering the original borehole BAC1-1. Therefore, the vertical borehole BAC1-1 was used again for the remaining investigations. For easier communication and labelling, the name BAC1-1 is generally used for this borehole, including the sidetrack, unless stated otherwise. A detailed description of all technical details about the drilling process can be found in Dossier I.

Tab. 1-1: General information about the BAC1-1 borehole

Siting region	Nördlich Lägern
Municipality	Bachs (Canton Zürich / ZH), Switzerland
Drill site	Bachs-1 (BAC1)
Borehole	Bachs-1-1 (BAC1-1) including sidetrack Bachs-1-1B (BAC1-1B)
Coordinates	LV95: 2'674'769.089 / 1'264'600.698
Elevation	Ground level = top of rig cellar: 450.35 m above sea level (asl)
Borehole depth	1'306.26 m measured depth (MD) below ground level (bgl)
Drilling period	10th September 2021 – 23rd April 2022 (spud date to end of rig release)
Drilling company	Daldrup & Söhne AG
Drilling rig	Wirth B 152t
Drilling fluid	Water-based mud with various amounts of different components such as[2]: 0 – 700 m: Bentonite & polymers 700 – 1'057 m: Potassium silicate & polymers[3] 1'057 – 1'129 m: Water & polymers 1'129 – 1'306.26 m: Sodium chloride brine & polymers

The lithostratigraphic profile and the casing scheme are shown in Fig. 1-3. The main lithostratigraphic boundaries in the BAC1-1 borehole are shown in Fig. 1-4.

[1] Measured depth (MD) refers to the position along the borehole trajectory, starting at ground level, which for this borehole is the top of the rig cellar. For a perfectly vertical borehole, MD below ground level (bgl) and true vertical depth (TVD) are the same. In all Dossiers depth refers to MD unless stated otherwise.

[2] For detailed information see Dossier I.

[3] Including sidetrack.

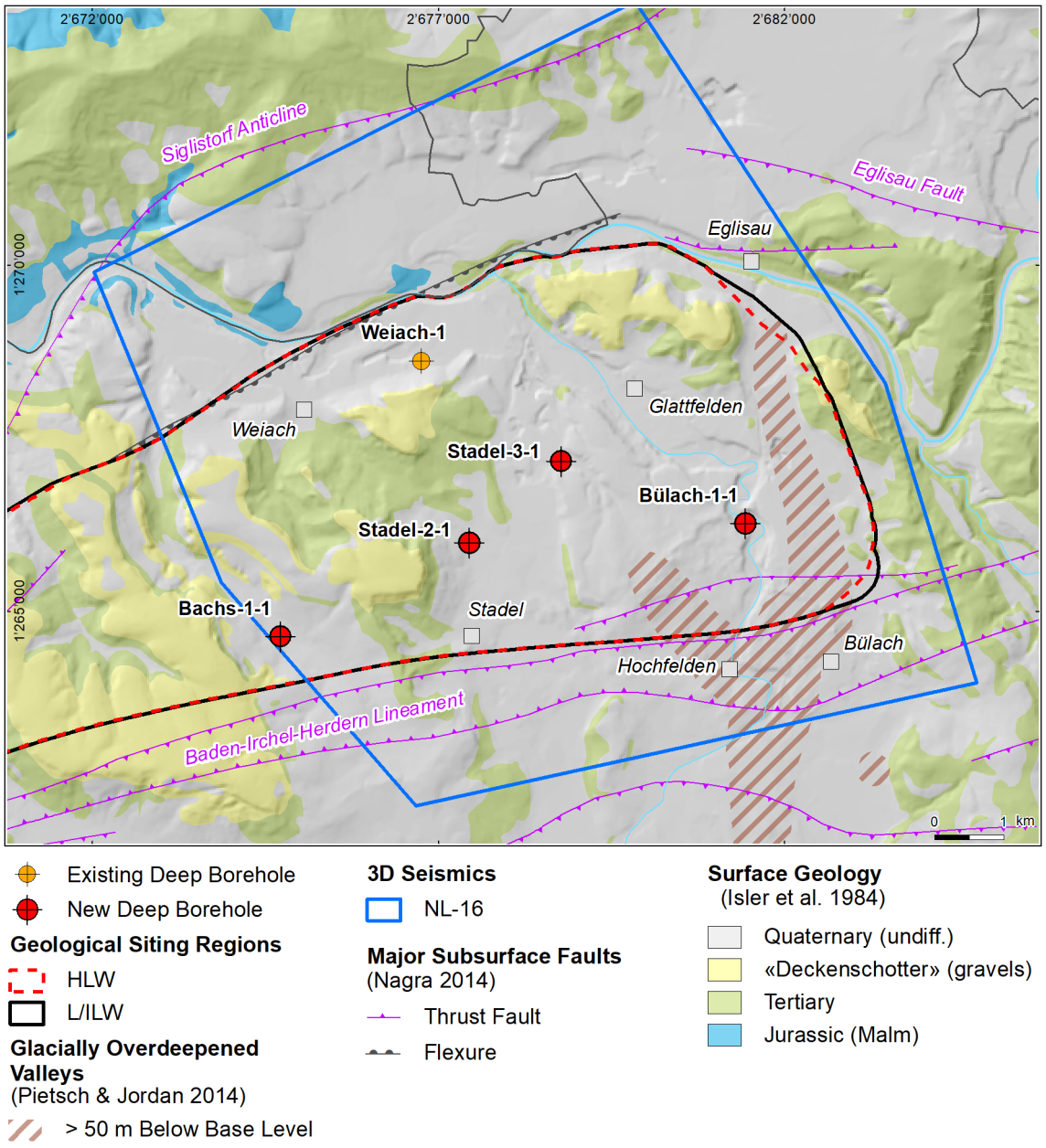

Fig. 1-2: Overview map of the investigation area in the Nördlich Lägern siting region with the location of the BAC1-1 borehole in relation to the boreholes Weiach-1, BUL1-1, STA3-1 and STA2-1

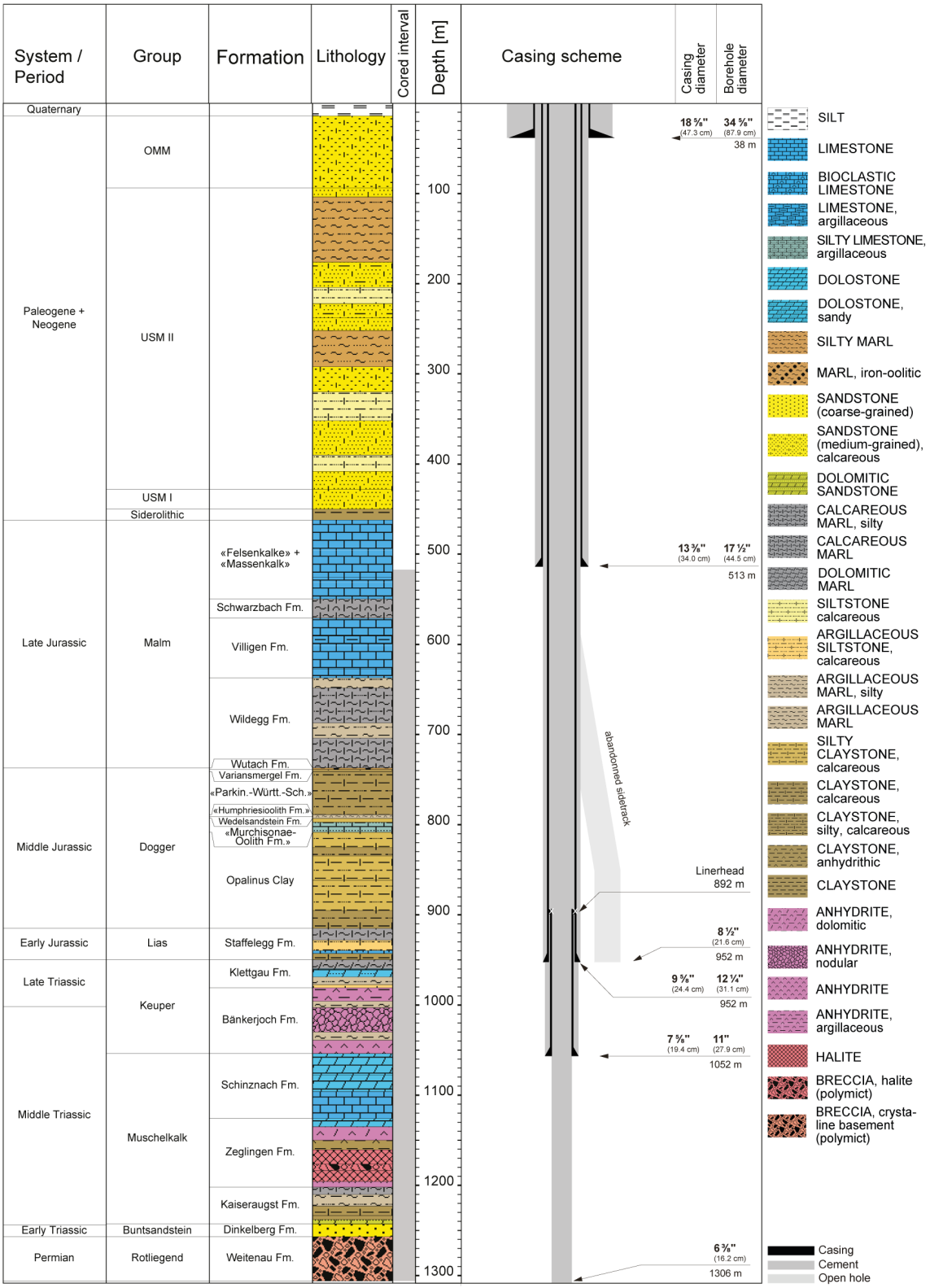

Fig. 1-3: Lithostratigraphic profile and casing scheme for the BAC1-1 borehole[4]

[4] For detailed information see Dossier I and III.

1.3 Documentation structure for the BAC1-1 borehole

NAB 22-04 documents the majority of the investigations carried out in the BAC1-1 borehole, including laboratory investigations on core material. The NAB comprises a series of stand-alone dossiers addressing individual topics and a final dossier with a summary composite plot (Tab. 1-2).

This documentation aims at early publication of the data collected in the BAC1-1 borehole. It includes most of the data available approximately one year after completion of the borehole. Some analyses are still ongoing (e.g. diffusion experiments, analysis of veins, hydrochemical interpretation of water samples) and results will be published in separate reports.

The current borehole report will provide an important basis for the integration of datasets from different boreholes. The integration and interpretation of the results in the wider geological context will be documented later in separate geoscientific reports.

Tab. 1-2: List of dossiers included in NAB 22-04

Black indicates the dossier at hand.

Dossier	Title	Authors
I	TBO Bachs-1-1: Drilling	P. Hinterholzer-Reisegger
II	TBO Bachs-1-1: Core Photography	D. Kaehr, M. Stockhecke & Hp. Weber
III	TBO Bachs-1-1: Lithostratigraphy	P. Jordan, P. Schürch, M. Schwarz, R. Felber, H. Naef, T. Ibele & F. Casanova
IV	TBO Bachs-1-1: Microfacies, Bio- and Chemostratigraphic Analyses	S. Wohlwend, H.R. Bläsi, S. Feist-Burkhardt, B. Hostettler, U. Menkveld-Gfeller, V. Dietze & G. Deplazes
V	TBO Bachs-1-1: Structural Geology	A. Ebert, E. Hägerstedt, S. Cioldi, L. Gregorczyk & F. Casanova
VI	TBO Bachs-1-1: Wireline Logging, Micro-hydraulic Fracturing and Pressure-meter Testing	J. Gonus, E. Bailey, J. Desroches & R. Garrard
VII	TBO Bachs-1-1: Hydraulic Packer Testing	R. Schwarz, R. Beauheim, L. Schlicken-rieder, E. Manukyan & A. Pechstein
VIII	TBO Bachs-1-1: Rock Properties, Porewater Characterisation and Natural Tracer Profiles	E. Gaucher, L. Aschwanden, T. Gimmi, A. Jenni, M. Kiczka, M. Mazurek, P. Wersin, C. Zwahlen, U. Mäder & D. Traber
IX	*The geomechanical campaign in BAC-1-1 was limited to two oedometric tests. Hence, no dedicated Dossier IX was produced for NAB 22-04. The hydraulic conductivity values derived from the oedometric tests are documented in the Summary Plot.*	
X	TBO Bachs-1-1: Petrophysical Log Analysis	S. Marnat & J.K. Becker
	TBO Bachs-1-1: Summary Plot	Nagra

1.4 Scope and objectives of this dossier

The dossier at hand complements the lithostratigraphic report (Dossier III) on the BAC1-1 borehole. The report documents data on microfacies analysis, ammonite- and palynostratigraphy as well as detailed geochemical (C, O and N isotopes) analyses. Preliminary results of these analyses already existed at data-freeze (11.07.2022), two months after the end of drilling operations and were integrated into the lithostratigraphic discussion and lithostratigraphic boundary definition (Dossier III).

The objectives of this report focusing on the Opalinus Clay and its confining units are:

- to specify the macroscopic description by a detailed microfacies analysis (components, matrix, cements),
- to allow a microfacies comparison of specific horizons, for example hardgrounds of the upper Opalinus Clay,
- to provide additional data on the diagenetic history of the sediment,
- to recover macrofossils from the stratigraphic interval of interest which are significant for facies changes and chronostratigraphic data,
- to compile an additional independent dataset of palynomorphs for chronostratigraphic data,
- to provide detailed geochemical (C, O and N isotopes) analyses with one metre spacing from the stratigraphic interval of interest,
- to allow a chemostratigraphic correlation (stable isotopes) with other deep boreholes in the three siting regions,
- to support the definition of the lithostratigraphic units.

The detailed stratigraphy of the BAC1-1 borehole with core depth in metres can be found in Fig. 1-4. The stratigraphic intervals of interest for the different investigations (microfacies analysis, ammonite- and palynostratigraphy and geochemical analyses) and their specific sampling intervals are visualised in Fig. 1-5 with respect to the 1:5'000 lithostratigraphic profile.

All depths labelled with metres [m] in this report refer to "m MD core depth" if not stated otherwise.

TBO BACHS-1-1

System / Period		Group	Formation	Metres MD	Member / Sub-unit
Quaternary				14	
Paleogene / Neogene		OMM		94	
		USM	USM II	428	
			USM I	450	
		Siderolithic		462	
Jurassic	Late	Malm	«Felsenkalke» + «Massenkalk»	549.69	
			Schwarzbach Fm.	570.98	
			Villigen Fm.	589.42	Wangental Mb.
				589.52	«Knollen Bed»
				627.20	Küssaburg Mb.
				637.31	Hornbuck Mb.
			Wildegg Fm.	736.40	Effingen Mb.
				737.05	Birmenstorf Mb. and «Glaukonitsandmergel Bed»
	Middle	Dogger	Wutach Fm.	738.81	
			Variansmergel Fm.	741.22	
			«Parkinsoni-Württembergica-Sch.»	788.92	
			«Humphriesioolith Fm.»	791.05	
			Wedelsandstein Fm.	793.11	
			«Murchisonae-Oolith Fm.»	808.34	
			Opalinus Clay	834.57	«Sub-unit with silty calcareous beds»
				861.63	«Upper silty sub-unit»
				895.17	«Mixed clay-silt-carbonate sub-unit»
				914.91	«Clay-rich sub-unit»
	Early	Lias	Staffelegg Fm.	919.64	Gross Wolf Mb.
				925.49	Rietheim Mb.
				928.12	Grünschholz Mb., Breitenmatt Mb. and Rickenbach Mb.
				939.52	Frick Mb.
				943.04	Beggingen Mb.
				949.73	Schambelen Mb.
Triassic	Late	Keuper	Klettgau Fm.	959.75	Gruhalde Mb.
				966.03	Seebi Mb.
				968.75	Gansingen Mb.
				980.93	Ergolz Mb.
	?1002		Bänkerjoch Fm.	1'002.78	«Claystone with anhydrite nodules»
				1'029.89	«Cyclic sequence»
				1'046.84	«Thin-layered anhydrite and claystone sequence»
				1'050.90	«Banded massive anhydrite»
	Middle	Muschelkalk	Schinznach Fm.	1'053.90	«Dolomite and anhydrite»
				1'057.9	Asp Mb.
				1'095.95	Stamberg Mb.
				1'100.66	Liedertswil Mb.
			Zeglingen Fm.	1'125.75	Leutschenberg Mb. and Kienberg Mb.
				1'134.87	«Dolomitzone»
				1'160.56	«Obere Sulfatzone»
				1'195.79	«Salzlager»
			Kaiseraugst Fm.	1'202.03	«Untere Sulfatzone»
				1'210.01	«Orbicularismergel»
				1'233.50	«Wellenmergel»
	?1244			1'242.82	«Wellendolomit»
	E.	Bsst.	Dinkelberg Fm.	1'256.86	
Permian		Rotlieg.	Weitenau Fm.	1'306.26	Final depth

Fig. 1-4: Bachs-1-1 stratigraphy with core depth in metres [m MD]

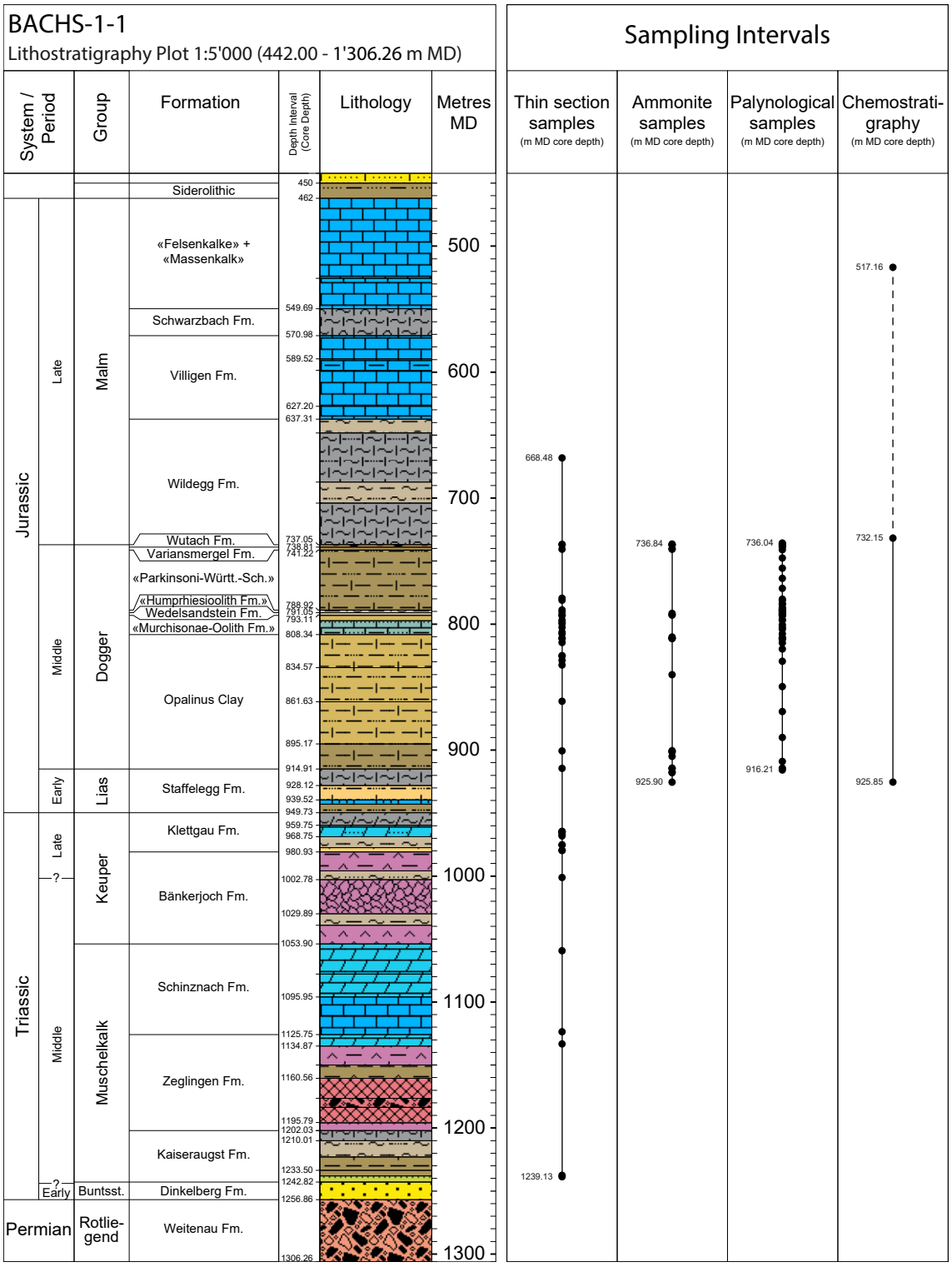

Fig. 1-5: Lithostratigraphy plot (1:5'000) from the Mesozoic succession with the individual sampling intervals for thin sections, macrofossils, palynological analysis and chemostratigraphy.

1:5'000 stratigraphic plot modified from Dossier III, shown is the stratigraphic range from 442.00 m to final depth at 1'306.26 m. The chemostratigraphic interval indicated by the dashed line was analysed for inorganic (carbonate) samples only.

2 Methods

2.1 Microfacies

Thin section preparation

All 40 thin sections (TS) were cut edgewise from the core so that the long side is parallel to the coring direction and therefore covers as much of the stratigraphy as possible. The mean depth of the thin section corresponds to the Sample ID. Therefore, thin sections containing lithological boundaries may have Sample IDs that fall into only one of the two described intervals. However, the lower or upper range on the thin section still covers the interval. A list of all thin sections with their sampling range and Sample ID can be found in Appendix A1 of this report.

The thin sections from calcareous lithologies with a standard length of 4 cm were prepared at the University of Basel. Lithologies sensitive to water such as claystones and argillaceous sediments (swelling of clay minerals) or evaporates (dissolution of evaporitic minerals) were prepared by the Thin Section Lab (TSL) using petroleum, they are only 3 cm long. For better identification of the carbonate minerals calcite, Fe-calcite and Fe-dolomite, the left half of the thin sections was stained applying the technique of Dickson (1965). Thin sections with a macroscopic porosity were impregnated during preparation using a blue coloured epoxy resin to estimate the percentage of their porosity.

Thin section analyses

The thin sections were analysed using a Zeiss polarisation microscope. First, all allochemical components, biogenic particles, siliciclastics, matrix and diagenetic alterations as neomorphic minerals, cements and replacements were studied. Then, to obtain the percentage of the components etc., 100 points were counted with a net micrometre ocular. For detrital quartz-bearing thin sections, the average grain size was evaluated in millimetres. To count inhomogeneous sediments, two different sections were looked at and averaged. A selection of 21 thin section photographs for microfacies analysis is documented in Appendix B (Figs. B-1 to B-21).

Components, matrix and cements (definitions)

To describe thin sections, several allochemical components (described below) were counted, and their numbers are documented in Section 3.1 ('Microfacies'). Some of the specific terms used for the components or matrix are explained as follows:

Clay matrix, micrite, microsparite (or pseudosparite): Sedimented mud consisting of clay minerals, other very small silicate grains, heavy minerals (i.e. clay matrix) and/or microcrystalline carbonate ooze (i.e. micrite). Microsparite is defined as a mosaic of small calcite crystals formed by aggrading neomorphism; originally, it was micrite and not a diagenetic pore-filling cement. Alternatively, microsparite could also be the product of dedolomitisation as seen in the «Felsenkalke» and «Massenkalk».

Dolomitic matrix: primary microcrystalline dolostone ooze.

Limonitic matrix: Calcite micrite mixed with microcrystalline limonitic grains grown during diagenesis.

Limonitic echinoderms, limonitic bivalves: Fragments, parts of echinoderms and bivalves, with limonite filling the skeletal structure of the fossil.

Pellets, peloids, aggregates: the column of pellets also contains aggregates (lumps); that means "carbonate grains of various kinds are clumped together to form compound grains" (Bathurst 1975).

Fe-stromatolites and stromatolitic clasts: Iron-mineralised microbial mats and/or microbial clasts.

Fe-ooids or iron-ooids: Limonitic/goethitic or chamositic ooids, with a visible concentric structure; some iron-ooids are replaced by calcite (calcitic iron-ooids), a few of them show relicts of iron mineral layers (see BAC1-1-825.52, Fig. B-9, Appendix B).

Intraclasts: Rock fragments of early diagenetic cemented sediment, reworked and sedimented in the same sedimentary environment.

Calcite cement (sparite): "Normal" cement, calcite crystals grown – filled in – within the primary pore space or in leached components. In this column, the amount of calcite crystal pseudomorphs after gypsum was noted.

"Stellate cement": Calcite "cement" grown within the matrix and not filling primary or secondary pore space. The calcite crystals form small "stellates" (e.g. thin sections BAC1-1-861.65, 815.04 and 790.85), i.e. a habitus typical for "hiatus beds" (firm-, hardgrounds; Wetzel & Allia 2000) or "hiatus concretions" (Voigt 1968).

Cone-in-cone calcite: Rows of piled calcite cones grown during diagenesis which were named "Tutenmergel" in the Swabian realm (e.g. BAC1-1-901.06).

(Fe)-Dolomite: Normally dolomite rhombohedrons that originated during diagenesis; in special cases, the dolomite replaces gypsum crystals that were sedimented as detritical gypsum crystals. In some cases, the rhombohedrons consist of iron-dolomite, which are stained blue after the thin section staining.

Dedolomite: Calcite replacement of dolomite: each single dolomite rhombohedron is replaced by a few smaller calcite crystals. When it was a total dolostone and the calcitic replacement has been completed, the result is a thoroughly crystalline, sparitic/microsparitic limestone. In addition, another dedolomite type exists with larger calcite crystals jointly replacing a few dolomite crystals, thus forming a calcite mosaic similar to marble.

Anhydrite: Present in various forms: as a rock-forming mineral, as a vein mineral, mainly replacing "Fasergips", and as cement in sandstones (e.g. Ergolz Member of the Klettgau Formation).

Quartz cement: Authigenic quartz rims grown during diagenesis around detrital quartz grains; quartz/chalcedony in silicified bivalves (MAR1-1-569.18; Wohlwend et al. 2021c).

Porosity: Thin sections with a macroscopic porosity were impregnated during preparation using a blue coloured epoxy resin to estimate the volume percentage (vol.-%) of their porosity.

Hardground: Thin sections from hardgrounds document synsedimentarily cemented and lithified carbonate layers which have been exposed on the seafloor. During that time period, the hardgrounds are therefore mostly encrusted and bored by organisms and may consist of early marine calcite cements and are in parts mineralised by iron and manganese oxides or calcium phosphates.

2.2 Ammonite preparation

The BAC1-1 cores were carefully examined for macrofossils at the Würenlingen (Canton Aargau) core storage facility. The cores were examined for ammonites and other macrofossils on the bedding and fractured surfaces as well as on the outer surface of the core; the core itself was not broken open. A list of all 22 samples with their sampling range and Sample ID can be found in Appendix A2 of this report. In addition to ammonites, other conspicuous fossils were identified to the extent possible and entered in the list (Appendix A3), even when they were not subsequently, or only occasionally, recovered. The ammonites were then secured from the core and brought to Glovelier (Canton Jura) where they were prepared and documented. Afterwards they were archived in the earth sciences collection of the Natural History Museum in Bern.

For the preparation, we used mechanical methods such as air tools and fine sandblasting equipment as well as a chemical etching method using potassium hydroxide (KOH). Sodium hydrogen carbonate was mainly used as abrasive. Residual material from sawing and/or preparing two ammonite samples (marked in grey in Appendix A4) was additionally used as material for palynological samples. Before being photographed, ammonium chloride steam was applied to the fossils to compensate for variation in contrast caused by different colouring. A selection of ammonites is documented on four plates (Plate I – IV) in Appendix C.

2.3 Palynological sample preparation and quantitative analysis

Palynological processing of the rock samples was carried out by MB Stratigraphy Limited (Sheffield, S11 7JH, UK). Processing followed the standard protocol using concentrated HCl and concentrated HF, followed by a short oxidation with HNO_3 and, if necessary, treatment with ultrasound (e.g. Wood et al. 1996). The residues were sieved at a mesh size of 15 µm. Residues were mounted on microscope slides and analysed using transmitted light microscopy. A list of all samples with their sampling range and Sample ID can be found in Appendix A4 of this report.

Two consecutive counts were carried out in the quantitative microscopic analysis. In a first count 200 grains of all palynomorphs were counted and the number of dinoflagellate cysts was noted (column 'DA *Dinocysts (count 1)*' in Appendix D1). In a second count, only dinoflagellate cysts were counted until a total of 100 dinoflagellate cysts was reached. The reminder of the slide was checked for additional, out-of-count species. Taxa recorded out of count are marked with a '+' in the range chart. Taxa only questionably identified are marked with a '?' in the range chart. Occurrences of fungal remains are recorded semi-quantitatively (R = Rare, O = Occasional, C = Common, A = Abundant, S = Superabundant).

Results are illustrated using the software package StrataBugs v2.1 (Appendices D1 and D2, in the digital version only). Numerical age dates used for the Composite Standard and the Depth/Age plot are in line with those of the *Geologic Time Scale 2016* (Ogg et al. 2016). On the range chart (Appendix D1) several abbreviations are used (AC = Acritarchs, ALBO = Algae, *Botryococcus* and *Pediastrum*, ALPR = Algae, Prasinophytes, ALZY = Algae, Zygnematophyceae, DA = Dinocyst abundance, DC = Dinoflagellate cysts, FT = Foraminiferal test linings, FU = Fungi, MP = Miscellaneous palynomorphs, SP = Spores and pollen. Several dinoflagellate cyst taxa contain a question mark in the name, as for example in *Evansia*? *eschachensis*. The question mark after the genus name indicates uncertainty regarding the correct taxonomical assignment of the species to the genus.

2.4 Chemostratigraphy

The sampling of the BAC1-1 borehole focused primarily on the Dogger and Lias Groups and therefore primarily on clay mineral-rich layers of the Opalinus Clay. However, the above following 215 m from the Malm Group were sampled in addition to have an impression about the inorganic isotopic variation above the interval of main interest. The sampling resolution was one metre, except for some intervals with denser sampling density (mainly condensed intervals, e.g. Rietheim Member and lowermost part of Wildegg Formation). All 486 samples were drilled with a micro-drill. In general, clay mineral-rich lithologies were sampled. Diagenetic calcite and siderite veins and nodules were avoided. The drilled powder amounted to around 1 g of material. A list of specific samples (n = 27) with results mainly from calcareous beds, calcareous concretions and septarian nodules can be found in Appendix E1 of this report.

Inorganic (carbonate) analyses

486 samples, including additional 216 samples from the Malm Group, were analysed for **stable carbon** ($\delta^{13}C_{carb}$) and **oxygen isotope** ($\delta^{18}O_{carb}$) of bulk carbonate, 459 continuous samples (roughly in metre resolution) and additional 27 samples from specific calcareous beds and concretions from the Opalinus Clay and neighbouring units (Appendix E1). Varying amounts of powder to reach approximately 120 µg of carbonate in the vial were weighed using a Mettler Toledo MT5 Fact microbalance in 12 ml vacutainers. The headspace was flushed with pure He, and then the samples were reacted with 100% phosphoric acid at 72 °C in a ThermoFisher GasBench II carbonate device connected to a ThermoFisher Delta V PLUS mass spectrometer. The instrument is calibrated with international carbonate standards NBS19 and NBS18 distributed by the International Atomic Energy Agency (IAEA), Vienna and internal standards (MS2 "Carrara marble"; $\delta^{13}C_{carb}$ = 2.16 ‰, $\delta^{18}O_{carb}$ = -1.85 ‰). The reproducibility of the measurements based on replicated standards was ± 0.05 ‰ for $\delta^{13}C_{carb}$ and ± 0.06 ‰ for $\delta^{18}O_{carb}$. All isotope measurements were performed at the Stable Isotope Laboratory of the ETH Zurich (Geological Institute). The isotope values are reported in the conventional delta notation with respect to the Vienna Pee Dee Belemnite (VPDB).

The **Total Carbonate content** (TCarb) was calculated based on a calibration using extracted CO_2 from the known weight of the internal standard material (MS2), which is composed to 100% of carbonate (calcite). The mean area of the m/z 44 peak (corresponding to the most abundant isotopologue $^{12}C^{16}O_2$) in the mass spectrometer allows the carbonate content to be estimated from the individual bulk rock samples. The individual uncertainty for TCarb, represents the average from all standard deviations from the MS2 and is ± 5.42%. However, the TCarb values calculated from the reaction of the phosphoric acid with the bulk rock, only reflect the carbonate that was able to react during the reaction time (~ 60 min). However, ankerite and especially siderite, for example, roughly require 60 h reaction time for full dissolution at 70 °C (Fernandez et al. 2016). Therefore, the calculated carbonate content (TCarb) does not completely represent the total amount of all different carbonates. The data reflect a mixed signal composed mostly of calcite and dolomite with a smaller component of the other more resistant carbonates (see also Wohlwend et al. 2019b).

Organic analyses

The powders remaining after inorganic analysis from 217 samples were decarbonated in quantities of less than 1 g in 10 ml of 3 M HCl for 12 h in 15 ml centrifuge tubes, to ensure the complete removal of carbonate. For neutralisation purposes, the residue was subsequently washed three times with deionised water, and then centrifuged and decanted. After drying at 70 °C in an oven

for at least 72 h the samples were homogenised with a mortar and pestle. Depending on the organic carbon content of each specific sample, a different amount was weighed in a tin capsule using a Mettler Toledo MT5 Fact microbalance, so that approximately the same amount of organic carbon was always measured.

$\delta^{13}C_{org}$ and **$\delta^{15}N_{org}$** were measured by flash combustion on a ThermoFisher Scientific FlashEA elemental analyser connected to a Delta V isotope ratio mass spectrometer (IRMS) operated in continuous flow mode. The samples were combusted in an O_2 atmosphere in a quartz reactor at 1'020 °C packed with $(Co_3O_4)Ag$ and Cr_2O_3 to form CO_2, N_2, NO_X and H_2O. These gases were then transferred through a reduction reactor containing elemental Cu at 600 °C to remove excess O_2 and to reduce NO_X to N_2. H_2O and SO_X were subsequently removed using anhydrous $Mg(ClO_4)_2$ and elemental Ag. Then, N_2 and CO_2 were separated in a packed gas chromatographic column and analysed for their isotopic composition using the IRMS. Isotope ratios are reported in conventional delta notation with respect to atmospheric N_2 (AIR) and VPDB standards, respectively. The methods were calibrated with the International Atomic Energy Agency (IAEA)-N1 ($\delta^{15}N$ = 0.45 ‰), IAEA-N2 ($\delta^{15}N$ = +20.41 ‰) and IAEA-N3 ($\delta^{15}N$ = +4.72 ‰) reference materials for nitrogen, and NBS22 ($\delta^{13}C$ = -30.03 ‰) and IAEA-CH-6 ($\delta^{13}C$ = -10.46 ‰) for carbon. Reproducibility of the measurements is better than ± 0.2 ‰ for both nitrogen and carbon. Reproducibility and accuracy of the measurements are based on replicate analyses of the internal laboratory standards atropine, peptone and nicotinamide. All geochemical measurements were performed at the Stable Isotope Laboratory of the ETH Zurich (Geological Institute).

The **Total Organic Carbon** (TOC_{decarb}) and **Total Nitrogen** (TN_{decarb}) contents of the decarbonised samples were calculated based on the known carbon and nitrogen contents of atropine (70.56 wt.-% C, 4.84 wt.-% N). The individual uncertainty for TOC_{decarb} represents the average from all standard deviations from atropine during that calculation and is ± 1.80 %, respectively ± 0.13 % for the TN_{decarb}. The calculated TN_{decarb} reflects a mixture of bound inorganic and organic nitrogen and therefore also contains ammonium, which substitutes for K^+ in the interlayer exchange sites of illite (Scheffer & Schachtschnabel 1984).

The **Carbon-to-Nitrogen ratio** (C/N ratio) is a ratio of the mass of carbon to the mass of nitrogen. In this study, the ratio was calculated using the TOC_{decarb} and the TN_{decarb}. As mentioned above, the C/N ratios can also be influenced by inorganic nitrogen in the form of soil-derived ammonium (Scheffer & Schachtschnabel 1984). Due to this inorganic nitrogen, the C/N ratios of sediments containing additional inorganic nitrogen will decrease. Therefore, C/N ratios are referred to as organic carbon/total nitrogen (TOC_{decarb}/TN_{decarb}) giving the ratio of the C and N masses of the decarbonised samples (C_{org}/N_{org}). The calculated ratios allow to distinguish between marine (C/N ≤ 10; Parsons 1975) *versus* terrigenous matter (C/N ≥ 12; Kukal 1971) in marine sediments.

$$\frac{C_{org}}{N_{org}} = \frac{TOC_{decarb}}{TN_{decarb}} * \frac{atomic\ mass\ (C)}{atomic\ mass\ (N)} = \frac{TOC_{decarb}}{TN_{decarb}} * \frac{14.007}{12.011}$$

The **Total Organic Carbon** (TOC**)** of the whole/bulk sample was calculated using the semi-quantitative carbonate content (TCarb) and semi-quantitative TOC_{decarb} content based on the following equation:

$$TOC = (1 - TCarb) * TOC_{decarb}$$

3 Results

3.1 Microfacies

Kaiseraugst Formation (BAC1-1-1239.13, 1237.99)

The Kaiseraugst Formation is a marly and argillaceous formation with sandy dolostones and dolomitic sandstones in their lowermost unit, in the «Wellendolomit». Only with a macroscopic description is it not always clear whether the siliciclastic grains or the dolomite dominate. If marine components are included, the affiliation to the Kaiseraugst Formation is unambiguous in comparison with the underlying terrestrial Dinkelberg Formation.

Thin section BAC1-1-1239.13 shows a dolomitic sandstone with 60 vol.-% quartz and siliciclastic rock fragments (Tab. 3-1; for all vol.-% data in this section) and 25 vol.-% dolomite rhombohedrons. Dolomitic intraclasts (4 vol.-%), echinoderm skeletal elements (3 vol.-%) and pyrite (3 vol.-%) are also present, as well as some porosity (5 vol.-%). Finer-grained sand layers (0.3 mm mean grain size) with fine crystalline dolomite (0.05 mm) are alternating with coarser-grained (0.5 mm) sand layers with coarse crystalline dolomite (0.5 mm).

The sample BAC1-1-1237.99 is a sandy dolostone, consisting of 30 vol.-% quartz and siliciclastic rock fragments and 53 vol.-% dolomite crystals. Most of these have rhombohedral shapes, but some have "banana" forms, perhaps they enclose bivalves, others enclose echinoderm skeletal elements (10 vol.-%). Pyrite (3 vol.-%) and porosity (4 vol.-%) complete the composition.

Zeglingen Formation (BAC1-1-1133.68)

Thin section BAC1-1-1133.68, taken near the base of the «Dolomitzone» is an anhydritic dolostone, composed of dolomicrite (65 vol.-%), without any components or lamination, but with small anhydrite nodules (35 vol.-%).

Schinznach Formation (BAC1-1-1124.02, 1059.71)

The Schinznach Formation consists of numerous carbonate beds with different lithologies and microfacies. Many of them are partly or totally dolomitised, so that the primary composition is hardly recognisable macroscopically after deposition. The two selected beds shed some light on this problem.

Sample BAC1-1-1124.02 shows a bioclastic limestone (partly dolomitised), which consists of echinoderm skeletal elements (11 vol.-%), bivalves (7 vol.-%), other biogenes, predominant codiacean green algae (6 vol.-%), pellets (7 vol.-%) and ooids (5 vol.-%) with micrite matrix (10 vol.-%) and calcite cement (13 vol.-%). Numberless dolomite rhombohedrons (35 vol.-%), with sizes up to 0.2 mm and few bigger (up to 1 mm) anhydrite single crystals (6 vol.-%) are scattered over the whole thin section.

BAC1-1-1059.71 comes from the Stamberg Member, the dolostone member of Schinznach Formation. It is now a dolostone, but three layers of different primary composition are still recognisable: an oolite, a coquina and a bioclastic limestone. Their mean composition is 42 vol.-% ooids, 9 vol.-% pellets, 8 vol.-% bivalves and 29 vol.-% micrite matrix. Anhydrite (4 vol.-%) is found in leached bivalves and open pores (8 vol.-%) in the oolite layer. Regarding only the oolite layer, 17 vol.-% porosity – primary porosity in the original pore space – has been found.

Bänkerjoch Formation (BAC1-1-1001.57)

The Bänkerjoch Formation is an anhydrite/claystone/dolomitic marl formation with little siliciclastic interlayers. One of them was analysed in thin section BAC1-1-1001.57: it is a fine-bedded dolomitic siltstone, composed of quartz grains and siliciclastic rock fragments (48 vol.-%), clay/dolomicritic matrix (36 vol.-%), anhydrite (14 vol.-%) and micas (2 vol.-%). The mean grain size of the siliciclastic grains is 0.04 mm. The anhydrite is located as cement in matrix-free siltstone layers.

Klettgau Formation (BAC1-1-980.07, 975.74, 975.61, 968.57, 967.44, 965.90, 965.08, 964.96)

We focused our microfacies analyses on the two members with sandstones (Ergolz Member and Seebi Member) and the dolostone member (Gansingen Member). The thin sections BAC1-1-980.07, 975.74 and 975.61 are sandstones of the Ergolz Member. They were taken to study the cementation and potential porosity of these beds. The next two, BAC1-1-968.57and 967.44, provide insight into the microfacies of the Gansingen Member. The three Seebi Member thin sections BAC1-1-965.90, 965.08 and 964.96 were selected for analysing cementation and porosity.

All three samples of the Ergolz Member BAC1-1-980.07, 975.74 and 975.61 are very fine to fine-grained sandstones, consisting of quartz and siliciclastic rock fragments (70 vol.-%, resp. 60 and 68 vol.-%). All contain clay matrix, as well as anhydrite cement, but they differ in the amount. BAC1-1-980.07 has 8 vol.-% clay matrix and 12 vol.-% anhydrite filling primary pore space, but some porosity (4 vol.-%) rests (Figs. B-1 and B-2; Appendix B for all figures in this section). BAC1-1-975.74 has more clay matrix (26 vol.-%), only little anhydrite cement (3 vol.-%) and a higher porosity (10 vol.-%), whereby matrix-free, porous horizons alternate with matrix-rich, non-porous layers (Fig. B-3 and B-4). Sample BAC1-1-975.61 contains clay matrix (17 vol.-%) and anhydrite cement (12 vol.-%) in "sufficient" content, so no porosity has been recognised.

Thin section BAC1-1-968.57 of the Gansingen Member is a micritic dolostone (dolomicritic matrix: 75 vol.-%) with dolomitic intraclasts (15 vol.-%) and an open fenestrate structure (small, irregularly distributed pores) (porosity: 8 vol.-%). Such are generated by repeated drying and wetting during sedimentation and early diagenesis in inter- to supratidal depositional environments. BAC1-1-967.44 shows a dolomitic stromatolite, a microbial mat (93 vol.-%, counted in the column of other biogenes) with some porosity (7 vol.-%).

The three samples BAC1-1-965.90, 965.08 and 964.96 come from the lowermost section of the Seebi Member. BAC1-1-965.90 is a sandy dolostone to a dolomitic sandstone, consisting of coarse-grained (0.1 – 4 mm) quartz and siliciclastic rock fragments (32 vol.-%) and dolostone intraclasts (15 vol.-%), as well as one tooth of unknown origin (1 vol.-%), few pores (4 vol.-%) and dolomicritic matrix (48 vol.-%).

BAC1-1-965.08, a coarse-grained sandstone, is composed of quartz and siliciclastic rock fragments (57 vol.-%) and dolostone intraclasts (15 vol.-%), whereby some of these are quartz-dolomite-nodules of pedogene origin (Fig. B-5), sedimented with dolomicritic matrix (17 vol.-%), little quartz cement (4 vol.-%) and some pores (7 vol.-%).

Thin section BAC1-1-964.96, a coarse-grained sandstone too, with quartz and siliciclastic rock fragments (62 vol.-%) and dolostone intraclasts (10 vol.-%) shows a very nice cementation: all components have first a thin dolomite cement fringe (8 vol.-%) and second a quartz cement

(10 vol.-%) in optical continuity around the quartz grains (Fig. B-6 and B-7). There are moreover few pores (7 vol.-%) and dolomitic, original calcite ooids (3 vol.-%) (Fig. B-7), similar to those, known from the Gansingen Member of other places.

Staffelegg Formation (BAC1-1-914.92)

Thin section BAC1-1-914.94 was selected for analysing the uppermost limestone bed of the Gross Wolf Member, at the boundary to the Opalinus Clay. This bioclastic limestone is composed of thin-shelled bivalves (38 vol.-%) and a fine acicular calcite cement (46 vol.-%). Echinoderms (3 vol.-%), micrite matrix (4 vol.-%) and some pyrite nodules (9 vol.-%) are present too.

Opalinus Clay (BAC1-1-901.06, 861.65, 832.90, 829.17, 825.58, 825.52, 815.04, 811.84, 811.57)

We focussed our Opalinus Clay microfacies analyses again on calcareous beds/layers or nodules, which interrupt the silty claystone (calcareous) succession. Iron-ooids have often been replaced by calcite, but some have retained their original iron-mineral composition. The here mentioned calcitic iron-ooids (applies for all following thin section descriptions) have been noted in the "Fe-ooids" column in Tab. 3-1 with an asterisk behind the number.

The sample BAC1-1-901.06, taken from a marly layer with micritic limestone nodules and a kind of "calcite cement", consists of a micritic nodule (70 vol.-%), clay matrix (10 vol.-%) with bivalves (2 vol.-%), serpulids (1 vol.-%), quartz-silt (3 vol.-%), pyrite (2 vol.-%), mica (1 vol.-%) and cone-in-cone calcite (11 vol.-%).

A nodular, bioclastic limestone (argillaceous) bed, which is also known from equivalent depths in the Opalinus Clay in STA3-1 and STA2-1 (Wohlwend et al. 2022c and 2022d), delivered thin section BAC1-1-861.65 with erratic shaped micritic nodules (22 vol.-%, Fig. B-8), echinoderms (12 vol.-%), bivalves (6 vol.-%), other biogenes (3 vol.-%), quartz-sand (12 vol.-%) and clay matrix (12 vol.-%) with "stellate cement" (17 vol.-%), siderite (10 vol.-%) and pyrite (6 vol.-%).

BAC1-1-832.90 comes from a nodular bioclastic limestone (argillaceous, sideritic) to calcareous marl bed above the interval with the numerous sandstone lenses. A similar "hiatus beds" is also found in STA3-1 and STA2-1. Siderite (34 vol.-%) marks the bed, together with bioclasts (totally 18 vol.-%), micrite nodules (5 vol.-%), quartz-silt (5 vol.-%), pyrite (2 vol.-%), mica (1 vol.-%) and clay matrix (35 vol.-%).

The sample BAC1-1-829.17 from a "hiatus bed" is part of a nodular limestone (iron-oolitic) bed, composed of iron-oolitic nodules and a silty, bioclastic calcareous marl. It consists of 34 vol.-% iron-ooids, whereof most are totally replaced by calcite, bioclasts (overall 11 vol.-%), intraclasts (4 vol.-%), which are components within the iron-oolitic nodule, quartz-silt (3 vol.-%), then 44 vol.-% micrite matrix, incl. 4 vol.-% limonitic matrix and 4 vol.-% calcite cement.

BAC1-1-825.58 and 825.52 have a similar origin as BAC1-1-829.17: both are nodular limestones (iron-oolitic), composed of calcitic iron-ooids (30, resp. 15 vol.-%), bioclasts (11, resp. 10 vol.-%) and micrite (incl. some clay) matrix (51, resp. 54 vol.-%) and are representing "hiatus beds". BAC1-1-825.58 contains quartz-silt (5 vol.-%) and BAC1-1-825.52 few different intraclasts (5 vol.-%) and siderite (8 vol.-%). Both have pyrite (3, resp. 8 vol.-%), which looks in some parts very eye-catching (Fig. B-9).

Thin section BAC1-1-815.04 from a "hiatus bed" shows a bioclastic limestone (silty), consisting of quartz-silt (25 vol.-%), thin-shelled bivalves (15 vol.-%), echinoderms (4 vol.-%), pellets (6 vol.-%), "stellate cement" (40 vol.-%), micrite matrix (7 vol.-%) and pyrite (3 vol.-%).

And then, the uppermost calcareous bed of the Opalinus Clay contains beautiful iron-ooids, which consist of iron-minerals (Fig. B-10). BAC1-1-811.84 and 811.57 are bioclastic limestones (iron-oolitic, argillaceous), composed of iron-ooids (25, resp. 26 vol.-%), echinoderms (13, resp. 14 vol.-%), bivalves (13 vol.-%), limonitic bioclasts (7, resp. 6 vol.-%), other biogenes (0, resp. 4 vol.-%), sedimented with a micritic, partly marly, partly limonitic matrix (26, resp. 18 vol.-%), few quartz grains (5 vol.-%) and siderite (11, resp. 8 vol.-%). Many of the limonitic iron-ooids are on one side half-moon shaped replaced by calcite (Fig. B-10).

«Murchisonae-Oolith Formation» (BAC1-1-808.11, 806.84, 803.00, 799.99, 799.00, 797.34, 793.63)

The «Murchisonae-Oolith Formation» of BAC1-1 shows a big variation of bioclastic limestones: some of them are sandy, some are iron-oolitic, some are dominated by limonitic bioclasts, often they are interbedded with sandy marls.

Sample BAC1-1-808.11 represents the lowermost sand-rich beds: it is a calcareous sandstone (bioclastic) or sandy limestone (bioclastic) with 40 vol.-% quartz-sand, echinoderms (23 vol.-%), bivalves (5 vol.-%), other biogenes (2 vol.-%), pellets (3 vol.-%), and micrite matrix (17 vol.-%), as well as calcite cement (10 vol.-%).

Thin section BAC1-1-806.84 shows one of the lower limestones. Carbonate components dominate (Fig. B-11): echinoderms (15 vol.-%), bivalves (13 vol.-%), pellets (13 vol.-%), other biogenes (3 vol.-%, with different foraminifera), moreover quartz-sand (26 vol.-%), calcite cement (16 vol.-%), micrite matrix (8 vol.-%), iron-dolomite (4 vol.-%) and pyrite (2 vol.-%).

Then BAC1-1-803.00 comes from one of the lower limonitic bioclast and iron-ooid bearing limestones. Small iron-ooids (12 vol.-%), limonitic bioclasts (12 vol.-%), echinoderms (8 vol.-%), bivalves (10 vol.-%) and quartz-sand (18 vol.-%) lie in micritic and limonitic matrix (totally 14 vol.-%) with calcite cement (9 vol.-%) and iron-dolomite rhombohedrons (17 vol.-%).

The impressive red-brown unit higher up in the «Murchisonae-Oolith Formation» delivered BAC1-1-799.99 and 799.00. These consist mostly of relatively small (0.1 – 0.3 mm) iron-ooids (30, resp. 26 vol.-%) and limonitic bioclasts (26, resp. 28 vol.-%) (Fig. B-12). They are accompanied by biogenic components (totally 15, resp. 17 vol.-%), quartz-sand (15, resp. 7 vol.-%), calcite cement (6, resp. 22 vol.-%) and limonitic matrix (BAC1-1-799.99: 8 vol.-%).

Sample BAC1-1-797.34, a light grey bioclastic limestone above the red-brown unit, has iron-ooids too, but no limonitic bioclasts. The components are: 17 vol.-% echinoderms, 21 vol.-% bivalves, 3 vol.-% serpulids, 2 vol.-% other biogenes and 22 vol.-% iron-ooids, as well as 4 vol.-% quartz-sand. But the calcite cement (23 vol.-%) within several generations (Fig. B-13) is the most impressive of this microfacies. Present is also some pyrite (8 vol.-%).

The uppermost limestone bed (30 cm thick) is represented by BAC1-1-793.63: different small layers with iron-stromatolites or bored stromatolite-intraclasts (Fig. B-14 und B-15) document an impressive hardground. Only a small cut-out, as usual by thin section analyses, is expressed by the analyse: iron-stromatolite (60 vol.-%), iron-ooids (5 vol.-%), echinoderms (4 vol.-%), bivalves (2 vol.-%), other biogenes (3 vol.-%), quartz-sand (6 vol.-%), micrite matrix (7 vol.-%), calcite cement (4 vol.-%), pyrite (4 vol.-%) and siderite (5 vol.-%). The greenish colour of the iron-stromatolite points to a chamositic composition (Fig. B-14).

Wedelsandstein Formation (BAC1-1-792.99)

Near the base of the Wedelsandstein Formation a further iron-ooid bearing sandy limestone (argillaceous) is developed, which we analysed with BAC1-1-792.99. The thin section contains iron-ooids (17 vol.-%), up to 1 mm big, quartz-sand (23 vol.-%), echinoderms (8 vol.-%), bivalves (7 vol.-%) and other biogenes (1 vol.-%) in a marly micrite matrix (40 vol.-%) with mica (2 vol.-%) and pyrite (2 vol.-%).

«Humphriesioolith Formation» (BAC1-1-790.85, 789.14)

The «Humphriesioolith Formation» of BAC1-1 consists predominantly of claystones and marls, but with two intercalated limestone beds: an iron-oolitic one at the base, represented by BAC1-1-790.85 and a bioclast-rich higher-up, analysed by BAC1-1-789.14.

BAC1-1-790.85 is composed of calcitic iron-ooids (21 vol.-%, Fig. B-16), bivalves (5 vol.-%) and other biogenes (2 vol.-%), with micrite matrix (38 vol.-%), "stellate cement" (30 vol.-%) and pyrite (4 vol.-%).

Thin section BAC1-1-789.14 shows a bioclastic limestone of 38 vol.-% echinoderm skeletal elements, 2 vol.-% bivalves and 2 vol.-% other biogenes with quartz-silt (8 vol.-%), pyrite (3 vol.-%), mica (1 vol.-%) and micrite matrix (46 vol.-%).

«Parkinsoni-Württembergica Schichten» (BAC1-1-781.44, 779.86)

A succession within the «Parkinsoni-Württembergica-Schichten» stands out: a strongly limonitised bioclastic calcareous marl which is analysed by BAC1-1-781.44. Limonitic bioclasts – echinoderms and bivalves (15 vol.-%, Fig. B-17) and limonitic matrix (18 vol.-%) give the special look. Further echinoderms (18 vol.-%), bivalves (6 vol.-%), other biogenes (3 vol.-%), quartz-silt (8 vol.-%), marly matrix (15 vol.-%), dolomite (7 vol.-%) and pyrite (6 vol.-%) are present. But the most wondering components are ooids (4 vol.-%), "normal" calcite ooids (Fig. B-18) with an outer microbial rim, comparable with those from the oolites of the Hauptrogenstein in BOZ1-1 (Figures B-14 and B-15 in Wohlwend et al. 2022a) and the quarry in Auenstein (Figure 5F in Wetzel et al. 2013). As nuclei most of the ooids have fragments of bioclasts, mainly fragments from echinoderms, but some also show presumed fragments from corals (Fig. B-18, the two on the right).

Sample BAC1-1-779.86 concerns a small bivalve horizon, which is probably also a "hiatus bed", composed of bivalves (27 vol.-%), echinoderms (16 vol.-%), limonitic biogenes (10 vol.-%), other biogenes, mainly belemnites and gastropods (12 vol.-%), quartz-silt (6 vol.-%), micrite matrix (5 vol.-%), "stellate cement" (18 vol.-%) and pyrite (6 vol.-%).

Variansmergel Formation (BAC1-1-740.96)

Thin section BAC1-1-740.96, taken near the base of the Variansmergel Formation, from a bioclastic limestone contains limonitic bioclasts (18 vol.-%) and few, partly calcitic, iron-ooids (6 vol.-%), then echinoderms (8 vol.-%), bivalves (5 vol.-%), other biogenes (1 vol.-%), quartz-silt (5 vol.-%) and pyrite (3 vol.-%). The components are embedded in microsparitic matrix (18 vol.-%) and "stellate cement" (36 vol.-%).

Wutach Formation (BAC1-1-737.20, 737.14)

Firstly these samples were analysed because the uppermost beds of the Wutach Formation show a quite different evolution of the iron-ooids and secondly, to look for glauconite grains. Could glauconite already appear in the Wutach Formation or does it mark the lithological base of the Wildegg Formation? However, BAC1-1-737.14 contains a few glauconite grains.

The sample BAC1-1-737.20 is an iron-oolite or better an "ironstone", consisting predominantly of iron-ooids (60 vol.-%). Most of the original chamositic iron-ooids are replaced – layer for layer – by calcite (Figs. B-19 and B-20), and the iron has been moved into the matrix around the ooids. Intraclasts (5 vol.-%), micrite matrix (13 vol.-%) and limonitic matrix (16 vol.-%), as well as calcite cement (6 vol.-%) are present too.

Thin section BAC1-1-737.14 comes from an iron-oolitic calcareous nodule, consisting of limonitic iron-ooids (27 vol.-%, Fig. B-21), echinoderms (3 vol.-%), bivalves (3 vol.-%), other biogenes (6 vol.-%, especially belemnites), and micrite matrix (44 vol.-%) with quartz-silt (5 vol.-%), dolomite (9 vol.-%), mica (2 vol.-%) and glauconite (1 vol.-%).

Wildegg Formation (BAC1-1-668.48)

The Wildegg Formation consists of calcareous marls and argillaceous marls with some limestone beds. One of them was analysed by BAC1-1-668.48: It is nearly a pure micritic limestone (92 vol.-%), with only few pellets (3 vol.-%), biogenes (2 vol.-%), quartz-silt (2 vol.-%) and pyrite (1 vol.-%).

Tab. 3-1: Microfacies analysis from BAC1-1 (1'239.13 – 668.48 m; numbers in vol.-%)

Microfacies analysis BAC1-1 (1'239.13 - 668.48 m)	clay matrix, micrite, microsparite	dolomitic matrix	limonitic matrix	components (and biohermal organisms)															cements, diagenesis											
				calcitic biogenes								allochems																			
				echinoderms	bivalves	limonitic echinod. + bivalves	serpulids	corals	sponges, spicules	other biogenes	Fe-stromatolite + stromatolitic clasts	pellets, peloids, aggregates	ooids	oncoids	Fe-ooids	intraclasts, nodules	detritial quartz + silic. rock fragm.	quartz grainsize (mm)	calcite cement	"stellate cement" (s) cone-in-cone calcite (c)	(Fe)-dolomite	dedolomite	anhydrite, gypsum	quartz cement	pyrite	limonite, Fe-min. nodules	siderite	glauconite	mica	porosity
668.48m: limestone (mudstone) *Wildegg Fm. (Effingen Mb.)*	92									2		3					2	0.04							1					
737.14m: calcareous nod. (Fe-oolitic) *Wutach Fm.*	44			3	3					6					27		5	0.05			9							1	2	
737.20m: iron-oolite ("ironstone") *Wutach Fm.*	13		16												60	5			6											
740.96m: biocl. limestone, "hiatus bed" *Variansmergel Fm.*	18			8	5	18				1					6		5	0.05		36				3					
779.86m: biocl. limestone, "hiatus bed" *«Parkinsoni-Württembergica-Sch.»*	5			16	27	10				12							6	0.05		18				6					
781.44m: biocl. calc. marl (limonitic) *«Parkinsoni-Württembergica-Sch.»*	15		18	18	6	15				3			4				8	0.07			7			6					
789.14m: bioclastic limestone *«Humphriesioolith Fm.»*	46			38	2					2							8	0.05						3				1	
790.85m: limestone (iron-oolitic) *«Humphriesioolith Fm.»*	38				5					2					21*					30				4					
792.99m: sandy limestone (Fe-oolitic) *Wedelsandstein Fm.*	40			8	7					1					17		23	0.07						2				2	
793.63m: iron-stromatolite, hardground *«Murchisonae-Oolith Fm.»*	7			4	2					3	60				5		6	0.10	4					4		5			
797.34m: biocl. limestone (Fe-oolitic) *«Murchisonae-Oolith Fm.»*				17	21		3			2					22		4	0.10	23					8					
799.00m: biocl. limestone (Fe-oolitic) *«Murchisonae-Oolith Fm.»*				4	13	28									26		7	0.10	22										
799.99m: biocl. limestone (Fe-oolitic) *«Murchisonae-Oolith Fm.»*			8	4	10	26				1					30		15	0.15	6										
803.00m: bioclastic limestone (sandy) *«Murchisonae-Oolith Fm.»*	5		9	8	10	12									12		18	0.15	9		17								
806.84m: bioclastic limestone (sandy) *«Murchisonae-Oolith Fm.»*	8			15	13					3		13					26	0.10	16		4			2					
808.11m: sandy limestone (bioclastic) *«Murchisonae-Oolith Fm.»*	17			23	5					2		3					40	0.10	10										
811.57m: biocl. limestone (Fe-oolitic) *Opalinus Clay*	13		5	14	13	6	1			3					26		5	0.10	6							8			
811.84m: biocl. limestone (Fe-oolitic) *Opalinus Clay*	26			13	13	7									25		5	0.10								11			
815.04m: biocl. lmst. (silty), "hiatus b." *Opalinus Clay*	7			4	15							6					25	0.06		40				3					
825.52m: limest. (Fe-ool) nodule, h.g. *Opalinus Clay*	54			5	4					1					15*	5								8		8			
825.58m: limest. (Fe-ool) nod., "h. b." *Opalinus Clay*	51			6	5										30*		5	0.05						3					
829.17m: limest. (Fe-ool) nod., "h. b." *Opalinus Clay*	40		4	4	5					2					34*	4	3	0.05	4										
832.90m: biocl. lmst. (argill.), "h. b." *Opalinus Clay*	35			9	7					2						5	5	0.05						2		34		1	
861.65m: biocl. limest. + nod., "h. b." *Opalinus Clay*	12			12	6					3						22	12	0.08		17				6		10			
901.06m: micritic nodule *Opalinus Clay*	10				2		1									70	3	0.04		11				2				1	
914.92m: bioclastic limestone *Staffelegg Fm. (Gross Wolf Mb.)*	4			3	38														46					9					
964.96m: sandstone (dolomitic) *Klettgau Fm. (Seebi Mb.)*													3			10	62	0.70			8			10					7
965.08m: sandstone (dolomitic) *Klettgau Fm. (Seebi Mb.)*		17														15	57	0.70						4					7
965.90m: sandy dolost. - dolo. sandst. *Klettgau Fm. (Seebi Mb.)*		48								1						15	32	0.80											4
967.44m: microbial mat, dolomitic *Klettgau Fm. (Gansingen Mb.)*										93																			7
968.57m: dolostone *Klettgau Fm. (Gansingen Mb.)*		75														15								2					8
975.61m: sandstone (argillaceous) *Klettgau Fm. (Ergolz Mb.)*	17																68	0.15	2					12				1	
975.74m: sandstone (argillaceous) *Klettgau Fm. (Ergolz Mb.)*	26																60	0.10						3				1	10
980.07m: sandstone (anhydritic) *Klettgau Fm. (Ergolz Mb.)*	8																70	0.08			3			12		2		1	4
1'001.57m: dolomitic siltstone *Bänkerjoch Fm.*		36															48	0.04						14				2	
1'059.71m: dolostone, form. oolit. limest. *Schinznach Fm. (Stamberg Mb.)*	29				8							9	42											4					8
1'124.02m: bioclast. limestone (dolomi.) *Schinznach Fm. (Leutschenberg & Kienberg Mb.)*	10			11	7					6		7	5						13		35			6					
1'133.68m: anhydr. dolostone with nod. *Zeglingen Fm. («Dolomitzone»)*		65																						35					
1'237.99m: sandy dolostone *Kaiseraugst Fm. («Wellendolomit»)*				10													30	0.60			53					3			4
1'239.13m: dolomitic sandstone *Kaiseraugst Fm. («Wellendolomit»)*				3												4	60	0.50			25					3				5

3.2 Ammonite stratigraphy

From BAC1-1 twenty-two macrofossil specimens (mainly ammonites) were recovered, only two of them (depth 925.90 m and 737.38 m) could not be extracted because there was no separation between the rock matrix and the fossil, and the rock matrix did not react to potassium hydroxide. In both cases, an albeit uncertain determination was made based on the characteristic cross section.

Several ammonites were unfortunately so damaged by drilling or sampling that the genus or species could not be determined. Typically, the ammonites are distributed differently over the individual time periods drilled by the borehole. They are relatively common in the Toarcian and Early Aalenian, where ammonite fragments and cross sections are locally common in the range between 905.41 m and 900.90 m, and between 811.90 m and 811.44 m (see Appendices A2 and A3). In the Late Aalenian and Early Bajocian ammonites are rare and in the Late Bajocian no ammonites were found. In the Early Bathonian ammonites are somewhat more common, in the Late Bathonian and Callovian somewhat rarer. Due to the generally small sample size and the poor, often incomplete preservation of the ammonites, a more-or-less large uncertainty in the age determinations must be expected, and this can have an effect on the biostratigraphic classification.

We documented a selection of ammonites and additional macrofossils with photographs on four plates (Plates I – IV) in Appendix C. In addition to ammonites, other conspicuous fossils were identified to the extent possible (Appendix A3), even when they were not subsequently, or only occasionally, recovered.

In general, the more ammonites are present in a specific profile section, the more precisely the biostratigraphic classification of that section can be determined (Tab. 3-2). Furthermore, it must be considered that not all ammonites have the same index value and that the state of preservation of the objects also plays an important role in the biostratigraphic determination. In this respect, a certain error must always be expected. This error is in the range of about one ammonite Subzone (SZ) but can be as high as one ammonite Zone (Z) when the available data is insufficient.

Staffelegg Formation

925.90 m: *Pleuroceras* sp.? Phosphatic steinkern, could not be extracted because there was no separation between the rock matrix and the fossil. Age: probably Spinatum Zone (Late Pliensbachian). Lithology: dark grey-green glauconitic calcareous marl with phosphatised intraclasts. Other fossils are belemnites (*Passaloteuthis* sp.?). The ammonite is not illustrated.

918.38 m: *Perilytoceras jurense* (Zieten, 1833). Truncated steinkern with calcitic inner whorl preservation. Age: Thouarsense Zone (Late Toarcian). Lithology: grey, splintery, nodular limestone, overlain by a darker calcareous marl. Other fossils in both lithologies are ammonite fragments and belemnites. The ammonite is not illustrated.

917.97 m: *Pseudogrammoceras* sp. Flattened steinkern. Age: Thouarsense Zone, probably Fallaciosum Subzone. Lithology: grey bioclastic calcareous marl, rich in bioclasts. The bioclasts consists mainly of echinoderm skeletal elements. Other fossils: fragments of *Pseudogrammoceras* sp., belemnites, and a bivalve fragment. The ammonite is illustrated on Plate I, Fig. 1 (Appendix C, for all figures in this chapter).

915.09 m: The sampled interval (915.14 – 915.06 m) contains ammonites on two levels (915.09 m and 915.06 m):

915.09 m: *Pleydellia leura* (Buckman, 1890) and *Cotteswoldia* ex gr. *lotharingica* (Branco, 1879) or *pseudolotharingica* (Maubeuge, 1950). Body chamber with a somewhat compressed phosphoritic steinkern, inner whorl flattened, sulfidic. Age: Aalensis Zone, Torulosum Subzone. Lithology: grey bioclastic calcareous marl. The bioclasts consist mainly of shell fragments and crinoid skeletal elements. Other fossils are ammonite fragments. The ammonites are illustrated on Plate I, Fig. 2.

915.06 m: *Pleydellia* ex gr. *buckmani* (Maubeuge, 1947). Flattened phosphorite steinkern. Age: Aalensis Zone, Torulosum Subzone. Lithology: grey bioclastic calcareous marl. The biodetritus consists mainly of shell fragments and crinoid skeletal elements. Other fossils are ammonite fragments. The ammonite is illustrated on Plate I, Fig. 3.

Opalinus Clay

914.72 m: *Pleydellia* ex gr. *buckmani*? (Maubeuge, 1947). Flattened phosphorite steinkern. Age: Aalensis Zone, Torulosum Subzone. Lithology: grey biodetritic calcareous marl. The ammonite is not illustrated.

905.41 m: *Leioceras* ex gr. *subglabrum* (Buckman, 1902). Flattened steinkern. Age: Opalinum Zone, Opalinum Subzone. Lithology: dark-grey, somewhat silty claystone. The ammonite is illustrated on Plate II, Fig. 1.

901.82 m: *Leioceras* ex gr. *opalinum* (Reinecke, 1818). Truncated specimen, body chamber not flattened. Age: Opalinum Zone, Opalinum Subzone. Lithology: dark-grey, slightly calcareous, bioclast-bearing claystone with sulphidic burrows. The ammonite is illustrated on Plate II, Fig. 2.

901.63 m: *Leioceras* ex gr. *opalinum* (Reinecke, 1818). Truncated specimen with body chamber only partially flattened. Age: Opalinum Zone, Opalinum Subzone. Lithology: somewhat silty, dark claystone with some bioclasts. An additional fossil is a juvenile ammonite at 901.65 m. The ammonite is illustrated on Plate II, Fig. 3.

900.90 m: *Leioceras* ex gr. *subglabrum* (Buckman, 1902). Truncated specimen with calcitic shell preservation. Lithology: dark-grey, claystone with some bioclasts. The bioclasts comprise ammonite shells among other fragments. Other fossils are ammonites and a burrow. The ammonite is illustrated on Plate II, Fig. 4.

840.57 m: *Leioceras* sp. Specimen with partially calcitic shell preservation. Age: Opalinum Zone, Opalinum Subzone. Lithology: grey, silty claystone with sand lenses. The ammonite is illustrated on Plate II, Fig. 5.

811.90 m: *Leioceras* ex gr. *goetzendorfense* (Dorn, 1935), smooth morphology. Truncated steinkern with calcitic shell preservation. Age: Opalinum Zone, Bifidatum Subzone. Lithology: dark-green bioclastic limestone (somewhat argillaceous) with limonitised components. Also present is a large, calcitic intraclast several cm in size. The bioclasts comprise echinoderm skeletal elements among other components. Other

fossils in the sampled interval from 811.93 m to 811.87 m: ammonites at 811.92 m and at 811.89 m (both undeterminable) and shell fragments. The ammonite at 811.90 m is illustrated on Plate III, Fig. 1.

811.75 m: *Leioceras* sp. Truncated steinkern with calcitic shell preservation. Age: Opalinum Zone. Lithology: dark green to dark-grey bioclastic limestone (somewhat argillaceous) with small limonitic/goethitic iron-ooids. Other fossils are bivalves and shell fragments. The ammonite is not illustrated.

811.49 m: The sampled interval (811.54 – 811.44 m) contains ammonites on two levels (811.52 m and 811.50 m):

811.52 m: *Leioceras* ex gr. *goetzendorfense* (Dorn, 1935), smooth morph. Calcitic shell preservation. Age: Opalinum Zone, Bifidatum Subzone. Lithology: dark-green to dark-grey bioclastic limestone (somewhat argillaceous) with limonitised components and small iron-ooids (< 0.5 mm). Other fossils are ammonites. The ammonite is illustrated on Plate III, Fig. 2.

811.50 m: *Leioceras* ex gr. *goetzendorfense* (Dorn, 1935), smooth morph. Truncated ammonite with calcitic shell preservation. Age: Opalinum Zone, Bifidatum Subzone. Lithology: dark-green to dark-grey bioclastic limestone (somewhat argillaceous) with limonitised components and small iron-ooids (< 0.5 mm). Other fossils are ammonites and a gastropod. The ammonite is illustrated on Plate III, Figs. 3a and 3b.

810.64 m: *Leioceras* sp. Incomplete, flattened argillaceous steinkern. Age: probably Early Aalenian. Lithology: dark-grey, mica-bearing calcareous marl. Other fossils are sulfidic burrows. The ammonite is illustrated on Plate III, Fig. 4.

«Murchisonae-Oolith Fm.»

793.26 m: *Hyperlioceras* sp. Truncated steinkern. Age: Concavum or Discites Zone, probably Early Bajocian. Lithology: dark-grey iron-ooid and mica-bearing calcareous marl. The iron-ooids have diameters ranging up to 0.5 mm, mostly smaller. Other fossils are belemnites (*Holcobelus blainvillei*?) and bivalves (*Myophorella* sp. u.a.). The ammonite is illustrated on Plate III, Fig. 5.

Wedelsandstein Formation

793.05 m: Sonniniidae indet.?, ammonite with calcitic shell preservation. Age: Discites Zone? Lithology: light-grey, argillaceous limestone with iron-ooids (diameter ca. 1 mm). The ammonite is not illustrated.

791.88 m: Probably fragment of a crocodile vertebra, the fragment did not look promising and therefore the sample was not prepared.

Variansmergel Formation

741.00 m: *Oxycerites* ex gr. *limosus* (Buckman, 1925). Age: Zigzag Zone. Lithology: brown-grey, bioclastic limestone (somewhat argillaceous) with limonitised components. Other fossils are bivalve fragments and burrows. The ammonite is illustrated on Plate IV, Figs. 1a and 1b.

740.56 m: *Parkinsonia* (*Oraniceras*) ex gr. *wuerttembergica* (Oppel, 1857). Truncated ammonite with calcitic shell preservation. Age: Zigzag Zone. Lithology: brown-grey iron-ooid bearing to iron-oolitic, somewhat nodular calcareous marl with limonitised components. Other fossils are bivalve fragments and an ammonite of the genus *Procerites*. The ammonite is illustrated on Plate IV, Figs. 2a and 2b.

Wutach Formation

737.53 m: *Oecotraustes* sp. Truncated ammonite with calcitic shell preservation. Age: Bathonian. Lithology: red-brown iron-oolite. Other fossils are a belemnite and a bivalve. The ammonite is illustrated on Plate IV, Figs. 3a and 3b.

737.38 m: *Macrocephalites* sp.?. Truncated ammonite with partial shell preservation, could not be extracted because there was no separation between the rock matrix and the fossil. Age: Bathonian to probably Callovian. Lithology: dark iron-oolite with limonitic/goethitic iron-ooids (diameter up to 1 mm) and limonite-encrusted intraclasts. Other fossils: bivalve shell fragments. The ammonite is not illustrated.

Wildegg Formation

736.84 m: *Euaspidoceras* sp.? or *Peltoceras* sp.?, Hecticoceratidae indet. Fragment of a flattened steinkern. Age: Late Callovian or Early Oxfordian. Lithology: dark, grey-brown calcareous marl with some iron-ooids. The iron-ooids are limonitic/goethitic, most diameters are < 1 mm. Other fossils are ammonite fragments (Hecticoceratidae indet.). The ammonites are illustrated on Plate IV, Fig. 4.

Tab. 3-2: Ammonite and other macrofossil determination from BAC1-1

Depth [m MD]	**Identification**	**Ammonite Zone (Subzone) or Age**
736.84	*Euaspidoceras* sp.? or *Peltoceras* sp.?	Late Callovian or Early Oxfordian
737.38	*Macrocephalites* sp.?	Bathonian to probably Callovian
737.53	*Oecotraustes* sp.	Bathonian
740.56	*Parkinsonia* (*Oraniceras*) ex gr. *wuerttembergica* (Oppel, 1857)	Zigzag Zone
741.00	*Oxycerites* ex gr. *limosus* (Buckman, 1925)	Zigzag Zone
791.88	Probably a vertebra of a crocodile	
793.05	Soniniidae indet.?	Discites Zone?
793.26	*Hyperlioceras* sp.	Concavum or Discites Zone, probably Early Bajocian
810.64	*Leioceras* sp.	Early Aalenian?
811.50	*Leioceras* ex gr. *goetzendorfense* (Dorn, 1935)	Opalinum Zone (Bifidatum Subzone)
811.52	*Leioceras* ex gr. *goetzendorfense* (Dorn, 1935)	Opalinum Zone (Bifidatum Subzone)
811.75	*Leioceras* sp.	Opalinum Zone
811.90	*Leioceras* ex gr. *goetzendorfense* (Dorn, 1935)	Opalinum Zone (Bifidatum Subzone)
840.57	*Leioceras* sp.	Opalinum Zone (Opalinum Subzone)
900.90	*Leioceras* ex gr. *subglabrum* (Buckman, 1902)	Opalinum Zone (Opalinum Subzone)
901.63	*Leioceras* ex gr. *opalinum* (Reinecke, 1818)	Opalinum Zone (Opalinum Subzone)
901.82	*Leioceras* ex gr. *opalinum* (Reinecke, 1818)	Opalinum Zone (Opalinum Subzone)
905.41	*Leioceras* ex gr. *subglabrum* (Buckman, 1902)	Opalinum Zone (Opalinum Subzone)
914.72	*Pleydellia* ex gr. *buckmani*? (Maubeuge, 1947)	Aalensis Zone (Torulosum Subzone)
915.06	*Pleydellia* ex gr. *buckmani* (Maubeuge, 1947)	Aalensis Zone (Torulosum Subzone)
915.09	*Pleydellia leura* (Buckman, 1890) and *Cotteswoldia* ex gr. *lotharingica* (Branco, 1879) or *pseudolotharingica* (Maubeuge, 1950)	Aalensis Zone (Torulosum Subzone)
917.97	*Pseudogrammoceras* sp.	Thouarsense Zone (Fallaciosum SZ?)
918.38	*Perilytoceras jurense* (Zieten, 1833)	Thouarsense Zone
925.90	*Pleuroceras* sp.?	Spinatum Zone?

System		Stage		Zone	Subzone
Jurassic	Late	Oxfordian	Late	Bifurcatus	Grossouvrei
					Stenocycloides
			Middle	Transversarium	Rotoides
					Schilli
					Luciaeformis
					Parandieri
				Plicatilis	Antecedens
					Vertebrale
			Early	Cordatum	Cordatum
					Costicardia
					Bukowski
				Mariae	Praecordatum
					Scarburgense
	Middle	Callovian	Late	Lamberti	Lamberti
					Henrici
				Athleta	Spinosum
					Proniae
					Phaeinum
			Middle	Coronatum	Grossouvrei
					Obductum
				Jason	Jason
					Medea
			Early	Calloviense	Enodatum
					Calloviense
				Koenigi	Galilaeii
					Curtilobus
					Gowerianus
				Herveyi	Kamptus
					Terebratus
					Keppleri
		Bathonian	Late	Discus	Discus
					Hollandi
				Orbis	Hannoveranus
					Blanazense
				Hodsoni	
			Middle	Morrisi	
				Subcontractus	
				Progracilis	
			Early	Zigzag	Tenuiplicatus
					Yeovilensis
					Macrescens
					Convergens
		Bajocian	Late	Parkinsoni	Bomfordi
					Truellei
					Acris
				Garantiana	Tetragona
					Garantiana
					Dichotoma
				Niortense	Baculata
					Polygyralis
					Banksii
			Early	Humphriesianum	Blagdeni
					Humphriesianum
					Romani
					Pinguis
				Sauzei	Macrum
					Kumaterum
				Laeviuscula	Laeviuscula
					Trigonalis
				Ovale	
				Discites ?	
		Aalenian	Late	Concavum ?	Formosum
					Concavum
			Middle	Bradfordensis	Gigantea
					Bradfordensis
				Murchisonae	Murchisonae
					Haugi
			Early	Opalinum	Bifidatum *
					Opalinum

System		Stage		Zone	Subzone
Jurassic	Early	Toarcian	Late	Aalensis	Torulosum
					Aalensis
				Levesquei	Moorei
					Levesquei
				Insigne	Dispansum
					Insigne
				Thouarsense	Fallaciosum ?
					Thouarsense
				Variabilis	
			Early	Bifrons	Crassum
					Fibulatum
					Commune
				Falcifer	Falcifer
					Elegans
					Exaratum
					Elegantulum
				Tenuicostatum	Semicelatum
					Clevelandicum
					Paltum
		Pliensbachian	Late	Spinatum ?	Hawskerense
					Apyrenum
				Margaritatus	Gibbosus
					Subnodosus
					Stokesi
			Early	Davoei	Figulinum
					Capricornus
					Maculatum
				Ibex	Luridum
					Valdani
					Masseanum
				Jamesoni	Jamesoni
					Brevispina
					Polymorphus
					Taylori
		Sinemurian	Late	Raricostatum	Aplanatum
					Macdonnelli
					Raricostatum
					Densinodulum
				Oxynotum	Oxynotum
					Simpsoni
				Obtusum	Denotatus
					Stellare
					Obtusum
			Early	Turneri	Turneri
				Semicostatum	Sauzeanum
					Scipionanum
					Charlesi
				Bucklandi	Bucklandi
					Rotiforme
					Conybeari
		Hettangian		Angulata	Complanata
					Extranodosa
				Liasicus	Laquaeus
					Portlocki
				Planorbis	Johnstoni
					Planorbis

BAC1-1

Grey highlighted zones and subzones are documented in the drill core with ammonites. Fields with additional interrogation points are not surely proven with ammonites.

Biostratigraphy modified after Cariou & Hanzpergue (1997)
* after Dietze et al. (2021), former «Comptum» Subzone

Fig. 3-1: Zones and subzones which are documented by ammonites in BAC1-1

3.3 Palynostratigraphy

The 47 studied samples yielded mostly a good palynological residue with rich and diverse palynofloras. Preservation is good. The palynomorph assemblages are composed of mainly dinoflagellate cysts and pollen and spores. Minor components are prasinophytes, acritarchs, foraminiferal test linings and green algae (e.g. *Botryococcus*). A total of 168 dinoflagellate cyst taxa, 21 other aquatic palynomorphs and 55 pollen and spore taxa are recorded.

Some reworked sporomorphs (*Densosporites* spp., *Ovalipollis* spp., *Rhaetipollis germanicus*, *Ricciisporites tuberculatus*) indicate erosion of Triassic sediments in the source area. Other reworking is indicated by the occurrence of a few single specimens of the dinoflagellate cyst *Luehndea spinosa*, a typical Early Jurassic species with a main distribution in the Late Pliensbachian and earliest Toarcian.

The studied samples from BAC1-1 cores are dated to span the interval from the latest Toarcian to the Middle Oxfordian. There are 20 sample intervals differentiated and, where possible, assigned to ammonite biostratigraphy. A list of the analysed samples and the age dating of each sample is given in Tab. 3-3. The indicated ages, zones (Z) and subzones (SZ) for each sample are the result of the palynostratigraphical analysis and interpretation. The results of the quantitative analysis are illustrated in a Range Chart (Appendix D1) and a Depth/Age plot (Appendix D2); both in the digital version only.

Sample 916.21 m (1 sample): Late Toarcian, Aalensis Zone

The palynoflora in this sample is rich in dinoflagellate cysts. The dinoflagellate cyst assemblage is of relatively low diversity and is composed of representatives of the families Phallocystaceae (*Dodekovia bullula, Dodekovia* spp., *Susadinium scrofoides*) and Valvaeodiniaceae (questionable *Comparodinium punctatum*, *Valvaeodinium vermipellitum, Valvaeodinium* spp.) as well as *Evansia*? cf. *granochagrinata*, *Hystrichodinium*? sp. in Feist-Burkhardt & Pross (2010), *Kallosphaeridium praussii*, *Mancodinium semitabulatum, Nannoceratopsis gracilis* s.s. and s.l., *Nannoceratopsis* spp., *Scriniocassis priscus* and *Wallodinium laganum*. The species *Kallosphaeridium praussii* is superabundant, while *Evansia*? cf. *granochagrinata* is common.

The sample interval is defined by the first occurrence of *Kallosphaeridium praussii* to the first dominant occurrence (superabundance) of *Evansia*? cf. *granochagrinata* in the interval above.

The FAD (First Appearance Datum) of *Evansia*? cf. *granochagrinata* is in the Late Toarcian, probably Levesquei Zone, that of *Kallosphaeridium praussii* is in the Late Toarcian Aalensis Zone. The very high abundance or dominance of *Evansia*? cf. *granochagrinata* is typical for a slightly younger age, straddling the Toarcian / Aalenian boundary (Aalensis Zone to Opalinum Zone, Opalinum Subzone).

The Interval is interpreted Late Toarcian, Aalensis Zone.

Sample 914.70 m (1 sample): Late Toarcian, Aalensis Zone to Early Aalenian, Opalinum Zone, Opalinum Subzone

The palynoflora in this sample is characterised by the very high abundance of one dinoflagellate cyst species, *Evansia*? cf. *granochagrinata*. The species dominates the palynoflora, reaching 72% of all palynomorphs counted. Other dinoflagellate cysts present, though in low numbers, are a

few representatives of the families Phallocystaceae (*Reutlingia cardobarbata*) and Valvaeodiniaceae (*Valvaeodinium vermipellitum, Valvaeodinium* spp.) as well as *Kallosphaeridium praussii* (occasional), *Mancodinium semitabulatum, Nannoceratopsis gracilis* s.s., *Nannoceratopsis* spp., *Scriniocassis limbicavatus, S. weberi* and *Wallodinium laganum.*

The sample interval is defined by the dominant occurrence (superabundance) of *Evansia*? cf. *granochagrinata*.

The composition of the dinoflagellate cyst assemblage is typical for the interval straddling the Toarcian / Aalenian boundary. The very high abundance or dominance of *Evansia*? cf. *granochagrinata* is typical for an age of the sample straddling the Toarcian / Aalenian boundary (Aalensis Zone to Opalinum Zone, Opalinum Subzone). This characteristic bioevent at the Early to Middle Jurassic boundary defines the palynostratigraphic unit A of Feist-Burkhardt & Pross (2010).

Sample interval 909.41 – 812.56 m (8 samples): Early Aalenian, Opalinum Zone, Opalinum Subzone

The dinoflagellate cyst assemblages of this sample interval are rich and diverse. They are composed of common to abundant *Evansia*? cf. *granochagrinata*, diverse Phallocystaceae (*Andreedinium* spp., *Andreedinium* sp. 2, *Dodekovia* spp., *D. bullula*, *D. knertensis*, *D.* "*penicillus*", *D. pinna*, *D. pseudochytroeides*, *D. syzygia*, *Ovalicysta hiata*, *Parvocysta bjaerkei*, *P.? tricornuta*, *Phallocysta*? *frommernensis*, *Reutlingia cardobarbata, R. cracens*, *R. fausta*, *Susadinium scrofoides*) and Valvaeodiniaceae (*Comparodinium punctatum*, *Valvaeodinium* spp., *V. cavum*, *V. sphaerechinatum*), species of *Nannoceratopsis* (*Nannoceratopsis* spp., *N. dictyambonis*, *Nannoceratopsis gracilis* s.s. and s.l., *Nannoceratopsis* sp. 1, *Nannoceratopsis* sp. B in Feist (1987), *N. triangulata, N. triceras,* higher up in the section also *N. plegas brevicorna, N. plegas dictyornata, N. plegas plegas)* and *Scriniocassis (S. limbicavatus*, *S. priscus, S. weberi*) as well as *Bradleyella* spp., *Hystrichodinium*? sp. in Feist-Burkhardt & Pross (2010), *Kallosphaeridium praussii*, *Mancodinium semitabulatum* and *Wallodinium laganum*. The species *Phallocysta*? *frommernensis* is fairly common throughout and shows an acme up to 850.03 m. In the two topmost samples *Nannoceratopsis plegas* sets in with its subspecies *N. plegas brevicorna, N. plegas dictyornata* and *N. plegas plegas.* Last occurrences within the interval have *Wallodinium laganum* at the top, as well as *Nannoceratopsis triangulata* and *Phallocysta*? *frommernensis* slightly below the top.

The interval is defined from the first occurrence of *Phallocysta*? *frommernensis* to the last occurrence of *Wallodinium laganum*.

According to Feist-Burkhardt & Pross (2010) there are four marker species for the Early Aalenian Opalinuston Formation (German stratigraphy): *Kallosphaeridium praussii, Phallocysta*? *frommernensis, Nannoceratopsis triangulata* and *Wallodinium laganum*. All four marker species occur in this interval. An acme of *Phallocysta*? *frommernensis* defines the palynostratigraphical unit B of Feist-Burkhardt & Pross (2010) of the Opalinuston Formation.

The sample interval is dated Early Aalenian Opalinum Zone, Opalinum Subzone and corresponds largely to palynostratigraphic unit B of Feist-Burkhardt & Pross (2010).

The occurrence of *Luehndea spinosa* in the topmost sample at 812.56 m indicates reworking of Early Jurassic Late Pliensbachian to earliest Toarcian sediments in the source area.

Sample interval 811.85 – 811.55 m (2 samples): Early Aalenian, Opalinum Zone, Bifidatum Subzone

The assemblages in this interval are reduced in diversity of the phallocystacean dinoflagellate cysts. The samples are characterised by the first and superabundant to common occurrence of the genus *Batiacasphaera* with *Batiacasphaera* sp. A in Feist-Burkhardt & Pross (2010) and *Batiacasphaera* sp. B in Feist-Burkhardt & Pross (2010). The genus *Nannoceratopsis* is diverse including i.a. *Nannoceratopsis plegas* with its subspecies *N. plegas brevicorna, N. plegas dictyornata, N. plegas plegas,* and *Nannoceratopsis* sp. 1. First occurrences in this interval include *Andreedinium elongatum* and *Moesiodinium raileanui*. Last occurrences in this interval include questionable *Nannoceratopsis triangulata* and unquestionable *Scriniocassis weberi*.

The interval is defined by the first occurrence of superabundant *Batiacasphaera* sp. A to the last occurrence of questionable *Nannoceratopsis triangulata* and unquestionable *Scriniocassis weberi*.

The FAD of the genus *Batiacasphaera* is in the upper part of the Opalinum Zone with *Batiacasphaera* sp. A often being abundant in the Bifidatum Subzone of Opalinum Zone. The LADs (Last Appearance Datums) of *Nannoceratopsis triangulata* and *Scriniocassis weberi* are considered to be at the top of the Opalinum Zone.

The sample is dated Bifidatum Subzone of the Opalinum Zone.

The occurrence of *Luehndea spinosa* in the sample at 811.55 m indicates reworking of Early Jurassic Late Pliensbachian to earliest Toarcian sediments in the source area.

Sample interval 811.11 – 802.95 m (4 samples): Early Aalenian, Opalinum Zone to Middle Aalenian, Murchisonae Zone

The samples in this interval are relatively lean in palynomorphs. The dinoflagellate cyst assemblages are quite similar to the top sample of the interval below, but *Batiacasphaera* sp. A is rare or recorded as questionable only. *Andreedinium elongatum* occurs in all samples and is sometimes common. Last occurrences in this interval include *Nannoceratopsis triceras* and questionable *Scriniocassis weberi* at the base. In the sample at 802.95 m *Phallocysta*? *frommernensis* is recorded and interpreted as reworked.

The interval is defined as from the last occurrence of unquestionable *Scriniocassis weberi* in the interval below to the first occurrence of *Evansia*? *spongogranulata* in the interval above.

The LAD of *Scriniocassis weberi* is considered to be at the top of the Opalinum Zone. The FAD of *Evansia*? *spongogranulata* is in the Murchisonae Zone.

The interval is interpreted Opalinum to Murchisonae Zone.

The occurrence of *Luehndea spinosa* in the sample at 811.11 m indicates reworking of Early Jurassic Late Pliensbachian to earliest Toarcian sediments in the source area.

Sample interval 800.94 – 797.31 m (2 samples): Middle Aalenian, Murchisonae Zone

The assemblages in this interval are quite similar to the interval below, but there is the first occurrence of a questionable specimen of *Evansia*? *spongogranulata* in the sample at the base. Representatives of the genus *Dissiliodinium* are not yet present but have their first occurrence in the interval above.

The interval is defined by the first occurrences of questionable *Evansia*? *spongogranulata* to the first occurrence of *Dissiliodinium* spp. in the interval above.

The FAD of *Evansia*? *spongogranulata* is in the Murchisonae Zone, that of *Dissiliodinium* spp. is within the Bradfordensis Zone.

The sample is interpreted Murchisonae Zone.

Sample interval 796.99 – 793.91 m (2 samples): Middle Aalenian, Bradfordensis Zone

The assemblages are characterised by the first representatives of the genus *Dissiliodinium*. Species of *Scriniocassis* (*S. limbicavatus* and *S. priscus*) have their last occurrence in this interval. *Nannoceratopsis dictyambonis* is superabundant. *Andreedinium elongatum* shows an acme in the interval.

The interval is defined by the first occurrence of *Dissiliodinium* spp. to the first occurrence of *Evansia*? *eschachensis* in the interval above.

The FAD of *Dissiliodinium* spp. is within the Bradfordensis Zone. The LAD of *Scriniocassis* spp. is in the Bradfordensis Zone. The FAD of *Evansia*? *eschachensis* is in the Concavum Zone.

The interval is dated Bradfordensis Zone.

Sample 793.13 m (1 sample): Late Aalenian, Concavum Zone

The assemblage in this sample differs from the interval below in that representatives of the genus *Dissiliodinium* are superabundant. There are the first occurrences of *Dissiliodinium lichenoides* (superabundant), *Evansia*? *eschachensis* and *Pareodinia* spp. *Andreedinium elongatum* is common.

The interval is defined by the first occurrence of *Evansia*? *eschachensis* to the first occurrence of *Dissiliodinium* aff. *giganteum* in the interval above.

The FAD of *Evansia*? *eschachensis* is in the Concavum Zone, that of *Dissiliodinium* aff. *Giganteum* is in the Discites Zone.

The interval is interpreted Concavum Zone.

Sample 792.89 m (1 sample): Early Bajocian, Discites Zone

The assemblage is characterised by the first occurrences of *Dissiliodinium* aff. *giganteum* and *Gongylodinium erymnoteichon*, both recorded with the first few specimens. *Nannoceratopsis* sp. B has its last occurrence.

The interval is defined by the first occurrences of *Dissiliodinium* aff. *giganteum* and *Gongylodinium erymnoteichon* to the last occurrence of *Nannoceratopsis* sp. B.

The FADs of *Dissiliodinium* aff. *giganteum* and *Gongylodinium erymnoteichon* are in the Discites Zone. The LAD of *Nannoceratopsis* sp. B is considered also in the Discites Zone.

The sample is interpreted Discites Zone.

Sample 792.55 m (1 sample): Early Bajocian, Ovale Zone

The assemblage is characterised by the first occurrence of *Dissiliodinium giganteum*. There are several last occurrences recorded, namely those of *Andreedinium elongatum*, *Evansia*? *eschachensis*, *Nannoceratopsis dictyambonis* and *N. plegas plegas*.

The interval is defined by the first occurrence of *Dissiliodinium giganteum* to the last occurrence of *Andreedinium elongatum* and *Evansia*? *eschachensis.*

The FAD of *Dissiliodinium giganteum* is in the Ovale Zone. The LADs of *Andreedinium elongatum* and *Evansia*? *eschachensis* are also in the Ovale Zone.

The sample is dated Ovale Zone.

Sample interval 791.67 – 791.12 m (2 samples): Early Bajocian, Laeviuscula Zone

Assemblages in this interval show the first occurrences of *Batiacasphaera laevigata*, *Cavatodissiliodinium hansgochtii* and *Durotrigia daveyi* (common to abundant) as well as the spore *Lycopodiumsporites gristhorpensis*. *Dissiliodinium giganteum* is abundant. Last occurrences in this interval include *Cavatodissiliodinium hansgochtii, Dissiliodinium giganteum, Evansia*? *spongogranulata, Hystrichodinium*? sp. in Feist-Burkhardt & Pross (2010) and *Mancodinium semitabulatum*. *Kallosphaeridium hypornatum* is not recorded.

The interval is defined by the first occurrences of *Batiacasphaera laevigata* and *Cavatodissiliodinium hansgochtii* while lacking *Kallosphaeridium hypornatum*.

The FADs of *Batiacasphaera laevigata* and *Cavatodissiliodinium hansgochtii* are in the Laeviuscula Zone. The FAD of *Kallosphaeridium hypornatum* is in the Sauzei Zone.

The interval is interpreted Laeviuscula Zone.

Sample interval 790.55 – 789.67 m (2 samples): Early Bajocian, Humphriesianum Zone

The assemblages in this interval are very different to below with e.g. superabundant *Acanthaulax crispa*. At the base of the interval there are numerous first occurrences including *Acanthaulax crispa, Atopodinium polygonale, Atopodinium* sp. 1 in Feist-Burkhardt & Götz (2016), *Durotrigia*

filapicata, "*Hypolytodinium*" sp., *Kallosphaeridium hypornatum, Meiourogonyaulax valensii, Nannoceratopsis spiculata, Rhynchodiniopsis*? sp. 1 in Feist-Burkhardt & Götz (2016), *Valensiella/Ellipsoidictyum* spp. as well as the spore *Foveotriletes* sp. 1.

The interval is defined by the first occurrence of *Acanthaulax crispa* to the last occurrence of "*Hypolytodinium*" sp.

The FAD of *Acanthaulax crispa* is in the Humphriesianum Zone. The range of "*Hypolytodinium*" sp. is considered to be restricted to the Humphriesianum Zone.

The interval is interpreted Humphriesianum Zone.

Sample interval 789.36 – 787.07 m (5 samples): Late Bajocian, Niortense Zone

The samples in this interval show a number of first occurrences including *Batiacasphaera* sp. 1, *Carpathodinium predae, Ctenidodinium continuum, Endoscrinium asymmetricum, Gonyaulacysta pectinigera, Korystocysta gochtii* and *Valvaeodinium spinosum*. The species *Nannoceratopsis gracilis* s.l. is last recorded in the topmost sample of the interval with some questionable specimens.

The interval is defined by the first occurrence of *Valvaeodinium spinosum* to the last occurrence of *Nannoceratopsis gracilis* s.l.

The FAD of *Valvaeodinium spinosum* is in the Niortense Zone. The LAD of *Nannoceratopsis gracilis* s.l. is also in the Niortense Zone.

The interval is dated Niortense Zone.

Sample interval 784.54 – 772.04 m (5 samples): Late Bajocian, Niortense to Parkinsoni Zone

Assemblages in this interval are quite similar to below but lack *Nannoceratopsis gracilis* s.l. In the topmost sample representatives of the genus *Ctenidodinium* become diverse and abundant and the first occurrence of *Dissiliodinium minimum* is recorded.

The interval is defined by the last occurrence of *Nannoceratopsis gracilis* s.l. in the interval below to the first occurrences of *Orobodinium automobile* and *Valvaeodinium vermicylindratum* in the interval above.

The LAD of *Nannoceratopsis gracilis* s.l. is in the Niortense Zone. The FADs of *Orobodinium automobile* and *Valvaeodinium vermicylindratum* are in the Parkinsoni Zone.

The interval is interpreted Niortense to Parkinsoni Zone.

Sample interval 764.07 – 741.38 m (4 samples): Late Bajocian Parkinsoni Zone

Assemblages in this interval are quite similar to below with e.g. superabundant *Ctenidodinium* spp., but there are some first occurrences including *Orobodinium automobile*, questionable *Sirmiodiniopsis* sp. in Feist-Burkhardt & Wille (1992) and *Valvaeodinium vermicylindratum* at the base, and *Gonyaulacysta eisenackii* higher up section. Last occurrences at the top of the interval include *Acanthaulax crispa, Meiourogonyaulax valensii* and *Rhynchodiniopsis*? *regalis*.

The interval is defined by the first occurrences of *Orobodinium automobile* and *Valvaeodinium vermicylindratum* to the last occurrence of *Acanthaulax crispa*.

The FADs of *Orobodinium automobile* and *Valvaeodinium vermicylindratum* are in the Parkinsoni Zone. The LAD of *Acanthaulax crispa* is also in the Parkinsoni Zone.

The interval is dated Parkinsoni Zone.

Sample 739.02 m (1 sample): Early Bathonian Zigzag Zone to Middle Bathonian Morrisi Zone

The sample is characterised by the first occurrence of *Ctenidodinium combazii*, which is common. Other first occurrences include questionable *Atopodinium prostatum, Gonyaulacysta jurassica* and *Lithodinia* spp. Last occurrences include *Carpathodinium predae*.

The interval is defined by the first occurrence of *Ctenidodinium combazii* to the last occurrence of *Carpathodinium predae*.

The FAD of *Ctenidodinium combazii* is in the Zigzag Zone. The LAD of *Carpathodinium predae* is in the Morrisi Zone.

The interval is dated Zigzag to Morrisi Zone.

Sample interval 738.79 – 737.53 m (2 samples): Late Bathonian, Hodsoni to Discus Zone

The base of the interval is characterised by the first occurrences of unquestionable *Atopodinium prostatum*, first complex skolochorate dinocysts indet., *Nannoceratopsis pellucida* and *Sirmiodiniopsis orbis*. At the top there are numerous last occurrences including *Atopodinium polygonale, Ctenidodinium combazii, Dissiliodinium minimum, Sirmiodiniopsis orbis, Valvaeodinium spinosum* and *V. vermicylindratum*.

The interval is defined by the first occurrences of unquestionable *Atopodinium prostatum* and *Sirmiodiniopsis orbis* to the last occurrence of *Valvaeodinium spinosum*.

The FADs of *Atopodinium prostatum* and *Sirmiodiniopsis orbis* are in the Hodsoni Zone. The LAD of *Valvaeodinium spinosum* is in the Discus Zone.

The interval is dated Hodsoni to Discus Zone.

Sample 737.19 m (1 sample): Middle Callovian, Jason to Coronatum Zone

Composition of the dinoflagellate cyst assemblage in this sample is distinctly different to below. Complex skolochorate dinocysts indet. are common and species of *Ctenidodinium* are less abundant. *Ctenidodinium combazii* is lacking. There are several first occurrences i.a. *Ambonosphaera* spp., *Hapsidaulax margarethae, Korystocysta pachyderma, Lithodinia caytonensis, Mendicodinium groenlandicum* (superabundant), *Rhynchodiniopsis cladophora, Rigaudella aemula* and *Stephanelytron redcliffense*. Last occurrences include *Hapsidaulax margarethae, Korystocysta gochtii, K. pachyderma, Lithodinia caytonensis, Nannoceratopsis spiculata* and *Rigaudella filamentosa*.

The interval is defined by the first occurrence of *Stephanelytron redcliffense* to the last occurrence of *Lithodinia caytonensis*.

The FAD of *Stephanelytron redcliffense* is in the Jason Zone. The LAD of *Lithodinia caytonensis* is in the Coronatum Zone.

The interval is interpreted Jason to Coronatum Zone.

Sample 736.62 m (1 sample): Late Callovian Lamberti Zone to Middle Oxfordian Plicatilis Zone

Composition of the dinoflagellate cyst assemblage in this sample is different to below. Chorate dinoflagellate cysts are superabundant. There are numerous first occurrences. These include *Compositosphaeridium polonicum, Endoscrinium galeritum, Liesbergia scarburghensis*, questionable *Limbodinium absidatum, Scriniodinium crystallinum, Wanaea fimbriata* and *W. thysanota.* Last occurrences in this sample include *Liesbergia scarburghensis*, questionable *Limbodinium absidatum, Rigaudella aemula, Scriniodinium crystallinum, Wanaea fimbriata, W. indotata* and *W. thysanota*.

The interval is defined by the first occurrences of *Endoscrinium galeritum, Liesbergia scarburghensis* and *Wanaea thysanota* co-occurring with *Wanaea indotata*, to the last occurrences of *Wanaea fimbriata* and *W. thysanota.*

The FADs of *Endoscrinium galeritum, Liesbergia scarburghensis* and *Wanaea thysanota* are in the Lamberti Zone. The LAD of *Wanaea indotata* is considered to be at the top of Athleta Zone. The LADs of *Wanaea fimbriata* and *W. thysanota* are in the Plicatilis Zone.

The interval is interpreted Lamberti to Plicatilis Zone.

Sample 736.04 m (1 sample): Middle Oxfordian, Plicatilis to Transversarium Zone

The sample shows the first occurrences of *Glossodinium dimorphum, Leptodinium arcuatum* and *Systematophora areolata*. Important taxa still present in the sample include *Compositosphaeridium polonicum, Endoscrinium galeritum* and *Gonyaulacysta eisenackii.*

The interval is defined by the first occurrences of *Glossodinium dimorphum, Leptodinium arcuatum* and *Systematophora areolata* to the last occurrences of *Compositosphaeridium polonicum, Endoscrinium galeritum* and *Gonyaulacysta eisenackii.*

The FADs of *Glossodinium dimorphum, Leptodinium arcuatum* and *Systematophora areolata* are in the Plicatilis Zone. The LADs of *Compositosphaeridium polonicum, Endoscrinium galeritum* and *Gonyaulacysta eisenackii* are in the Transversarium Zone.

The interval is interpreted Plicatilis to Transversarium Zone.

Tab. 3-3: List of analysed palynology samples from BAC1-1

The indicated ages, zones and subzones for each sample are the result of the palynostratigraphical analysis and interpretation.

Depth [m MD]	**Age**	**Zone & Subzone**
736.04	Middle Oxfordian	Transversarium – Plicatilis Zone
736.62	Middle Oxfordian – Late Callovian	Plicatilis – Lamberti Zone
737.19	Middle Callovian	Coronatum – Jason Zone
737.53	Late Bathonian	Discus – Hodsoni Zone
738.79	Late Bathonian	Discus – Hodsoni Zone
739.02	Middle – Early Bathonian	Morrisi – Zigzag Zone
741.38	Late Bajocian	Parkinsoni Zone
747.92	Late Bajocian	Parkinsoni Zone
756.02	Late Bajocian	Parkinsoni Zone
764.07	Late Bajocian	Parkinsoni Zone
772.04	Late Bajocian	Parkinsoni – Niortense Zone
780.58	Late Bajocian	Parkinsoni – Niortense Zone
781.44	Late Bajocian	Parkinsoni – Niortense Zone
784.10	Late Bajocian	Parkinsoni – Niortense Zone
784.54	Late Bajocian	Parkinsoni – Niortense Zone
787.07	Late Bajocian	Niortense Zone
788.41	Late Bajocian	Niortense Zone
788.89	Late Bajocian	Niortense Zone
789.06	Late Bajocian	Niortense Zone
789.36	Late Bajocian	Niortense Zone
789.67	Late Bajocian	Humphriesianum Zone
790.55	Late Bajocian	Humphriesianum Zone
791.12	Early Bajocian	Laeviuscula Zone
791.67	Early Bajocian	Laeviuscula Zone
792.55	Early Bajocian	Ovale Zone
792.89	Early Bajocian	Discites Zone
793.13	Late Aalenian	Concavum Zone
793.91	Middle Aalenian	Bradfordensis Zone
796.99	Middle Aalenian	Bradfordensis Zone
797.31	Middle Aalenian	Murchisonae Zone
800.94	Middle Aalenian	Murchisonae Zone
802.95	Middle – Early Aalenian	Murchisonae – Opalinum Zone
804.44	Middle – Early Aalenian	Murchisonae – Opalinum Zone
808.08	Middle – Early Aalenian	Murchisonae – Opalinum Zone
811.11	Middle – Early Aalenian	Murchisonae – Opalinum Zone
811.55	Early Aalenian	Opalinum Zone (Bifidatum SZ)
811.85	Early Aalenian	Opalinum Zone (Bifidatum SZ)
812.56	Early Aalenian	Opalinum Zone (Opalinum SZ)
815.34	Early Aalenian	Opalinum Zone (Opalinum SZ)
820.17	Early Aalenian	Opalinum Zone (Opalinum SZ)
829.90	Early Aalenian	Opalinum Zone (Opalinum SZ)
850.03	Early Aalenian	Opalinum Zone (Opalinum SZ)
869.83	Early Aalenian	Opalinum Zone (Opalinum SZ)
890.39	Early Aalenian	Opalinum Zone (Opalinum SZ)
909.41	Early Aalenian	Opalinum Zone (Opalinum SZ)
914.70	Early Aalenian – Late Toarcian	Opalinum Zone (Opalinum SZ) – Aalensis Zone
916.21	Late Toarcian	Aalensis Zone

3.4 Chemostratigraphy

The sampling of the BAC1-1 cores focused primarily on the upper part of the Lias Group (Figs. 3-2 and 3-3) and Dogger Group (Figs. 3-4 to 3-7) and, therefore inter alia on clay mineral-rich layers of the Opalinus Clay. In addition, the whole cored interval of the Malm Group was sampled and analysed for bulk carbonates in metre resolution up to 517.16 m (Fig. 3-8). The summary Figs. 3-9 and 3-10 illustrate the fully analysed interval from the upper part of the Staffelegg Formation up to the lowermost part of the Wildegg Formation (925.85 – 720.00 m). The data presented here (applies for all subsequent figures in this section) is shown in comparison to other data collected during the drilling campaign: Stratigraphic profile after Dossier III, DryClay (values in wt.-%, vertical axis in m MD log depth; *cf.* Dossier X), XRD measurements (horizontal bars; calcite: blue, dolomite and ankerite: green, siderite: red; *cf.* Dossier VIII) and C(org) measurements also with blue horizontal bars (*cf.* Dossier VIII). In addition, formation boundaries were highlighted with black lines and other formal or informal subintervals with grey lines. The following stratigraphic abbreviations were used in Figs. 3-2 to 3-10: Fm. = Formation; Mb. = Member; F. = Frick Mb.; G.B.R = Grünschholz Mb., Breitenmatt Mb. and Rickenbach Mb.; Rieth. = Rietheim Mb.; G. W. = Gross Wolf Mb.; «M.-O. Fm.» = «Murchisonae-Oolith Fm.»; Wedel. = Wedelsandstein Fm.; «H.o.» = «Humphriesioolith Fm.»; «P.-W.» = «Parkinsoni-Württembergica-Schichten»;Varians. and V. = Variansmergel Fm.; W. = Wutach Fm.; Hornb. = Hornbuck Mb.; Siderol. = Siderolithic Group.

In addition to the continuous samples (roughly in metre resolution), some specific samples were taken (Appendix E1) to complete the information about the calcareous beds. Some of the firm- to hardground samples were drilled directly from the remaining thin section blocks to correlate the bulk geochemical data with the microfacies analysis. All these data points are distinguished in different colours on Figs. 3-2, 3-4, 3-6 and 3-8 (in light blue: calcareous samples ("hiatus beds", calcareous and sideritic concretions); in violet: septarian nodules) but may not be shown on the individual plots because of the data ranges (see Appendix E1 for data).

The data will be discussed in four intervals: Lias Group, the lower part of the Dogger Group – mainly Opalinus Clay, the upper part of the Dogger Group, and the cored interval of the Malm Group. Not all data are discussed to the same extent as for example the $\delta^{18}O_{carb}$ and $\delta^{15}N_{org}$ data. The oxygen isotopes are strongly influenced by diagenesis. This can be exemplarily shown with the measured belemnites in the Lias Group in MAR1-1 (green points in Figure 3-2 in Wohlwend et al. 2021c). These are 3 to 4 ‰ more positive than the marlier bulk rock and therefore much less diagenetically overprinted. The nitrogen isotopes may not be as meaningful in some cases, because the combined $\delta^{13}C_{org}$ and $\delta^{15}N_{org}$ measurements showed a too low concentration of N in most of the measurements.

Although, the calculated carbonate content (TCarb) is only a semi-quantitative method, the values presented here correspond quite good to the XRD values measured at the University of Bern (*cf.* Dossier VIII). The XRD data are illustrated in the following Figs. 3-2, 3-4, 3-6 and 3-8 to provide a visual comparison between the data presented here and those from Dossier VIII. As discussed in Wohlwend et al. (2019b) based on measurements from the BDB-1 borehole at the Mont Terri Rock Laboratory, the values calculated here follow nicely the calcite and dolomite wt.-% with an additional mixed signal from the other carbonates (mainly siderite). Because during the reaction time of 60 min at 72 °C, a complete reaction for example for siderite does not take place. Therefore, the TCarb values are slightly too low in siderite-rich successions (red bars in the XRD data; e.g. Fig. 3-4).

In contrast to the carbonate measurements, the organic measurements were not always measured in metre resolution. If no major isotope changes were expected, as for example during the middle part of the Opalinus Clay, only every second sample (mainly 2 m interval) was analysed.

Lias Group

Starting from the bottom up (Fig. 3-2), the oldest sediments measured belong to the Early Jurassic (probably Late Pliensbachian). The lowermost two measurements (925.85 m and 925.55 m) belong to the uppermost combined Grünschholz Member, Breitenmatt Member and Rickenbach Member (G.B.R). The following ones, between 925.48 m and 914.92 m, represent the upper two members of the Staffelegg Formation.

The semi-quantitative carbonate content (TCarb, Fig. 3-2) in the Rietheim Member shows an increasing trend from around 13.7 wt.-% (924.99 m) to values around 65 wt.-%. The lowermost interval of the Rietheim Member from 925.48 m to 924.73 m (below the «Unterer Stein»), clearly contains less carbonate than the hanging part and is separated by the two clearly higher values measured from the above following calcareous interbeds («Unterer Stein»: 97.1 wt.-% at 924.50 m and «Homogene Kalkbänke»: 87.8 wt.-% at 924.03 m). The uppermost more calcareous interval is represented by one sample (questionable «Monotisbank»: 74.9 wt.-% at 920.50 m). The nomenclature of theses beds is *sensu* Kuhn & Etter (1994). The data is documented in Appendix E1 and marked by blue dots in Fig. 3-2. The overlying Gross Wolf Member shows similar values around 50 wt.-% measured from the argillaceous to calcareous marl sediments. The calcareous nodules to nodular layers, which are typical for the Gross Wolf Member, clearly show higher values 95.1, 86.9 and 76.8 wt.-% (917.50, 916.00 and 914.92 m).

The $\delta^{13}C_{carb}$ values document at the base of the Rietheim Member a negative trend with the most negative value coinciding with the «Unterer Stein» (-2.1 ‰ at 924.50 m). The negative trend is subsequently followed by a rapid increase. The most positive $\delta^{13}C_{carb}$ value thereafter was documented just below the «Oberer Stein» with +2.0 ‰ at 923.50 m. Further up to the top of the Gross Wolf Member the values show a continuous decreasing trend to values around +0.3 ‰ at 915.50 m with two more negative values (-1.3 ‰ at 916.00 m and -3.6 ‰ at 914.92 m), followed by a slight jump to values around -1 to -2 ‰ in the lowermost Opalinus Clay.

The above-mentioned negative carbon isotope excursion (CIE) below the «Unterer Stein» can also be seen by the $\delta^{13}C_{org}$ values (Fig. 3-3). The most negative one, with a value of -33.5 ‰ at 924.73 m, is slightly lower than the most negative one from the $\delta^{13}C_{carb}$ and clearly in the succession below the «Unterer Stein». The above following rapid positive shift is also documented in the organic matter, reaching the most positive value (-27.2 ‰) with the same sample as the $\delta^{13}C_{carb}$ value at 923.50 m. The discussed negative CIE below the «Unterer Stein» represents one of the major Mesozoic perturbations of the carbon cycle. It can be correlated with the global Toarcian-CIE (T-CIE). The whole isotopic expression of the T-CIE can be followed with a much higher resolution in BUL1-1 (Wohlwend et al. 2021a), where the resolution enables a direct comparison with the compilation made by Ruebsam & Al-Husseini (2020).

The Rietheim Member is very bituminous and is itself defined by the occurrence of bituminous shale. The TOC as well as the C/N ratio (both Fig. 3-3) limit the range of the member. The highest TOC value with 8.0 wt.-% was measured between the two calcareous beds at 924.31 m. The average range of the semi-quantitative TOC, with only one exception, is clearly above 2 wt.-% for the whole Rietheim Member and can therefore clearly be assigned as a black shale deposit. The hanging Gross Wolf Member has an obvious different lithological composition which is documented by the very stable but much lower TOC content, which is below 0.7 wt.-%.

The C/N ratios show the same trend as the TOC with the highest ratios mainly measured contemporaneously with the bituminous Rietheim Member (ratios mainly above 30 to a maximum of 40), compared to the overlying Gross Wolf Member with a much lower C/N ratio (9 – 16). Such high C/N ratios, measured in the Rietheim Member, are normally rather unusual for marine organic matter, see also discussion in e.g. BUL1-1 (Wohlwend et al. 2021a).

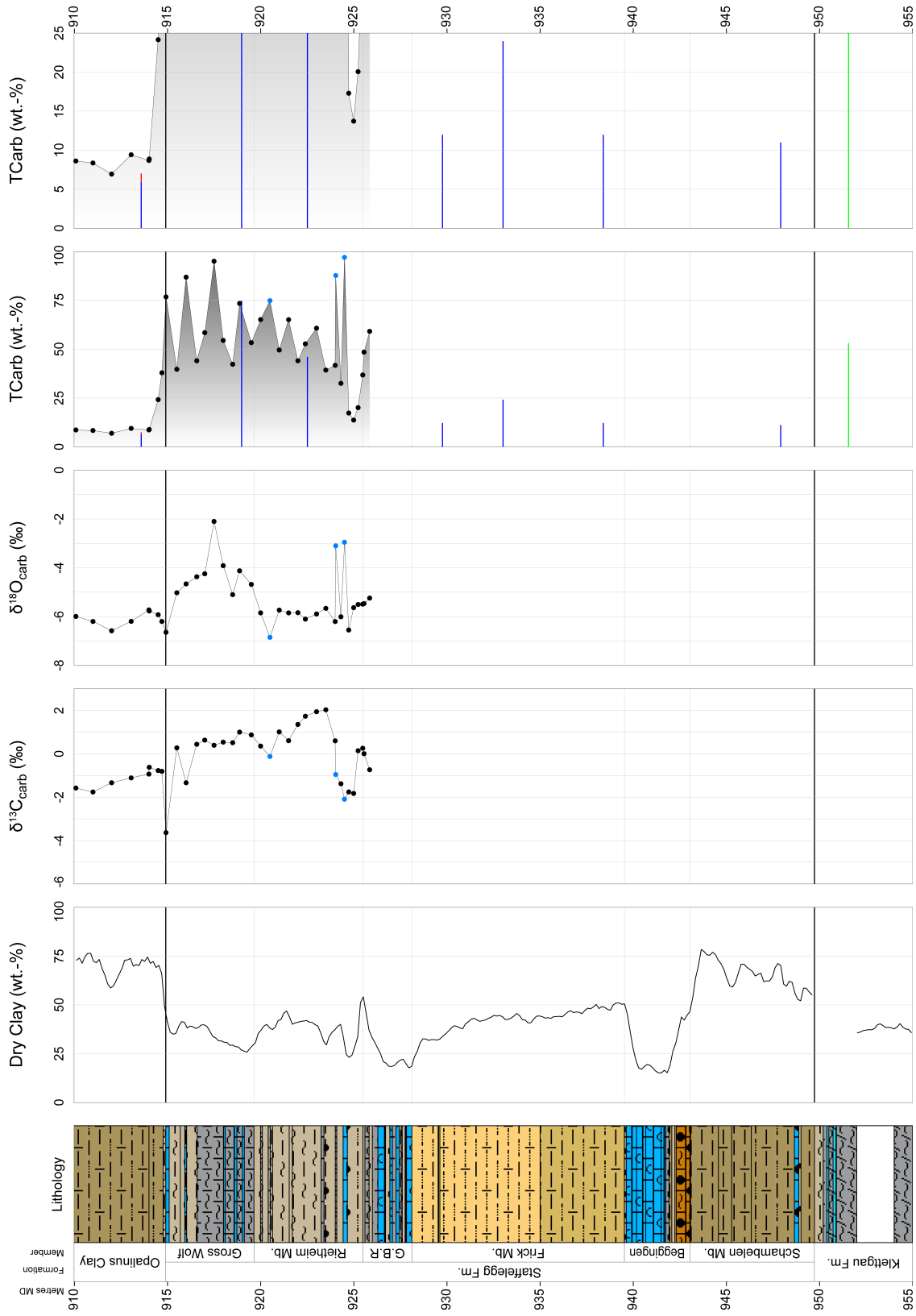

Fig. 3-2: Bulk rock (carbonate) isotopic data from the Lias Group

Geochemical data from 925.85 – 910.08 m, additional explanations and references see text at the beginning of Section 3.4.

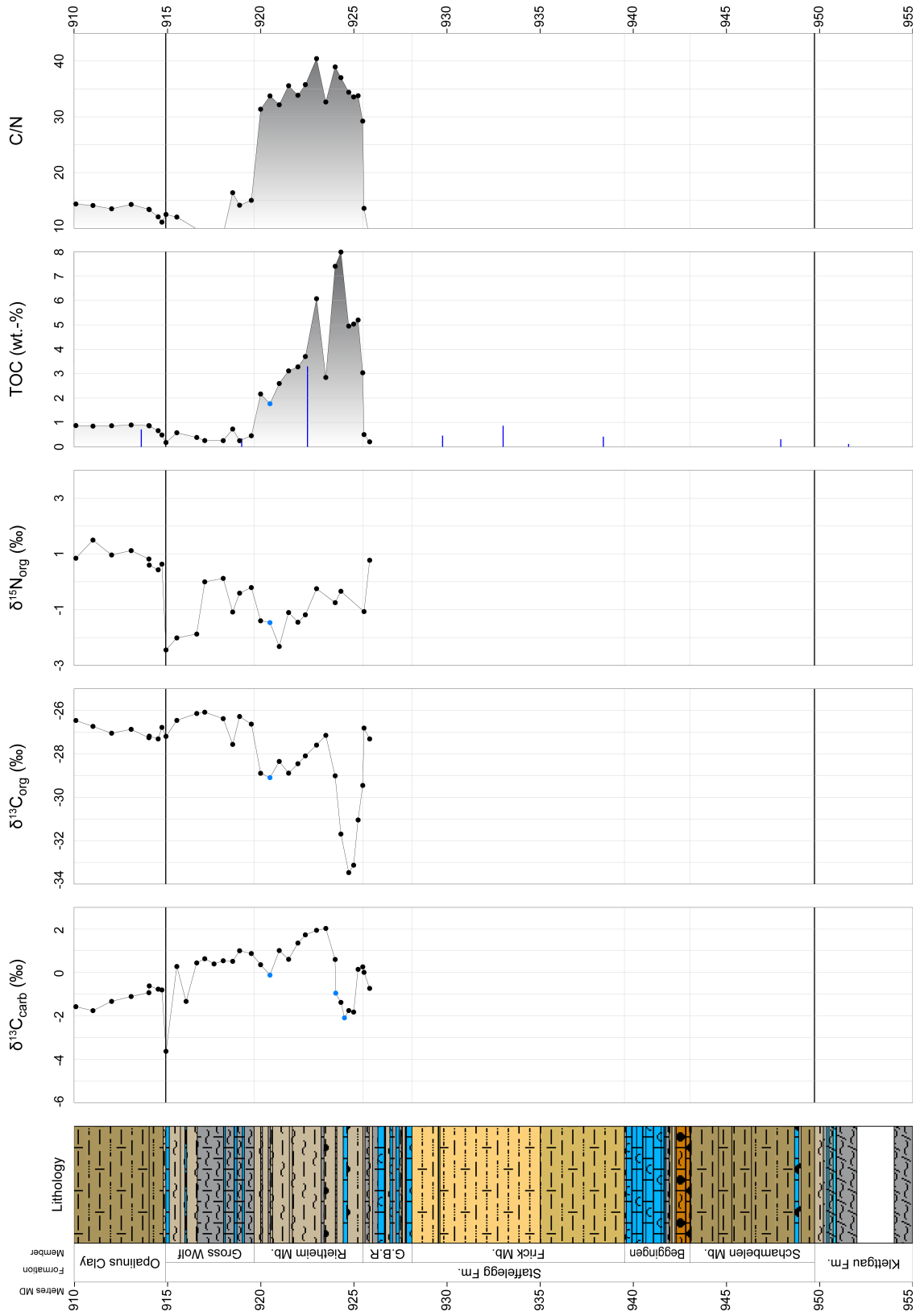

Fig. 3-3: Organic isotopic data from the Lias Group

Geochemical data from 925.85 – 910.08 m, additional explanations and references see text at the beginning of Section 3.4.

Lower part of the Dogger Group – mainly Opalinus Clay

The interval described in the following section, the lower part of the Dogger Group (the Opalinus Clay, the «Murchisonae-Oolith Formation» and the transition into the very condensed succession of the Wedelsandstein Formation and «Humphriesioolith Formation»), is also the interval at the main focus of these investigations (Figs. 3-4 and 3-5).

The semi-quantitative carbonate content (TCarb) values from the more homogeneous clay mineral-dominated lithologies are rather low and very stable compared to those from the underlying Staffelegg Formation (Fig. 3-4). In the lower three informal sub-units until 834.57 m the majority of the TCarb values range from 5 – 10 wt.-% with only a few more calcareous exceptions, the most striking of which is certainly at 876.77 m with 18.5 wt.-%. Upsection, the TCarb values document one major increasing trend up to the uppermost calcareous bed at 811.92 to 811.45 m with values up to 72.8 wt.-% (Appendix E1). The above following about 3 m, up to the top of the Opalinus Clay (808.34 m), are again remarkable less calcareous with TCarb values between 4.6 and 7.8 wt.-%. In the hanging «Murchisonae-Oolith Formation», two individual successions can be observed when looking at the TCarb contents: a lower one (808.09 – 798.00 m) with very variable values reaching up to 80.7 wt.-% at 798.00 m and an upper one (797.00 – 793.50 m) with very low TCarb values between 3.2 and 9.7 wt.-%. The above following condensed succession of the Wedelsandstein Formation and the «Humphriesioolith Formation» does not show a clear trend, also because the sampling density is not sufficient for this low thickness succession. The individual measurements depend very much on whether they were sampled from calcareous beds or from marly interlayers.

In the Opalinus Clay several calcareous beds can be observed and have been sampled (see also data in Appendix E1). Some of the samples analysed from these are classified as measurements from "hiatus beds" and calcareous or sideritic concretions. They are all illustrated in Figs. 3-4 and 3-6 by thicker light blue lines ending with blue dots marking the TCarb values. In addition to the blue values, also several septarian nodules were sampled, which are illustrated in violet (see Appendix E1 for data). The calcareous beds (marked in blue) comprise TCarb values that are typical for calcareous marl (50 – 75 wt.-%) and limestone (75 – 100 wt.-%). The septarian nodules (violet) can mainly be found in two specific intervals: the lower one between 901.87 m and 901.06 m and slightly above and the upper one between 827.81 m and 827.56 m. The lower one belongs to a level with typical calcareous concretions and septarian nodules in the «Clay-rich sub-unit», which can be correlated over several boreholes and siting regions (e.g. BUL1-1: Wohlwend et al. 2021a; TRU1-1: Wohlwend et al. 2021b; BOZ1-1: Wohlwend et al. 2022a).

The $\delta^{13}C_{carb}$ data reveal two negative CIE or negative intervals in the Opalinus Clay (Fig. 3-4): a lower negative CIE in the «Clay-rich sub-unit» and an upper CIE in the «Sub-unit with silty calcareous beds». The lower negative CIE is represented by a clear decreasing trend, reaching the most negative value (-5.9 ‰ at 902.00 m) just below the horizon with the calcareous concretions and septarian nodules between 901.87 m and 901.06 m. The above following increasing trend, documented in the $\delta^{13}C_{carb}$ data, shows a turning point almost coinciding with the transition from the «Clay-rich sub-unit» to the hanging «Mixed clay-silt-carbonate sub-unit». During the «Mixed clay-silt-carbonate sub-unit» the $\delta^{13}C_{carb}$ values fluctuate around 0 ‰ with ± 1 ‰ and with some larger outliers. Trough the «Upper silty sub-unit» the C-isotope data document a slight decrease to values around -0.5 ‰. In the «Sub-unit with silty calcareous beds», as mentioned above, an upper negative CIE can be observed with the most negative value of -5.2 ‰ at 828.90 m. The upper CIE is somehow bounded by two calcareous beds, which are located at: 829.26 – 829.00 m and 825.59 – 825.39 m (*cf.* Dossier III). From 825.00 m to the top of the Opalinus Clay the $\delta^{13}C_{carb}$ values show rather stable values, varying between -2.0 and -1.0 ‰. Crossing the lithological boundary to the hanging «Murchisonae-Oolith Formation», the $\delta^{13}C_{carb}$ data jump to a

mean value slightly below 0 ‰ and are slightly more positive to the top of the very calcareous interval (up to 798.00 m). In the hanging very monotonous and argillaceous succession an additional negative CIE can be observed with the most negative value of -4.0 ‰ at 795.00 m. Upsection, the $\delta^{13}C_{carb}$ values increase again and range between -1.0 and 0 ‰.

The $\delta^{13}C_{carb}$ data from the calcareous beds and/or bored and reworked intraclasts document possibly an early diagenetic signal (e.g. Wetzel & Allia 2000). The calcareous concretions and septarian nodules between 901.87 m and 901.06 m and at 826.30 m are the only macroscopic features with very negative $\delta^{13}C_{carb}$ values (-21.4 to -32.1‰, Appendix E1). However, very fine authigenic calcite was probably also precipitated in the very fine primary porosity of the Opalinus Clay as well as in the upper part of the «Murchisonae-Oolith Formation», which would lead to the more negative $\delta^{13}C_{carb}$ values in the lower and upper negative CIE in the Opalinus Clay and the CIE above (see also diagenetic discussion in Wohlwend et al. 2016).

The $\delta^{13}C_{org}$ data (Fig. 3-5) show a different picture compared to the $\delta^{13}C_{carb}$ values. The curve is above the negative shifts at the base relatively stable with a slight increasing trend for the middle to upper part of the Opalinus Clay. The formation of the Opalinus Clay can be subdivided, based on $\delta^{13}C_{org}$ values, into three subintervals: The lowest interval (914.70 – 896.00 m) can be described from the base of the Opalinus Clay and includes the three progressively more negative CIE (-27.3‰ at 914.50 m, -27.3 ‰ at 906.00 m and -28.3 ‰ at 899.50 m). The most negative $\delta^{13}C_{org}$ value at 899.50 m is 2.5 m above the most negative $\delta^{13}C_{carb}$ value at 902.00 m. As already mentioned above, the most part in the middle (896.00 – 812.00 m) is very stable and documents a slight +1.2 ‰ increasing trend from around -27.3 ‰ to values around -26.1 ‰. The upper interval (811.93 – 808.50 m) is easily observed as the $\delta^{13}C_{org}$ data is slightly shifted to more positive values and includes a prominent positive peak at 811.84 m with a $\delta^{13}C_{org}$ value of -24.9 ‰. The peak value was analysed from the sample taken from the uppermost calcareous bed (811.92 – 811.45 m) in the «Sub-unit with silty calcareous beds». The whole upper part until the top of the Opalinus Clay, as well as into the hanging «Murchisonae-Oolith Formation», shows a positive trend reaching the most positive value with -24.3 ‰ at 800.01 m. The $\delta^{13}C_{org}$ data from the condensed succession of the Wedelsandstein Formation and the hanging «Humphriesioolith Formation» document a clear decreasing trend, reaching the most negative value of -27.2 ‰ just above the scale of Fig. 3-5 (see also Fig. 3-7) at 788.99 m within the uppermost part of the «Humphriesioolith Formation».

The TOC as well as the C/N ratio will be discussed in the same paragraph. Both proxies document rather stable conditions throughout the lower part of the Opalinus Clay into the lowermost part of the «Upper silty sub-unit» at 841.00 m (TOC: ~ 0.8 – 1.0 wt.-%, C/N ratio ~ 15). From 840.00 m upwards, the C/N ratio starts to increase, reaching a first peak value of 20.3 at 835.01 m and a second shift to a ratio above 21.3 at 825.00 m just above the calcareous bed between 825.59 m and 825.39 m. With the same sample at 825.00 m the TOC reaches a maximum value of 1.4 wt.-%. In the upper part of the «Sub-unit with silty calcareous beds» both proxies show similar decreasing trends until the calcareous bed between 811.92 m and 811.45 m. Just above the before mentioned calcareous bed (811.92 – 811.45 m) the TOC and the C/N ratio reach again very positive values at 811.03 m (TOC: 1.5 wt.-%, C/N ratio 23.8) In the «Murchisonae-Oolith Formation» the same two times subdivision, as discussed above by the TCarb data, can be seen with the TOC dataset. The upper part (samples 797.00 m to 794.00 m) contains higher TOC values close to 1 wt.-% compared to the contents below reaching values between 0.1 and 0.4 wt.-%.

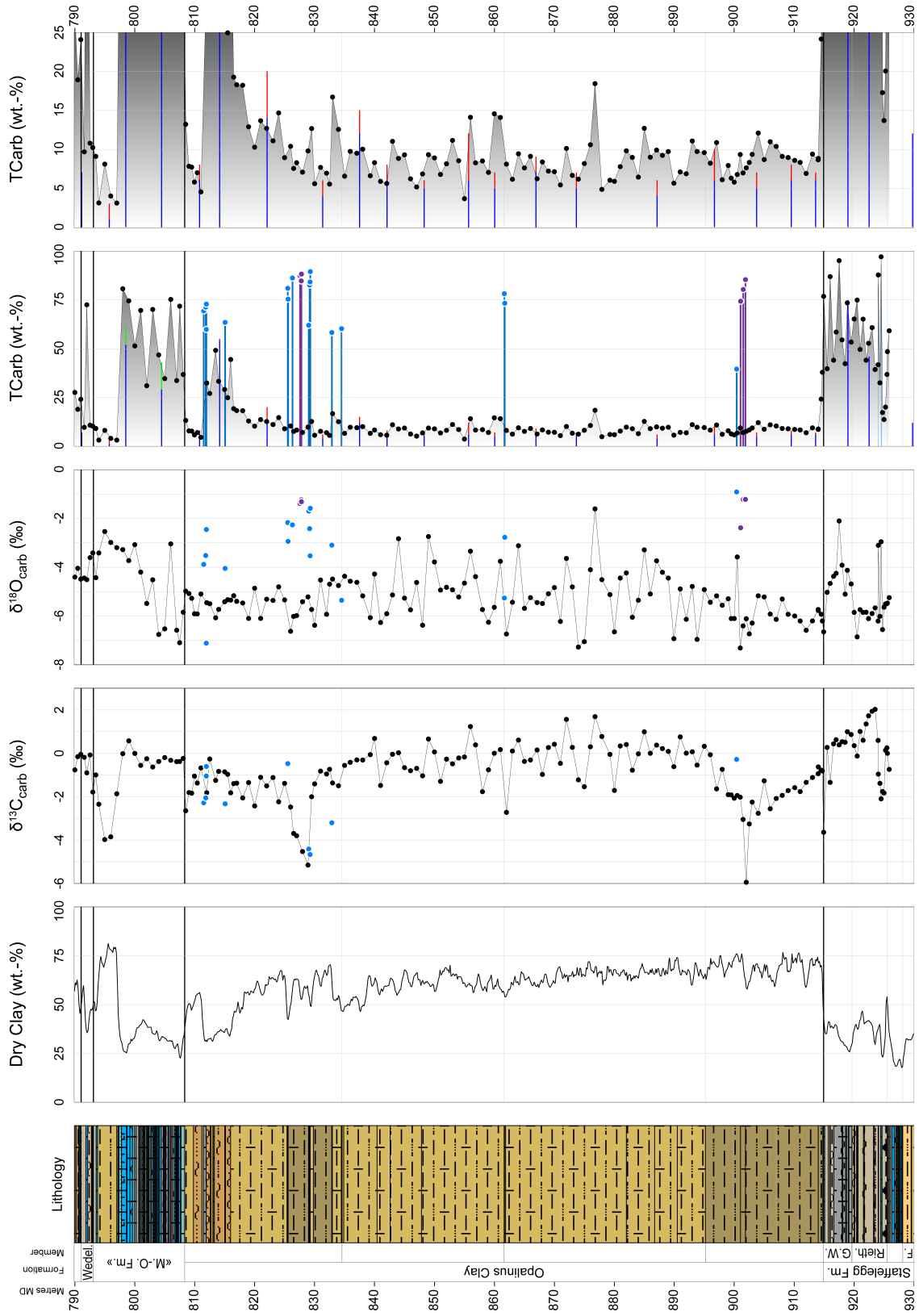

Fig. 3-4: Bulk rock (carb.) isotopic data from the lower Dogger Group – mainly Opalinus Clay

Geochemical data from 925.85 – 790.00 m, additional explanations and references see text at the beginning of Section 3.4.

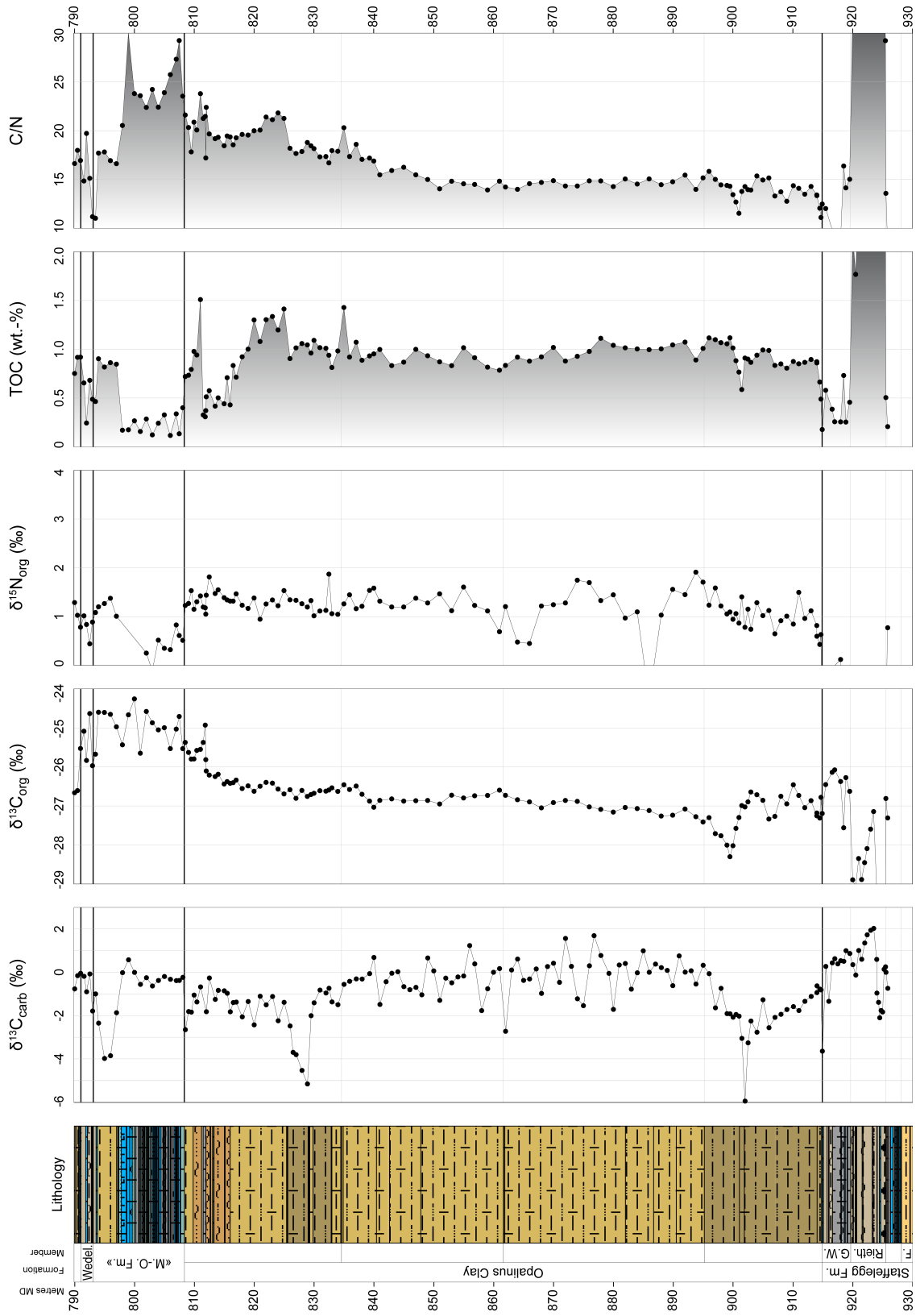

Fig. 3-5: Organic isotopic data from the lower Dogger Group – mainly Opalinus Clay

Geochemical data from 925.85 – 790.00 m, additional explanations and references see text at the beginning of Section 3.4.

Upper part of the Dogger Group

The following described interval, the upper Dogger Group («Murchisonae-Oolith Formation», condensed succession of the Wedelsandstein Formation and «Humphriesioolith Formation», «Parkinsoni-Württembergica-Schichten», Variansmergel Formation, Wutach Formation as well as the lower part of the Wildegg Formation) covers in time the whole Middle Aalenian to Middle Oxfordian substages (Figs. 3-6 and 3-7).

The semi-quantitative TCarb (Fig. 3-6) represents the alternation of silty claystone, argillaceous to calcareous marl and limestone. However, the TCarb contents are probably slightly underestimated because of the sampling strategy of not sampling every limestone bed (focus on the clay mineral-rich sediments). Nevertheless, the carbonate content curve reflects the inverse Dry Clay content curve (*cf.* Dossier X) and additionally shows where, besides clay minerals and carbonate, a siliciclastic component must also be present. As mentioned above, the «Murchisonae-Oolith Formation» can be divided into two parts: a lower calcareous and an upper represented by very low TCarb values. The Wedelsandstein Formation and the «Humphriesioolith Formation» are both very condensed in the drilling of BAC1-1, both together only reach a thickness of a good 4 m. In the above following «Parkinsoni-Württembergica-Schichten» there is a more calcareous interval present with the samples between 784.00 m and 781.00 m. In the upper half of the formation the TCarb values vary with values below and above 25 wt.-%. Only with the sediments from the Effingen Member of the Wildegg Formation a more calcareous succession is reached with values mainly above 50 wt.-%.

Although the oxygen isotope data were not discussed until now (too vulnerable to diagenetic overprint in the low-carbonate sediments), the $\delta^{18}O_{carb}$ values show an interesting trend in the here discussed succession (Fig. 3-6). Coming from the Opalinus Clay the $\delta^{18}O_{carb}$ data show more positive values until reaching the lower part of the «Parkinsoni-Württembergica-Schichten». The interval from 778.00 m to 743.00 m are, compared to the rest of the succession, very stable and lie mainly between -4.0 ‰ and -5.0 ‰.

The $\delta^{13}C_{carb}$ data (Figs. 3-6 and 3-7) indicate several quite stable intervals, mainly with a slight increasing trend, interrupted by two clear negative intervals. The lower negative interval was already discussed and can be found in the upper part of the «Murchisonae-Oolith Formation», as it is documented by the samples from 797.00 m to 794.00 m. The second and upper one is situated in the lower part of the «Parkinsoni-Württembergica-Schichten» between 782.90 m and 781.00 m. The more negative values were analysed from the three samples with enriched TCarb values, which are between 50 and 75 wt.-%. Above there is one outlier at 774.00 m with a $\delta^{13}C_{carb}$ value of -1.8 ‰, before the isotope data show a very narrow range and an increase from -0.7 ‰ to 0.6 ‰ through the middle and upper part of the «Parkinsoni-Württembergica-Schichten». The lower two of the three samples taken from the iron-ooid rich succession of the Wutach Formation (738.00 m and 737.53 m) document values close to +0.1 ‰, the third at 737.36 m, which is 21 cm below the top of the formation, already +0.7 ‰. The $\delta^{13}C_{carb}$ data from the following Wildegg Formation document an increasing trend which is already at 736.62 m above +2.0 ‰. The several per mil positive shift to values around +3.2 ‰ at 734.75 m is typical for the Callovian / Oxfordian boundary and was already documented by Rais et al. (2007) in other locations as well as the Weiach borehole and was for example also documented during this campaign in the BUL1-1 borehole (Wohlwend et al. 2021a). The most positive $\delta^{13}C_{carb}$ values were documented in the Middle Oxfordian (Transversarium Zone; see Rais et al. 2007).

The $\delta^{13}C_{org}$ data (Fig. 3-7) as briefly mentioned continues the rising trend from the uppermost part of the Opalinus Clay into the «Murchisonae-Oolith Formation». One sample from the Wedelsandstein Formation (-24.6 ‰ at 792.54 m) shows a similar more positive value as the uppermost samples from the underlying formation. However, the three samples 790.50 m, 790.00 m and

788.99 m from the «Humphriesioolith Formation» are clearly shifted to more negative values (-26.6 ‰, -26.7 ‰ and -27.2 ‰). The lowermost four samples from the «Parkinsoni-Württembergica-Schichten» (787.96 – 785.00 m) again document a slight increase to -26.0 ‰ before the isotopic data are clearly shifted a second time to more negative values (-27.0 ‰ at 784.00 m). The $\delta^{13}C_{org}$ data document a smooth negative trend, reaching the most negative value of -28.0 ‰ at 764.00 m, before the data increase again to the top of the «Parkinsoni-Württembergica-Schichten» (-26.6 ‰ at 742.01 m). One sample from the Wutach Formation (738.00 m) shows a quite negative value of -27.9 ‰. However, the other two (737.53 m and 737.36 m) are clearly more positive (-25.3 ‰ and -25.8 ‰). Like the $\delta^{13}C_{carb}$ data, the $\delta^{13}C_{org}$ data from the hanging Wildegg Formation also document the very striking positive shift close to the Callovian / Oxfordian boundary. Though, the most positive values are reached lower in the formation (-23.7 ‰ at 736.62 m and -23.6 ‰ at 736.50 m). Maybe, the two more positive values are the result of an incomplete decarbonatisation of ankerite and/or other iron-carbonates which would shift the isotopic data to more positive values. An additional, or second round of decarbonatisation at 70° C was not performed, as it was done with earlier questionable higher values (e.g. BOZ1-1; Wohlwend et al. 2022a). The $\delta^{13}C_{org}$ data stay at a more positive level up to 733.50 m (-24.4 ‰) and then decrease with the uppermost two analysed samples at 732.50 m and 732.15 m to a value of -25.6 ‰.

Both the C/N ratio and the TOC show less clear trends, except for the already discussed jump in the «Murchisonae-Oolith Formation» from the calcareous lower to the more argillaceous upper part. The slightly higher TOC values seem to last until the sample taken at 785.00 m. The calcareous interval in the lower «Parkinsoni-Württembergica-Schichten» also shows a lower TOC content (0.2 wt.-% at 782.90 m). Similar to the TCarb trend in the «Parkinsoni-Württembergica-Schichten» the TOC shifts to lower values in the upper half from 761.00 m upwards. The trend to lower TOC contents also continues in the lower part of the Wildegg Formation.

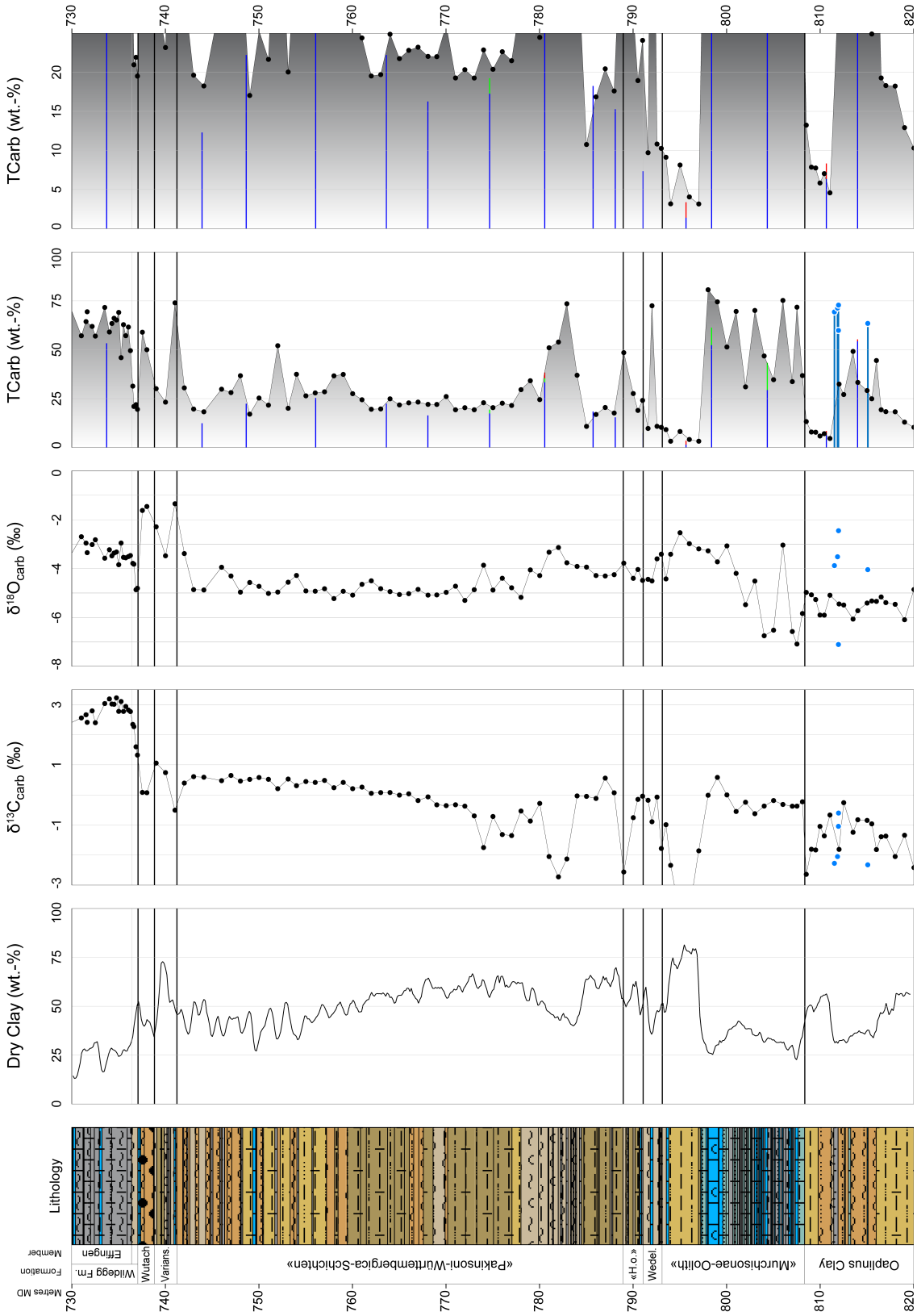

Fig. 3-6: Bulk rock (carbonate) isotopic data from the upper part of the Dogger Group

Geochemical data from 820.00 – 730.00 m, additional explanations and references see text at the beginning of Section 3.4.

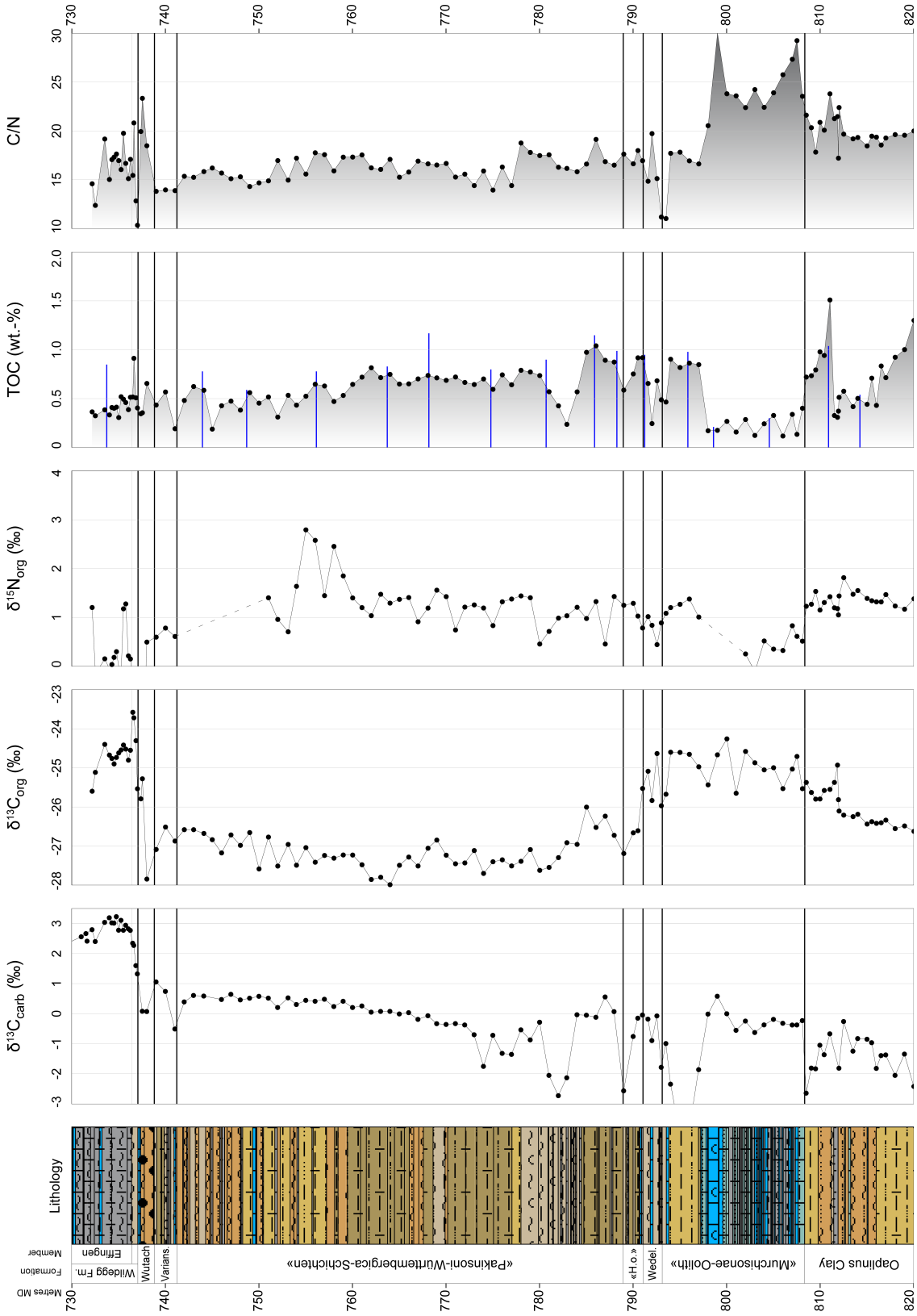

Fig. 3-7: Organic isotopic data from the upper part of the Dogger Group

Geochemical data from 820.00 – 730.00 m, additional explanations and references see text of Section 3.4.

Cored interval of the Malm Group

The following described interval, the whole cored interval of the Malm Group (Wildegg, Villigen and Schwarzbach Formations as well as the lower part of the «Felsenkalke» and «Massenkalk»), covers in time the Middle Oxfordian to Late Kimmeridgian substages (Fig. 3-8).

The semi-quantitative TCarb (Fig. 3-8) represents the more calcareous succession of the Malm Group. The majority of the TCarb contents of the Wildegg Formation range between 50 wt.-% and 75 wt.-% with mainly two exceptions. The three samples at 686.50 m, 686.00 m and 684.33 m were taken from the very striking light limestone beds with the lower one ending with a bored hardground (*cf.* Dossier III). The sampled interval between 673.00 m and 666.00 m clearly documents a calcareous interval within the Effingen Member, it can be correlated with the Gerstenhübel Bed (671.82 – 665.88 m; *cf.* Dossier III). The lower TCarb values nicely represent the different lithology of the Schwarzbach Formation within the overall very calcareous Malm Group. To summarise, the TCarb curve reflects the inverse Dry Clay content curve (*cf.* Dossier X), whereby the values have turned out to be rather calcareous.

The $\delta^{18}O_{carb}$ data somehow reflects the carbonate content. The very calcareous or just limestone intervals tend to have slightly lower values as the marlier ones, which can be seen by the interval from the Gerstenhübel Bed, as well as from the varying lithologies at the base of the combined succession of the «Felsenkalke» and «Massenkalk». The mainly silty marl succession (530.51 – 525.63 m; *cf.* Dossier III) is represented by the four samples between 530.00 m and 526.00 m. The interval corresponds to the «Glauconitic Marker Bed» after Gygi (2000). The boundary between the Küssaburg and the Wangental Members, which is formed by the «Knollen Bed» (589.52 – 589.42 m; *cf.* Dossier III) can also be seen in the $\delta^{18}O_{carb}$ data. Around the boundary the isotopic data were shifted from -3.1 ‰ to -4.1 ‰.

The $\delta^{13}C_{carb}$ data provides a few specific variations which probably could be used for further chemostratigraphic correlation within the Late Jurassic period (Wohlwend et al. 2022b). In the lowermost interval of the Wildegg Formation the Plicatilis/Transversarium positive excursion after Rais et al. (2007) is visible (+3.2 ‰ at 734.75 m). In the middle part of the Effingen Member the $\delta^{13}C_{carb}$ data were shifted to more negative values (+2.1 ‰ at 686.50 m) within the limestone beds with the bored hardground (687.30 – 686.00 m). In the upper part of the Effingen Member the $\delta^{13}C_{carb}$ data document a negative trend up to the top. Whereas the samples taken from the Villigen Formation (Hornbuck Member) have 0.3 to 0.4 ‰ more positive values, which even increase within the Küssaburg Member to nearly +3.0 ‰. The lithological change into the Wangental Member, as well as the top of the Villigen Formation, are both represented by a change in the $\delta^{13}C_{carb}$ data. The Schwarzbach Formation and the succession above are more negative than the Villigen Formation. The «Glauconitic Marker Bed» is also visible with the $\delta^{13}C_{carb}$ data, whereby they are more positive than the underlying succession (+2.6 ‰ at 530.00 m).

The hanging succession above the «Glauconitic Marker Bed» is documented by the $\delta^{13}C_{carb}$ data with an extreme negative shift. The sample taken from the lower part of the «Glauconitic Marker Bed» at 530.00 m has an isotopic value of +2.6 ‰, the one from the upper part at 526.88 m shows a value of +2.1 ‰. The following three samples 560.00 m, 525.00 m and 524.00 m document a decrease to already 0.5 ‰. However, this is not the whole scope of the negative trend. The above following values are all out of scale. The most negative one reaches -2.5 ‰ at 519.00 m and the uppermost sample taken at the top of the cored interval at 517.16 m has a $\delta^{13}C_{carb}$ value of -1.8 ‰. One possible explanation is that the interval above the «Glauconitic Marker Bed» may have undergone some dolomitisation and therefore the $\delta^{13}C_{carb}$ data is strongly shifted.

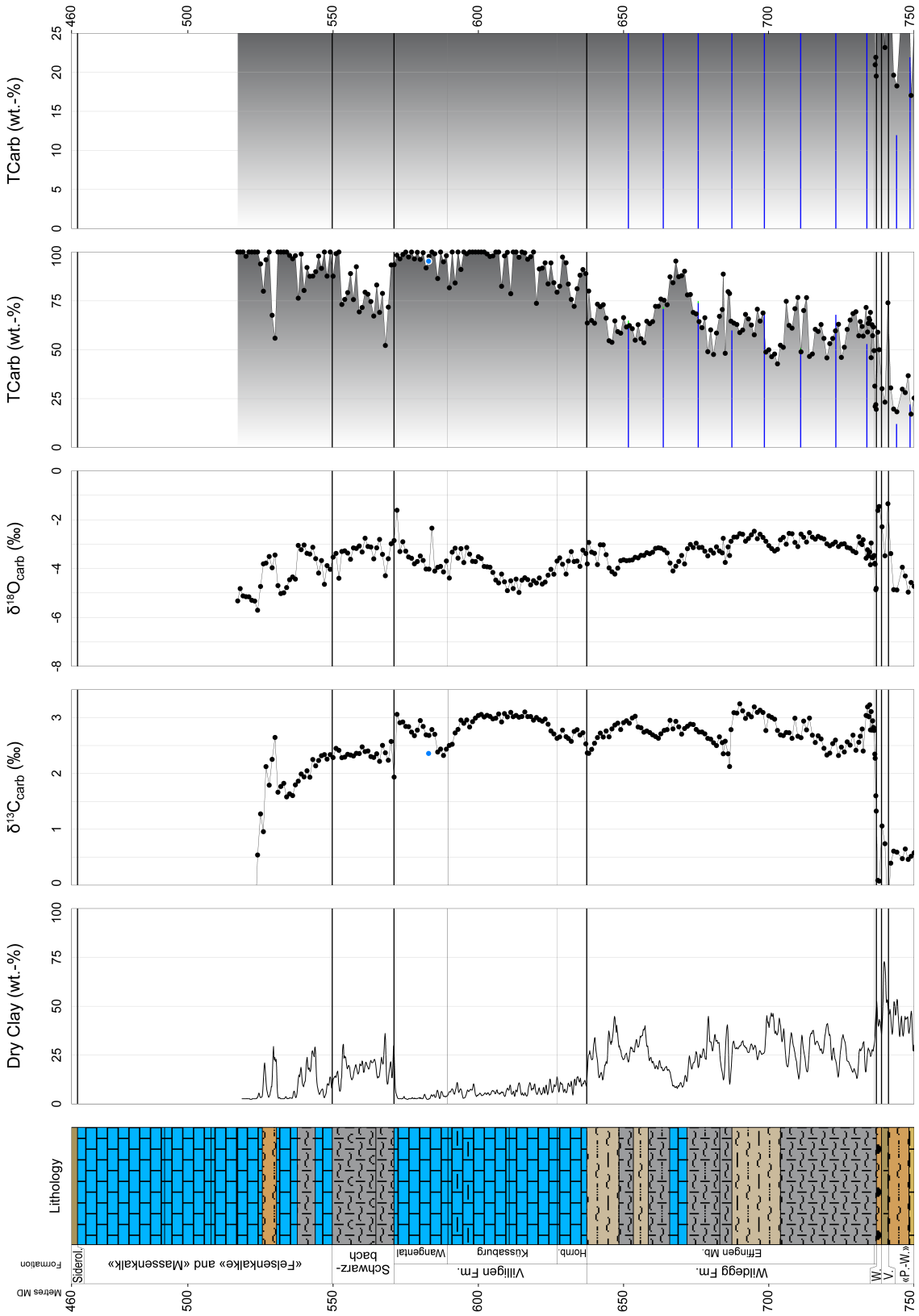

Fig. 3-8: Bulk rock (carbonate) isotopic data from the cored interval of the Malm Group

Geochemical data from 750.00 – 517.16 m, additional explanations and references see text at the beginning of Section 3.4.

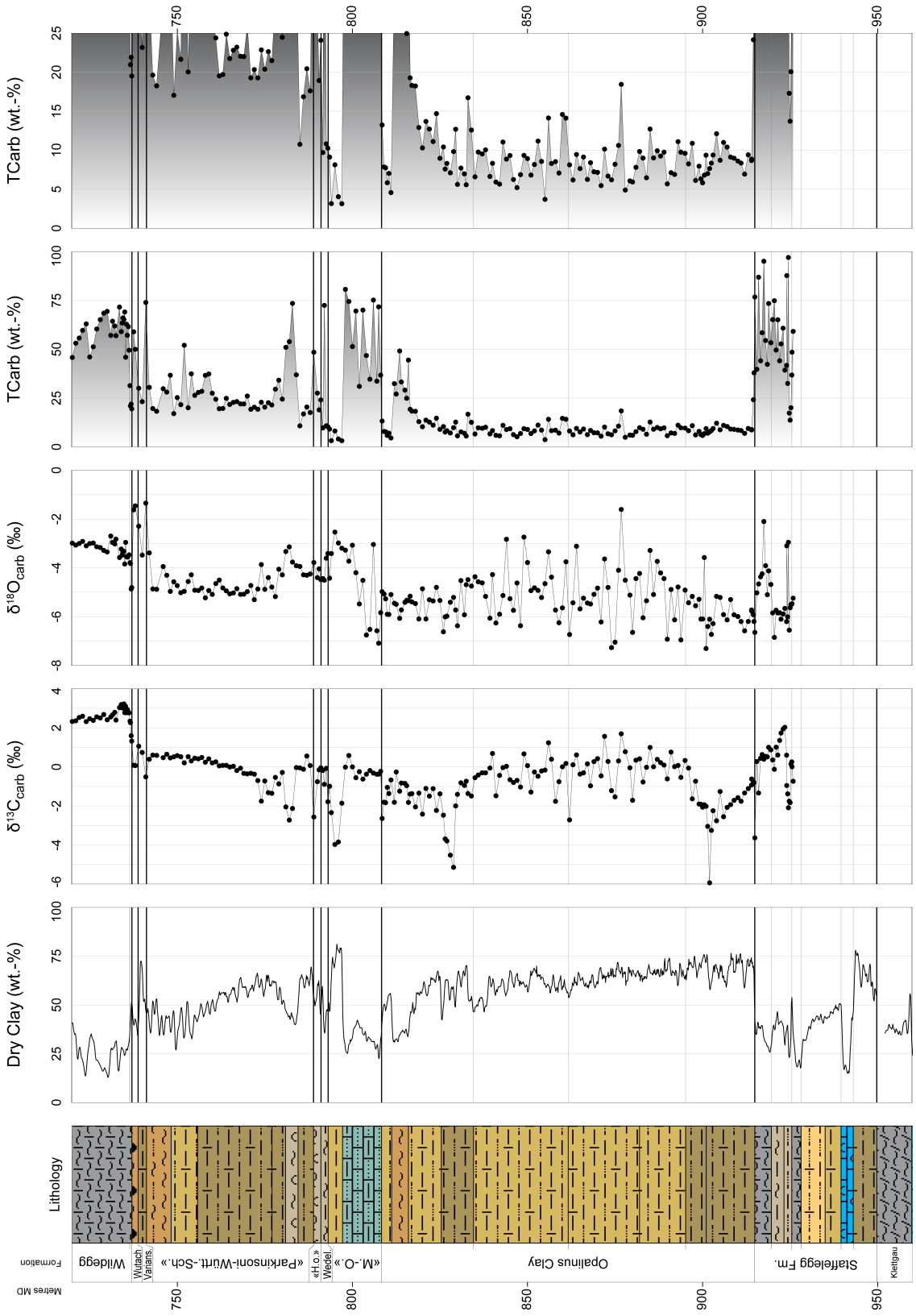

Fig. 3-9: Whole bulk rock (carbonate) isotopic data from the Lias and Dogger Groups

Geochemical data from 925.85 – 720.00 m, additional explanations and references see text at the beginning of Section 3.4.

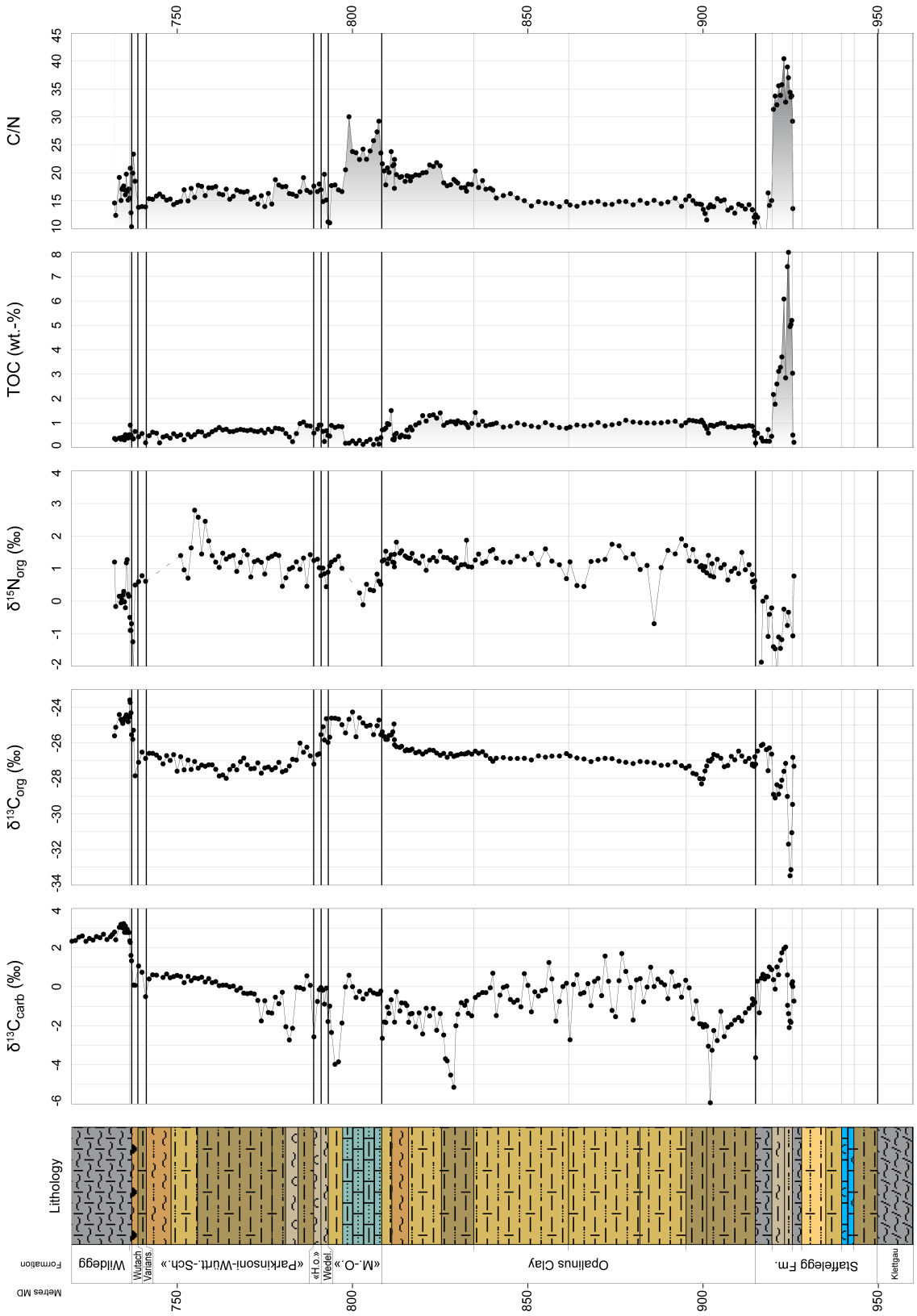

Fig. 3-10: Whole organic isotopic data from the Lias and Dogger Groups from BAC1-1

Geochemical data from 925.85 – 720.00 m, additional explanations and references see text at the beginning of Section 3.4.

4 Definition of specific lithostratigraphic boundaries

The boundaries between stratigraphical units, as also shown in the stratigraphical logs of the lithostratigraphy report (Dossier III), were mostly defined by using lithological criteria. According to the guidelines on stratigraphical nomenclature of Remane et al. (2005), the definition of lithostratigraphical units should be based, both vertically and horizontally, on lithological variations regardless of their age. In fact, the formation boundaries, as used by Nagra for the ongoing borehole campaign of Stage 3 of the Sectoral Plan for Geological Repositories (Jordan & Deplazes 2019), were not always obvious in the borehole and definitions were difficult to apply, either because of the small core diameter, because of differences in facies or strongly varying sedimentation rates and associated reduction or condensation. The exact location of some of the formation boundaries caused discussions during core description and the process of quality control. Most of the important data for questionable boundaries were already present before the data-freeze (11.07.2022) and were used for the log descriptions and drawings. In the following paragraphs, the underlying considerations are explained for providing a better understanding of how boundaries were demarcated, especially in the highly reduced successions of the Early Bajocian. We are aware of the fact that several boundaries are no longer based on lithological criteria alone and that chronostratigraphic criteria (ammonite, palyno- and chemostratigraphy) are included in the definitions.

Opalinus Clay (914.91 – 808.34 m)

The *lower boundary* of the Opalinus Clay is set at 914.91 m at the uppermost surface of a bed of limestone (argillaceous) from the underlying Staffelegg Formation, which is covered by a thin argillaceous marl layer followed by claystone (silty, calcareous) (*cf.* Dossier III). The lithological boundary is therefore evident above all in the carbonate content (TCarb: Figs. 3-2 and 3-4). The value decreases from 76.8 wt.-%, measured from the uppermost sample (914.92 m) of the Gross Wolf Member, to values of 38.0 and 24.2 wt.-% at 914.70 m and 914.50 m followed by values between 8.5 and 12.1 wt.-% in the basal Opalinus Clay (Fig. 3-2). The lithological change between the Gross Wolf Member and the Opalinus Clay is also visible in the slight increase in TOC from values mainly < 0.5 wt.-% to values mainly around 0.8 wt.-% in the lowermost Opalinus Clay (Fig. 3-5).

The described ammonites (Section 3.2, Appendices A2 and A3) document, that the lithological boundary is close to the Toarcian / Aalenian stage boundary. The two ammonites at 915.06 m and 914.72 m (both *Pleydellia* ex gr. *buckmani* (Maubeuge, 1947), the later questionable) yield Aalensis Zone (Torulosum Subzone). The second one is coming from the argillaceous marl just above the uppermost limestone bed, which is here lithologically defined as the basal bed of the Opalinus Clay. The lowermost provisionally determined *Leioceras* sp.? was found at 914.41 m (Appendix A3) and therefore just 0.5 m above the lithological boundary in the Opalinus Clay. The palynosample from 914.70 m also yields Aalensis Zone to Opalinum Zone (Opalinum Subzone). Therefore, the Toarcian / Aalenian stage boundary seems to be within this lowermost 0.5 m of the Opalinus Clay.

The *upper boundary* of the Opalinus Clay is set at 808.34 m at the base of a heterogenous succession of sandy to silty limestone and bioclastic limestone, which become more and more limonitic and iron-oolitic, both are intercalated by calcareous marl (*cf.* Dossier III). The boundary documents a clear change in lithology and coincides with the top of dark grey silty claystone, which is therefore also evident in the markedly higher carbonate content (TCarb) and is also supported by the analysis of FMI and GR logs in the hanging succession.

In BAC1-1 the uppermost calcareous bed (811.92 – 811.45 m) within the Opalinus Clay was quite rich in ammonites (811.90 m, 811.52 m and 811.50 m: *Leioceras* ex gr. *goetzendorfense*, 811.75 m: *Leioceras* sp.) With these determinations the bed can be dated as Bifidatum Subzone of the Opalinum Zone. The same dating derives from the two palynomorph samples (811.85 m and 811.55 m). The following four palynological samples (811.11 m, 808.08 m, 804.44 m and 802.95 m) are covering the lithological upper boundary of the Opalinus Clay. However, they cannot give a clear biostratigraphic resolution. The four samples were interpreted as Opalinum to Murchisonae Zone.

The positive chemostratigraphic shift or even jump in the organic C-isotopes within the uppermost calcareous bed (811.85 – 811.55 m), is typical for the Bifidatum Subzone of the Opalinum Zone (e.g. BUL1-1; Wohlwend et al. 2021a). The additional shift to even more positive $\delta^{13}C_{org}$ values at and above the lithological upper boundary of the Opalinus Clay also fits to similar shifts found in the same biostratigraphic intervals, mainly in the Murchisonae to Bradfordensis Zones. Although, in BUL1-1 the basal succession of the hanging «Murchisonae-Oolith Formation» is very condensed and therefore, the positive shift or trend is more compressed to a peak (Wohlwend et al. 2021a).

«Murchisonae-Oolith Formation» (808.34 – 793.11 m)

The *lower boundary* of the «Murchisonae-Oolith Formation» is set at 808.34 m at the base of a heterogenous succession of sandy to silty limestone and bioclastic limestone, which become more and more limonitic and iron-oolitic, both are intercalated by calcareous marl (*cf.* Dossier III). This succession overlies typical silty claystone from the Opalinus Clay and therefore, documents a clear change in lithology; see above for the detailed discussion about this boundary (upper boundary of the Opalinus Clay).

The *upper boundary* of the «Murchisonae-Oolith Formation», is defined at the subface of the «Sowerbyi-Oolith», which is per definition (Bloos et al. 2005) the basal bed of the hanging Wedelsandstein Formation (deposited during the Discites Zone). The 8 cm thick bed between 793.11 m and 793.03 m, with iron-ooids and an erosive base, may correlate with the "Austern-pflaster" of Weiach (539.17 – 538.85 m; Matter et al. 1988, Beilage 6.2b and Bläsi et al. 2013). Both "event-beds" can likely be linked to the «Sowerbyi-Oolith». Therefore, the top of the «Murchisonae-Oolith Formation» is set at the erosional surface at 793.11 m. However, the bio-clastic limestone bed between 793.82 m and 793.55 m shows in the upper part (793.67 – 793.55 m), with the oncoids, bored intraclasts and dispersed iron-ooids also a great similarity with the 15 cm thick bed between 786.85 m and 786.70 m in STA2-1 forming there the base of the Wedelsandstein Formation. A definition solely on lithological criteria is not unambiguous.

The lower age of the «Murchisonae-Oolith Formation» is interpreted by palynomorphs as Opalinum to Murchisonae Zone (see discussion above). The first palynological sample with a clearly Middle Aalenian age has been taken at 800.94 m (Murchisonae Zone). Unfortunately, no ammonites were found in the calcareous part of the «Murchisonae-Oolith Formation». The argillaceous interval in the hanging of that striking, reddish impregnated succession has been dated to Bradfordensis Zone by two samples (796.99 m and 793.91 m). The age of the uppermost part and the slightly questionable upper boundary can be narrowed by an ammonite at 793.26 m (*Hyperlioceras* sp.) and the two palynological samples taken at 793.13 m and 792.89 m. The two later samples were interpretated as Concavum Zone (793.13 m) and Discites Zone (792.89 m), whereas the ammonite yields Concavum or Discites Zone (probably Discites Zone). Therefore, the biostratigraphically defined ages were also considered and thus support the definition of the upper limit at 793.11 m dating into the Early Bajocian.

Wedelsandstein Formation (793.11 – 791.05 m)

The *lower boundary* of the Wedelsandstein Formation is set at the subface of the 8 cm thick iron-ooid bearing bed (793.11 – 793.03 m), which is believed to correspond to the «Sowerbyi-Oolith» and therefore defines the base of the Wedelsandstein Formation (German Stratigraphic Scheme; Bloos et al. 2005). See more details and the discussion about the boundary above (upper boundary of the «Murchisonae-Oolith Formation»).

The *upper boundary* of the Wedelsandstein Formation is set at 791.05 m at the base of an irregular, nodular 4 cm thick horizon consisting of iron-oolitic, bored and encrusted, micritic intraclasts, surrounded by a bioclastic calcareous marl. The boundary coincides with the onset of iron-ooids in the above following formation (*cf*. Dossier III). The stratigraphically following «Humphriesioolith Formation» in the hanging of the Wedelsandstein Formation is defined by the occurrence of iron-ooids and/or limonitic components.

However, a definition solely on lithological criteria is not unambiguous because the here defined Wedelsandstein Formation only reaches a thickness of approximately 2 m, which is in comparison to other drillings in the siting region of Nördlich Lägern extremely thin indicating very reduced sedimentation rates. Comparing the Wedelsandstein Formation in the more expanded drillings in Nördlich Lägern, the succession can always be subdivided by a calcareous horizon including a hardground at the top (e.g. STA2-1: 783.10 m; Wohlwend et al. 2022d or STA3-1: 760.86 m; Wohlwend et al. 2022c). The same subdivision may correspond to the limestone bed with the hardground top at 791.84 m.

For the identification of lithostratigraphic units in this interval in BAC1-1, additional information such as biostratigraphic dating has to be considered. This argument was also the reason for the very dense palynological sampling in this interval in question. From the approximately 2 m thin succession of the Wedelsandstein Formation four samples have been taken. They all show a clear younging from base to top: Discites Zone (792.89 m), Ovale Zone (792.55 m) and Laeviuscula Zone (791.67 m, 791.12 m). The proposed hardground horizon at 792.14 m to 791.84 m also seems to be at the limit between Ovale and Laeviuscula Zone as it is in other drillings. The sample taken from the above following iron-oolitic succession (at 790.55 m) is already interpreted as Humphriesianum Zone, which is not unusual, because during the Humphriesianum Zone mainly iron-oolitic successions were deposited. So, the onset of the iron-oolitic succession at 791.05 m seems to be a reasonable location for the boundary between the Wedelsandstein Formation and the «Humphriesioolith Formation».

«Humphriesioolith Formation» (791.05 – 788.92 m)

The *lower boundary* of the «Humphriesioolith Formation» is set at 791.05 m at the base of an irregular, nodular 4 cm thick horizon (measured on the yellow line on the core, otherwise up to 10 cm thick) consisting of iron-oolitic, bored and encrusted intraclasts, which are surrounded by a bioclastic calcareous marl. The onset of iron-ooids and iron-oolitic intraclasts defines the lithological lower boundary of the «Humphriesioolith Formation». The deposition of an iron-oolitic succession seems to be contemporaneous to other drillings, occurring during the Humphriesianum Zone. See more detailed discussion for the boundary above (upper boundary of the Wedelsandstein Formation).

The *upper boundary* is set at 788.92 m, where bioclastic argillaceous marl, rich in belemnites and crinoids, is overlain by claystone (silty, calcareous) without larger fossils (*cf*. Dossier III). The upper boundary is differing from the solely lithological definition by the on- and offset of iron-ooids and/or limonitic components. If one were to follow only the presence of iron-ooids, the

upper limit would have to be defined at 790.75 m. The thickness would then only be 30 cm, consisting of a horizon with iron-oolitic intraclasts (791.05 – 791.01 m) and an overlying iron-oolitic limestone bed (790.90 – 790.75m). The thin section taken from the above following bioclastic interval (BAC1-1-789.14) documents a bioclastic limestone of 38 vol.-% echinoderm skeletal elements, 5 vol.-% bivalves and 2 vol.-% other biogenes. This bioclast-rich interval up to 788.92 m is integrated into the «Humphriesioolith Formation». A definition solely on lithological criteria is not unambiguous and additional information from the palynomorph dating has been integrated (see detailed discussion below).

As mentioned before, the extremely reduced sedimentation rate in combination with differing lithologies, makes the lithostratigraphic grouping into formations very challenging and without additional information such as biostratigraphy (i.e. time control) hardly feasible. Because no ammonites are present in this interval, all the age information is based on the palynological interpretation. The samples taken at 790.55 m and 789.67 m are interpreted Humphriesianum Zone. The following five samples (789.36, 789.06, 788.89, 788.41, 787.07 m) are dated Niortense Zone. Therefore, the iron-oolitic succession between 791.05 m and 790.75 m was deposited during the Humphriesianum Zone, the above following bioclastic succession (until 788.92 m) still during the later Humphriesianum Zone and mainly during the earlier Niortense Zone. The biostratigraphic data together with the lithological changes allow a shift of the upper boundary to the offset of the bioclastic interval (mainly crinoids). However, in comparison to surrounding drillings, the iron-oolite or iron-oolitic succession of the «Subfurcaten-Oolith» was not deposited.

An even higher upper boundary for the formation was also discussed. The interval between 784.48 m and 780.90 m is dominated by bioclastic argillaceous and calcareous marl with several horizons of limonitised bioclasts (in Dossier III also marked with disperse iron-ooids). The interval is also represented with higher values in the TCarb log (Fig. 3-6) as well as in the FMI and GR logs. The thin section BAC1-1-781.44 was taken to test the occurrence of iron-ooids. The sample only contains limonitic bioclasts (echinoderms and bivalves: 15 vol. %) and limonitic matrix (18 vol. %). The striking thing is the occurrence of calcitic ooids (4 vol. %, Fig. B-18) with an outer microbial rim, like the ones from the Hauptrogenstein in BOZ1-1 and the quarry in Auenstein (Figures B-14 and B-15 in Wohlwend et al. 2022a and Figure 5F in Wetzel et al. 2013). Some of the ooids show presumed coral fragments as nuclei (Fig. B-18). The first impression was to correlate the interval with the «Parkinsoni-Oolith». The palynological samples covering that interval (784.54, 784.10, 781.44, 780.58 m) were interpreted as Niortense to Parkinsoni Zone. The temporal interpretation does not directly confirm the correlation, but the interpretation range does allow the correlation. There is also the possibility that the calcareous ooids are a very distal swell from the Hauptrogenstein platform, analogous to the calcareous ooids in the Klingnau Formation («Subfurcaten-Schichten» and «Untere Parkinsoni-Schichten»; Wohlwend et al. 2019a) or that they were eroded from another smaller platform nearby, perhaps in combination with the drowning of the «Herrenwis Unit», which probably already happened during the Humphriesianum Zone. An additional information is coming from the $\delta^{13}C_{org}$ data (Fig. 3-7). The negative shift, happening during the calcareous interval, from 785.00 m (-26.0 ‰) to 780.00 m (-27.6 ‰) is similar to the one observed in STA2-1 at the base of the «Parkinsoni-Württembergica-Schichten» (-26.8 ‰ at 767.39 m to -28.0 ‰ at 766.00 m; Wohlwend et al. 2022d) and can also be linked to Weiach (-25.7 ‰ at 520.57 m to -27.8 ‰ at 516.00 m; Wohlwend unpublished data). The probably same negative shift documented in the three drillings supports the correlation of the interval between 784.48 m and 780.90 m in BAC1-1 to the lower part of the «Parkinsoni-Württembergica-Schichten». Therefore, the upper boundary of the «Humphriesioolith Formation» at 788.92 m seems to be feasible.

However, the above discussed delimitation of the upper boundary of the «Humphriesioolith Formation» could also be drawn slightly deeper in BAC1-1 when looking at the cores of Weiach and the definition by Bläsi et al. (2013): «Humphriesioolith Formation» from 523.25 m to 520.29 m. There, the hardground at the top of the «Humphriesioolith Formation» at 520.29 m is overlain by a 5 cm thick layer rich in crinoid stems, oysters and belemnites. Belemnite-rich and up to 15 cm thick horizons can also be found in the interval between 519.40 m to 517.00 m (Matter et al. 1988). At around 518.34 m an up to 10 cm thick calcareous bed or nodular bed is represented in Weiach which is probably of a diagenetic origin, probably a septarian nodule. A similar horizon can probably also be seen in BAC1-1 between 789.53 m and 789.37 m. The calcite veins in the upper part led to an interpretation of a septarian nodule. Combining all these information, the interval in BAC1-1 from 790.75 m to 788.92 m (here included into the «Humphriesioolith Formation») may correlate to the interval in Weiach from 520.29 m to 517.00 m (basal part of the «Parkinsoni-Württembergica-Schichten»).

5 Conclusion

The present study documents data on microfacies analysis, ammonite stratigraphy and palyno-stratigraphy as well as detailed geochemical analyses (C, O and N isotopes). With this data collection, it was possible to predict the delimitation of the Mesozoic strata more accurately. Most of the important data for the boundaries in question were already present at the data-freeze (11.07.2022). Therefore, the present report complements the lithostratigraphic report of Dossier III for the deep borehole Bachs-1-1. The lithological boundaries, and therefore the stratigraphic profile, were mostly defined by lithological criteria. Nevertheless, the customary formal and informal formation boundaries were not always obvious in the drill cores, either because of the small core diameter or changing facies conditions. The exact location of specific formation boundaries led to discussions requiring additional data to determine the exact profile description and illustration. We are aware that certain boundaries are thus no longer based solely on lithological criteria, and that the definitions therefore also include chronostratigraphic criteria (ammonite stratigraphy, palyno- and chemostratigraphy).

6 References

Bathurst, R.G.C. (1975): Carbonate sediments and their diagenesis (2nd ed.), Developments in Sedimentology, Amsterdam, Elsevier, 658 pp.

Bläsi, H.R., Deplazes, G., Schnellmann, M. & Traber, D. (2013): Sedimentologie und Stratigraphie des 'Brauner Doggers' und seiner westlichen Äquivalente. Nagra Arbeitsbericht NAB 12-51.

Bloos, G., Dietl, G. & Schweigert, G. (2005): Der Jura Süddeutschlands in der Stratigraphischen Tabelle von Deutschland 2002. Newsletters on stratigraphy 41, 263-277.

Branco, C.W. (1879): Beiträge zur Entwickelungsgeschichte der fossilen Cephalopoden, Theil I: Die Ammoniten. Palaeontographica 26, 15-50.

Buckman, S.S. (1887 – 1907): A Monograph of the ammonites of the Inferior Oolite Series. Palaeontographical Society Monographs, London, The Palaeontographical Society, 456 pp.

Buckman, S.S. (1923 – 1925): Yorkshire Type Ammonites/Type Ammonites, 5. London (Wheldon & Wesley), 302 pp.

Cariou, E. & Hantzpergue, P. Coord. (1997): Biostratigraphie du Jurassique ouest-européen et méditerranéen: zonations parallèles et distribution des invertébrés et microfossiles. Bull. Centre Rech. Elf Explor. Prod.

Dickson, J.A. (1965): Modified staining technique for carbonates in thin section. Nature 205, 587.

Dietze, V., Gräbenstein, S., Franz, M., Schweigert, G. & Wetzel, A. (2021): The Middle Jurassic Opalinuston Formation (Aalenian, Opalinus Zone) at its type locality near Bad Boll and adjacent outcrops (Swabian Alb, SW Germany). Palaeodiversity 14/1, 15-113.

Dorn, P. (1935): Die Hammatoceraten, Sonninien, Ludwigien, Dorsetensien und Witchellien des süddeutschen, insbesondere fränkischen Doggers. Palaeontographica 82, 1-124.

Feist, S. (1987): Palynologische Untersuchungen im Braunjura beta und unteren Braunjura gamma (oberes Aalenium bis unteres Bajocium) der Bohrungen Hausen, nordöstliche Schwäbische Alb. Diploma Thesis, University of Tübingen. 78 pp.

Feist-Burkhardt, S. & Götz, A.E. (2016): Ultra-high-resolution palynostratigraphy of the Early Bajocian Sauzei and Humphriesianum zones (Middle Jurassic) from outcrop sections in the Upper Rhine area, southwest Germany. *In*: Montenari, M. (eds.): Stratigraphy & Timescales 1, 325-392.

Feist-Burkhardt, S. & Pross, J. (2010): Dinoflagellate cyst biostratigraphy of the Opalinuston Formation (Middle Jurassic) in the Aalenian type area in southwest Germany and north Switzerland. Lethaia 43, 10-31.

Feist-Burkhardt, S. & Wille, W. (1992): Jurassic palynology in southwest Germany – state of the art. Cahiers de Micropaléontologie 7/1-2, 141-164.

Fernandez, A., van Dijk, J., Müller, I.A. & Bernasconi, S.M. (2016): Siderite acid fractionation factors for sealed and open vessel digestions at 70°C and 100°C. Chemical Geology 444, 180-186.

Gygi, R.A. (2000): Annotated index of lithostratigraphic units currently used in the Upper Jurassic of northern Switzerland. Eclogae geol. Helv. 93/1, 125-146.

Isler, A., Pasquier, F. & Huber, M. (1984): Geologische Karte der zentralen Nordschweiz 1:100'000. Herausgegeben von der Nagra und der Schweiz. Geol. Komm.

Jordan, P. & Deplazes, G. (2019): Lithostratigraphy of consolidated rocks expected in the Jura Ost, Nördlich Lägern and Zürich Nordost regions. Nagra Arbeitsbericht NAB 19-14.

Kuhn, O. & Etter, W. (1994): Der Posidonienschiefer der Nordschweiz: Lithostratigraphie, Biostratigraphie und Fazies. Eclogae geol. Helv. 87/1, 113-138.

Kukal, Z. (1971): Geology of recent sediments. Academie Press, New York, 490 pp.

Matter, A., Peters, Tj., Bläsi, H.-R., Meyer, J., Ischi, H. & Meyer, Ch. (1988): Sondierbohrung Weiach – Geologie (Textband und Beilagenband). Nagra Technical Report NTB 86-01.

Maubeuge, P.L. (1947): Sur quelques ammonites de l'Aalénien ferrugineux du Luxembourg et sur l'échelle stratigraphique de la Formation ferrifère Franco–Belgo–Luxembourgeoise. Archives de l'Institut Grand–Ducal de Luxembourg, Section des Sciences naturelles, physique et mathématique, Nouvelle Série 17, 73-87.

Maubeuge, P.L. (1950): Nouvelles Recherches Stratigraphiques et Paléontologiques sur l'Aalénien Luxembourgeois (Parties Moyenne et Supérieure). Archives de l'Institut Grand–Ducal de Luxembourg, Section des Sciences naturelles, physique et mathématique, Nouvelle Série 19, 365-397.

Nagra (2014): SGT Etappe 2: Vorschlag weiter zu untersuchender geologischer Standortgebiete mit zugehörigen Standortarealen für die Oberflächenanlage. Geologische Grundlagen. Dossier II: Sedimentologische und tektonische Verhältnisse. Nagra Technical Report NTB 14-02.

Ogg, J.G., Ogg, G. & Gradstein, F.M. (2016): The Concise Geologic Time Scale. Cambridge University Press. 184 pp.

Oppel, A. (1856 – 1858): The Juraformation Englands, Frankreichs, und des südwestlichen Deutschlands. Ebner & Seubert, Stuttgart und Württ. Naturwiss. Jh. 12-14, 857 pp.

Parsons, T.R. (1975): Particulate organic carbon in the sea. *In*: Riey, J.P. & Skirrow, G. (eds.): Chemical oceanography. Academie Press, London, 338-425.

Pietsch, J. & Jordan, P. (2014): Digitales Höhenmodell Basis Quartär der Nordschweiz – Version 2013 (SGT E2) und ausgewählte Auswertungen. Nagra Arbeitsbericht NAB 14-02.

Rais, P., Louis-Schmid, B., Bernasconi, S.M. & Weissert, H. (2007): Palaeoceanographic and palaeoclimatic reorganization around the Middle–Late Jurassic transition. Palaeogeography, Palaeoclimatology, Palaeoecology 251/3-4, 527-546.

Reinecke, J.C.M. (1818): Maris protogaei Nautilos et Argonautae vulga Cornua Ammonis in Agro Coburgico et vicinio reperiundos; descripsit et delineavit, simul Observationes de Fossilum Protypis. L.C.A. Ahlii imp., Coburg, 90 pp.

Remane, J., Adatte, T., Berger, J.P., Burkhalter, R., Dall'Agnolo, S., Decrouez, D., Fischer, H., Funk, H., Furrer, H., Graf, H.R., Gouffon, Y., Heckendorn, W. & Winkler, W. (2005): Richtlinien zur stratigraphischen Nomenklatur. Eclogae geol. Helv. 98/3, 385-405.

Ruebsam, W. & Al-Husseini, M. (2020): Calibrating the Early Toarcian (Early Jurassic) with stratigraphic black holes (SBH). Gondwana Research 82, 317-336.

Scheffer, F. & Schachtschnabel, P. (1984): Lehrbuch der Bodenkunde. Enke Verlag, Stuttgart.

StrataBugs, version 2.1 (June 2016): StrataData Ltd., UK. http://www.stratadata.co.uk.

Timescale Creator, version 7.0 (30. July 2016): Geologic TimeScale Foundation. https://engineering.purdue.edu/Stratigraphy/tscreator/.

Voigt, E. (1968): Über Hiatus-Konkretionen (dargestellt an Beispielen aus dem Lias). Geologische Rundschau 58, 281-296.

Wetzel, A. & Allia, V. (2000): The significance of hiatus beds in shallow-water mudstones: an example from the Middle Jurassic of Switzerland. Journal of Sedimentary Research 70/1, 170-180.

Wetzel, A., Weissert, H., Schaub, M. & Voegelin, A.R. (2013): Sea-water circulation on an oolite-dominated carbonate system in an epeiric sea (Middle Jurassic, Switzerland). Sedimentology 60, 19-35.

Wohlwend, S., Hart, M. & Weissert, H. (2016): Chemostratigraphy of the Upper Albian to mid-Turonian Natih Formation (Oman) – How authigenic carbonate changes a global pattern. The Depositional Record 2/1, 97-117.

Wohlwend, S., Bläsi, H.R., Feist-Burkhardt, S., Hostettler, B., Menkveld-Gfeller, U., Dietze, V. & Deplazes, G. (2019a): Die Passwang-Formation im östlichen Falten- und Tafeljura: Fasiswald (SO) – Unt. Hauenstein (SO) – Wasserflue (AG) – Thalheim (AG) – Frickberg (AG) – Cheisacher (AG) – Böttstein (AG) – Tegerfelden (AG) – Acheberg (AG). Nagra Arbeitsbericht NAB 18-11.

Wohlwend, S., Bernasconi, S.M., Deplazes, G. & Jaeggi, D. (2019b): SO Experiment: Chemostratigraphic study of Late Aalenian to Early Bajocian. Mont Terri Technical Report TR 19-05. Federal Office of Topography (swisstopo), Wabern, Switzerland.

Wohlwend, S., Bläsi, H.R., Feist-Burkhardt, S., Hostettler, B., Menkveld-Gfeller, U., Dietze, V. & Deplazes, G. (2021a): TBO Bülach-1-1: Data Report – Dossier IV: Microfacies, Bio- and Chemostratigraphic Analysis. Nagra Arbeitsbericht NAB 20-08.

Wohlwend, S., Bläsi, H.R., Feist-Burkhardt, S., Hostettler, B., Menkveld-Gfeller, U., Dietze, V. & Deplazes, G. (2021b): TBO Trüllikon-1-1: Data Report – Dossier IV: Microfacies, Bio- and Chemostratigraphic Analysis. Nagra Arbeitsbericht NAB 20-09.

Wohlwend, S., Bläsi, H.R., Feist-Burkhardt, S., Hostettler, B., Menkveld-Gfeller, U., Dietze, V. & Deplazes, G. (2021c): TBO Marthalen-1-1: Data Report – Dossier IV: Microfacies, Bio- and Chemostratigraphic Analysis. Nagra Arbeitsbericht NAB 21-20.

Wohlwend, S., Bläsi, H.R., Feist-Burkhardt, S., Hostettler, B., Menkveld-Gfeller, U., Dietze, V. & Deplazes, G. (2022a): TBO Bözberg-1-1: Data Report – Dossier IV: Microfacies, Bio- and Chemostratigraphic Analysis. Nagra Arbeitsbericht NAB 21-21.

Wohlwend, S., Feist-Burkhardt, S., Hostettler, B., Menkveld-Gfeller, U., Bläsi, H.R., Bernasconi, S.M. & Deplazes, G. (2022b): A new combined high-resolution Jurassic C-isotope chemo- and biostratigraphic correlation from Northern Switzerland. 11th International Congress on the Jurassic System, 29 August – 2 September 2022, Budapest, Hungary.

Wohlwend, S., Bläsi, H.R., Feist-Burkhardt, S., Hostettler, B., Menkveld-Gfeller, U., Dietze, V. & Deplazes, G. (2022c): TBO Stadel-3-1: Data Report – Dossier IV: Microfacies, Bio- and Chemostratigraphic Analysis. Nagra Arbeitsbericht NAB 22-01.

Wohlwend, S., Bläsi, H.R., Feist-Burkhardt, S., Hostettler, B., Menkveld-Gfeller, U., Dietze, V. & Deplazes, G. (2022d): TBO Stadel-2-1: Data Report – Dossier IV: Microfacies, Bio- and Chemostratigraphic Analysis. Nagra Arbeitsbericht NAB 22-02.

Wood, G.D., Gabriel, A.M. & Lawson, J.C. (1996): Palynological techniques – processing and microscopy. *In*: Jansonius, J. & McGregor, D.C. (eds.): Palynology, principles and applications. American Association of Stratigraphic Palynologists Foundation 2, 29-50.

Zieten, C.H. von (1830 – 1833): Versteinerungen Württembergs, oder naturgetreue Abbildungen der in den vollständigsten Sammlungen, namentlich der in dem Kabinet des Oberamts-Arzt Dr. Hartmann befindlichen Petrefacten, mit Angabe der Gebirgs-Formationen, in welchen dieselben vorkommen und der Fundorte. Verlag & Lithographie der Expedition des Werkes unserer Zeit, Stuttgart, 102 pp.

Appendix A: List of all samples

Appendix A1: List of all thin sections from BAC1-1 (1'239.13 – 668.48 m)

For the description and individual counting of the thin sections see Section 3.1; selected photos can be found in Appendix B.

Top [m]	**Bottom** [m]	**Avg. depth** [m]	**Formation**	**Retrieval date** [dd.mm.yyyy]	**Sample ID**
668.46	668.50	668.48	Wildegg Fm.	23.02.2022	BAC1-1-668.48-TS
737.12	737.15	737.14	Wutach Fm.	23.02.2022	BAC1-1-737.14-TS
737.18	737.22	737.20	Wutach Fm.	23.02.2022	BAC1-1-737.20-TS
740.94	740.98	740.96	Variansmergel Fm.	23.02.2022	BAC1-1-740.96-TS
779.84	779.88	779.86	«Parkinsoni-Württembergica-Sch.»	23.02.2022	BAC1-1-779.86-TS
781.42	781.45	781.44	«Parkinsoni-Württembergica-Sch.»	23.02.2022	BAC1-1-781.44-TS
789.12	789.15	789.14	«Humphriesioolith Fm.»	01.06.2022	BAC1-1-789.14-TS
790.83	790.87	790.85	«Humphriesioolith Fm.»	01.06.2022	BAC1-1-790.85-TS
792.97	793.00	792.99	Wedelsandstein Fm.	01.06.2022	BAC1-1-792.99-TS
793.61	793.65	793.63	«Murchisonae-Oolith Fm.»	23.02.2022	BAC1-1-793.63-TS
797.32	797.36	797.34	«Murchisonae-Oolith Fm.»	23.02.2022	BAC1-1-797.34-TS
798.98	799.02	799.00	«Murchisonae-Oolith Fm.»	23.02.2022	BAC1-1-799.00-TS
799.97	800.01	799.99	«Murchisonae-Oolith Fm.»	23.02.2022	BAC1-1-799.99-TS
802.98	803.02	803.00	«Murchisonae-Oolith Fm.»	23.02.2022	BAC1-1-803.00-TS
806.82	806.86	806.84	«Murchisonae-Oolith Fm.»	01.06.2022	BAC1-1-806.84-TS
808.09	808.13	808.11	«Murchisonae-Oolith Fm.»	01.06.2022	BAC1-1-808.11-TS
811.55	811.59	811.57	Opalinus Clay	23.02.2022	BAC1-1-811.57-TS
811.82	811.86	811.84	Opalinus Clay	23.02.2022	BAC1-1-811.84-TS
815.02	815.06	815.04	Opalinus Clay	07.03.2022	BAC1-1-815.04-TS
825.50	825.54	825.52	Opalinus Clay	07.03.2022	BAC1-1-825.52-TS
825.56	825.60	825.58	Opalinus Clay	07.03.2022	BAC1-1-825.58-TS
829.15	829.19	829.17	Opalinus Clay	07.03.2022	BAC1-1-829.17-TS
832.88	832.92	832.90	Opalinus Clay	07.03.2022	BAC1-1-832.90-TS
861.63	861.67	861.65	Opalinus Clay	07.03.2022	BAC1-1-861.65-TS
901.04	901.07	901.06	Opalinus Clay	23.02.2022	BAC1-1-901.06-TS
914.90	914.94	914.92	Staffelegg Fm.	23.02.2022	BAC1-1-914.92-TS
964.94	964.98	964.96	Klettgau Fm. (Seebi Mb.)	01.06.2022	BAC1-1-964.96-TS
965.06	965.10	965.08	Klettgau Fm. (Seebi Mb.)	01.06.2022	BAC1-1-965.08-TS
965.88	965.92	965.90	Klettgau Fm. (Seebi Mb.)	01.06.2022	BAC1-1-965.90-TS
967.42	967.45	967.44	Klettgau Fm. (Gansingen Mb.)	01.06.2022	BAC1-1-967.44-TS
968.55	968.59	968.57	Klettgau Fm. (Gansingen Mb.)	01.06.2022	BAC1-1-968.57-TS
975.59	975.62	975.61	Klettgau Fm. (Ergolz Mb.)	01.06.2022	BAC1-1-975.61-TS
975.72	975.76	975.74	Klettgau Fm. (Ergolz Mb.)	01.06.2022	BAC1-1-975.74-TS
980.05	980.09	980.07	Klettgau Fm. (Ergolz Mb.)	01.06.2022	BAC1-1-980.07-TS
1'001.55	1'001.59	1'001.57	Bänkerjoch Fm.	01.06.2022	BAC1-1-1001.57-TS
1'059.69	1'059.73	1'059.71	Schinznach Fm.	04.07.2022	BAC1-1-1059.71-TS
1'124.00	1'124.04	1'124.02	Schinznach Fm.	04.07.2022	BAC1-1-1124.02-TS
1'133.66	1'133.70	1'133.68	Zeglingen Fm.	04.07.2022	BAC1-1-1133.68-TS
1'237.97	1'238.01	1'237.99	Kaiseraugst Fm.	04.07.2022	BAC1-1-1237.99-TS
1'239.11	1'239.15	1'239.13	Kaiseraugst Fm.	04.07.2022	BAC1-1-1239.13-TS

Appendix A2: List of all sampled macrofossils from BAC1-1 (925.90 – 736.84 m)

For the definitive determination of the individual macrofossils see Section 3.2 (Tab. 3-2).

Top [m]	**Bottom** [m]	**Sample depth** [m]	**Formation**	**Retrieval date** [dd.mm.yyyy]	**Sample ID**
736.84	736.86	736.84	Wildegg Fm.	10.02.2022	BAC1-1-736.84-BS(MF)
737.36	737.40	737.38	Wutach Fm.	10.02.2022	BAC1-1-737.38-BS(MF)
737.51	737.55	737.53	Wutach Fm.	10.02.2022	BAC1-1-737.53-BS(MF)
740.53	740.58	740.56	Variansmergel Fm.	10.02.2022	BAC1-1-740.56-BS(MF)
740.98	741.01	741.00	Variansmergel Fm.	10.02.2022	BAC1-1-741.00-BS(MF)
791.83	791.92	791.88	Wedelsandstein Fm.	10.02.2022	BAC1-1-791.88-BS(MF)
793.03	793.06	793.05	Wedelsandstein Fm.	10.02.2022	BAC1-1-793.05-BS(MF)
793.24	793.29	793.26	«Murchisonae-Oolith Fm.»	10.02.2022	BAC1-1-793.26-BS(MF)
810.61	810.64	810.64	Opalinus Clay	10.02.2022	BAC1-1-810.64-BS(MF)
811.44	811.54	811.49	Opalinus Clay	10.02.2022	BAC1-1-811.49-BS(MF)
811.72	811.78	811.75	Opalinus Clay	10.02.2022	BAC1-1-811.75-BS(MF)
811.87	811.93	811.90	Opalinus Clay	10.02.2022	BAC1-1-811.90-BS(MF)
840.57	840.60	840.57	Opalinus Clay	10.02.2022	BAC1-1-840.57-BS(MF)
900.88	900.90	900.90	Opalinus Clay	10.02.2022	BAC1-1-900.90-BS(MF)
901.63	901.67	901.63	Opalinus Clay	10.02.2022	BAC1-1-901.63-BS(MF)
901.82	901.83	901.82	Opalinus Clay	10.02.2022	BAC1-1-901.82-BS(MF)
905.39	905.41	905.41	Opalinus Clay	10.02.2022	BAC1-1-905.41-BS(MF)
914.68	914.75	914.72	Opalinus Clay	10.02.2022	BAC1-1-914.72-BS(MF)
915.06	915.14	915.09	Staffelegg Fm.	10.02.2022	BAC1-1-915.09-BS(MF)
917.94	917.99	917.97	Staffelegg Fm.	10.02.2022	BAC1-1-917.97-BS(MF)
918.33	918.42	918.38	Staffelegg Fm.	10.02.2022	BAC1-1-918.38-BS(MF)
925.85	925.92	925.90	Staffelegg Fm.	10.02.2022	BAC1-1-925.90-BS(MF)

Appendix A3: List of other provisionally determined conspicuous macrofossils from BAC1-1 (943.00 – 673.15 m)

Top [m]	**Bottom** [m]	**Fossil**	**Determination (provisional)**
673.15		Ammonite	*Perisphinctes* sp.? Microconch
738.78		Brachiopod	*Rhynchonelloidella alemanica*
897.75		Ammonite	*Leioceras opalinum*
900.40		Ammonite	*Leioceras subglabrum*
901.14		2 Ammonites	*Leioceras opalinum*
914.41		Ammonite	*Leioceras* sp.?
915.20		Ammonite	*Pleydellia* sp.
915.50		Ammonite	*Cotteswoldia* sp.
915.73		Nautilid	indet.
916.10		Ammonites	*Cotteswoldia* sp.
921.32		Wood	Wood
921.79		Belemnites	indet.
922.18		Bivalve	indet.
923.08		Ammonite	indet.
923.27		Ammonite	*Harpoceras* sp.
925.42	925.49	Rhynchonellids	indet.
925.41		Ammonite	indet.
943.00		Coral	*Montlivaltia* sp.

Appendix A4: List of all palynological samples from BAC1-1 (916.21 – 736.04 m)

Palynological samples in grey are taken from ammonite samples retrieved at specific depths. Sampling was always as close as possible to the ammonite.

Top [m]	**Bottom** [m]	**Avg. Depth** [m]	**Formation**	**Retrieval date** [dd.mm.yyyy]	**Sample ID**
736.03	736.05	736.04	Wildegg Fm.	23.02.2022	BAC1-1-736.04-BS(PA)
736.61	736.63	736.62	Wildegg Fm.	23.02.2022	BAC1-1-736.62-BS(PA)
737.18	737.20	737.19	Wutach Fm.	23.02.2022	BAC1-1-737.19-BS(PA)
737.51	737.55	737.53	Wutach Fm.	23.02.2022	BAC1-1-737.53-BS(PA)
738.78	738.80	738.79	Wutach Fm.	23.02.2022	BAC1-1-738.79-BS(PA)
739.01	739.03	739.02	Variansmergel Fm.	23.02.2022	BAC1-1-739.02-BS(PA)
741.37	741.39	741.38	«Parkinsoni-Württembergica-Sch.»	23.02.2022	BAC1-1-741.38-BS(PA)
747.91	747.93	747.92	«Parkinsoni-Württembergica-Sch.»	23.02.2022	BAC1-1-747.92-BS(PA)
756.01	756.03	756.02	«Parkinsoni-Württembergica-Sch.»	23.02.2022	BAC1-1-756.02-BS(PA)
764.05	764.08	764.07	«Parkinsoni-Württembergica-Sch.»	23.02.2022	BAC1-1-764.07-BS(PA)
772.03	772.05	772.04	«Parkinsoni-Württembergica-Sch.»	23.02.2022	BAC1-1-772.04-BS(PA)
780.57	780.59	780.58	«Parkinsoni-Württembergica-Sch.»	23.02.2022	BAC1-1-780.58-BS(PA)
781.42	781.45	781.44	«Parkinsoni-Württembergica-Sch.»	23.02.2022	BAC1-1-781.44-BS(PA)
784.09	784.11	784.10	«Parkinsoni-Württembergica-Sch.»	23.02.2022	BAC1-1-784.10-BS(PA)
784.53	784.55	784.54	«Parkinsoni-Württembergica-Sch.»	23.02.2022	BAC1-1-784.54-BS(PA)
787.06	787.08	787.07	«Parkinsoni-Württembergica-Sch.»	23.02.2022	BAC1-1-787.07-BS(PA)
788.40	788.42	788.41	«Parkinsoni-Württembergica-Sch.»	07.12.2021	BAC1-1-788.41-BS(PA)
788.87	788.90	788.89	«Parkinsoni-Württembergica-Sch.»	23.02.2022	BAC1-1-788.89-BS(PA)
789.05	789.07	789.06	«Humphriesioolith Fm.»	23.02.2022	BAC1-1-789.06-BS(PA)
789.35	789.36	789.36	«Humphriesioolith Fm.»	23.02.2022	BAC1-1-789.36-BS(PA)
789.66	789.68	789.67	«Humphriesioolith Fm.»	23.02.2022	BAC1-1-789.67-BS(PA)
790.54	790.56	790.55	«Humphriesioolith Fm.»	23.02.2022	BAC1-1-790.55-BS(PA)
791.10	791.13	791.12	Wedelsandstein Fm.	23.02.2022	BAC1-1-791.12-BS(PA)
791.66	791.68	791.67	Wedelsandstein Fm.	07.12.2021	BAC1-1-791.67-BS(PA)
792.54	792.56	792.55	Wedelsandstein Fm.	23.02.2022	BAC1-1-792.55-BS(PA)
792.88	792.90	792.89	Wedelsandstein Fm.	23.02.2022	BAC1-1-792.89-BS(PA)
793.12	793.14	793.13	«Murchisonae-Oolith Fm.»	07.12.2021	BAC1-1-793.13-BS(PA)
793.90	793.92	793.91	«Murchisonae-Oolith Fm.»	07.12.2021	BAC1-1-793.91-BS(PA)
796.97	797.00	796.99	«Murchisonae-Oolith Fm.»	07.12.2021	BAC1-1-796.99-BS(PA)
797.30	797.32	797.31	«Murchisonae-Oolith Fm.»	07.12.2021	BAC1-1-797.31-BS(PA)
800.93	800.95	800.94	«Murchisonae-Oolith Fm.»	07.12.2021	BAC1-1-800.94-BS(PA)
802.94	802.96	802.95	«Murchisonae-Oolith Fm.»	23.02.2022	BAC1-1-802.95-BS(PA)
804.43	804.45	804.44	«Murchisonae-Oolith Fm.»	07.12.2021	BAC1-1-804.44-BS(PA)
808.07	808.09	808.08	«Murchisonae-Oolith Fm.»	07.12.2021	BAC1-1-808.08-BS(PA)
811.10	811.12	811.11	Opalinus Clay	07.12.2021	BAC1-1-811.11-BS(PA)
811.54	811.56	811.55	Opalinus Clay	23.02.2022	BAC1-1-811.55-BS(PA)
811.84	811.86	811.85	Opalinus Clay	07.12.2021	BAC1-1-811.85-BS(PA)
812.55	812.57	812.56	Opalinus Clay	07.12.2021	BAC1-1-812.56-BS(PA)
815.33	815.35	815.34	Opalinus Clay	07.12.2021	BAC1-1-815.34-BS(PA)
820.16	820.18	820.17	Opalinus Clay	07.12.2021	BAC1-1-820.17-BS(PA)
829.89	829.91	829.90	Opalinus Clay	07.12.2021	BAC1-1-829.90-BS(PA)
850.02	850.04	850.03	Opalinus Clay	23.02.2022	BAC1-1-850.03-BS(PA)
869.82	869.84	869.83	Opalinus Clay	23.02.2022	BAC1-1-869.83-BS(PA)
890.38	890.39	890.39	Opalinus Clay	23.02.2022	BAC1-1-890.39-BS(PA)
909.40	909.42	909.41	Opalinus Clay	23.02.2022	BAC1-1-909.41-BS(PA)
914.68	914.72	914.70	Opalinus Clay	23.02.2022	BAC1-1-914.70-BS(PA)
916.20	916.22	916.21	Staffelegg Fm.	23.02.2022	BAC1-1-916.21-BS(PA)

Appendix B: Photos microfacies

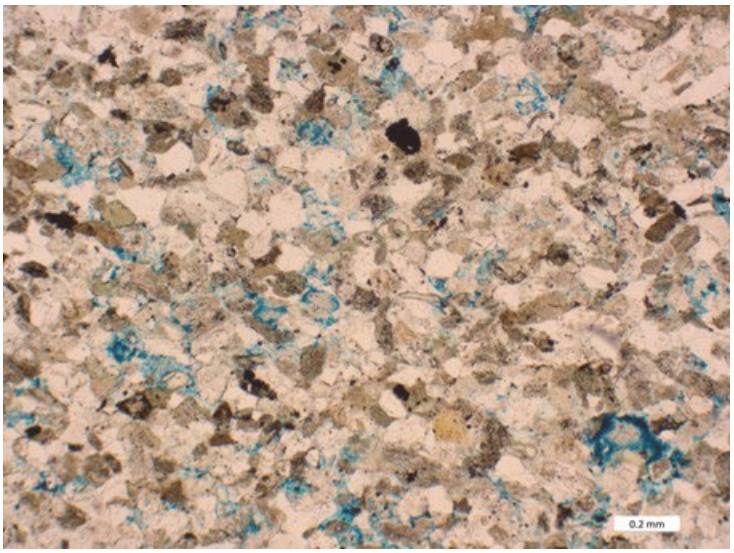	**Fig. B-1:** Sandstone (fine-grained, anhydritic): Composed of quartz-grains and different rock fragments, e.g. schist, as well as some clay matrix. Open pores filled with blue coloured glue Thin section photo BAC1-1-980.07 Klettgau Fm. (Ergolz Mb.)
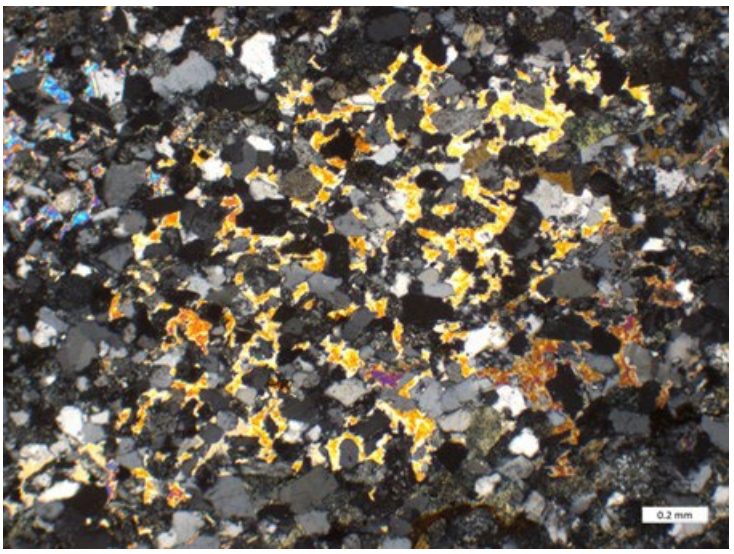	**Fig. B-2:** Sandstone (fine-grained, anhydritic): Same sample as above (Fig. B-1), showing anhydrite cement (yellow, orange, blue), filling primary pore space Thin section photo, crossed nicols BAC1-1-980.07 Klettgau Fm. (Ergolz Mb.)
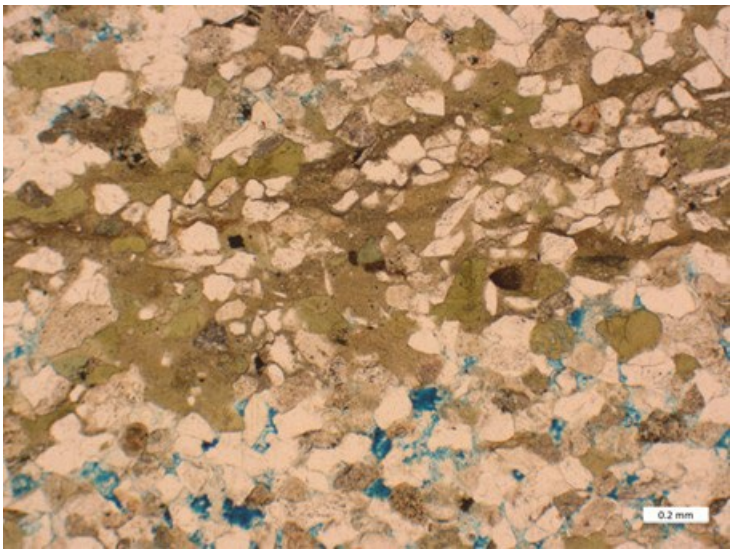	**Fig. B-3:** Sandstone (fine-grained, argillaceous): Composed of quartz-grains and numerous schist rock fragments (greenish and brown components, as well as clay matrix and open pores (filled with blue coloured glue) Thin section photo BAC1-1-975.74 Klettgau Fm. (Ergolz Mb.)

Selected photos of microfacies from Klettgau Fm.

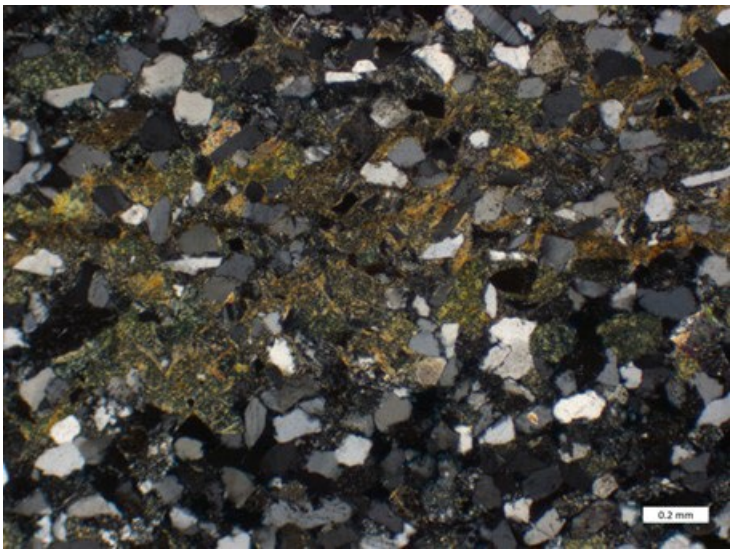	**Fig. B-4:** Sandstone (fine-grained, argillaceous): Same sample as above (Fig. B-3) Thin section photo, crossed nicols BAC1-1-975.74 Klettgau Fm. (Ergolz Mb.)
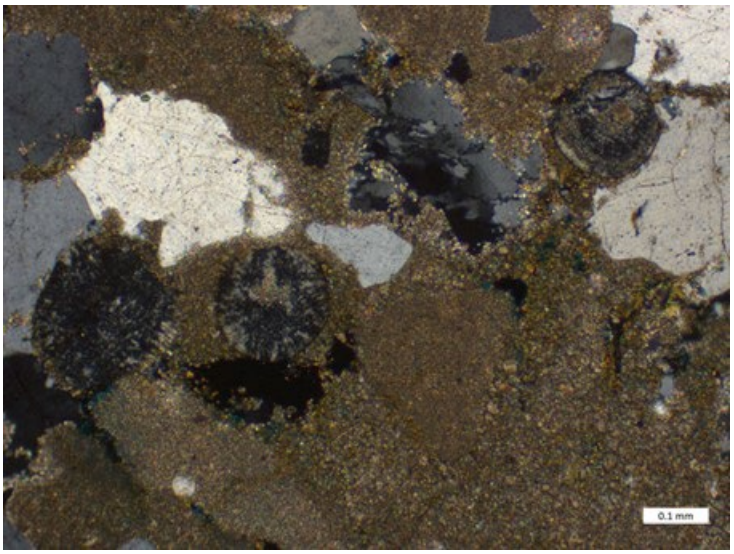	**Fig. B-5:** Sandstone (coarse-grained, dolomitic): Composed of quartz-grains (grey), dolostone rock fragments (brown) and few pedogenic quartz-dolomite nodules (middle left, grey-brown mixed) Thin section photo, crossed nicols BAC1-1-965.08 Klettgau Fm. (Seebi Mb.)
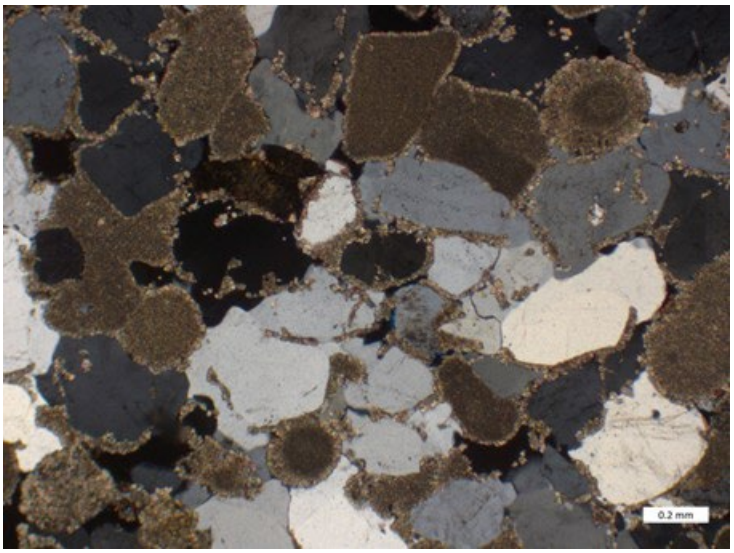	**Fig. B-6:** Sandstone (coarse-grained, dolomitic): Composed of quartz-grains, dolostone rock fragments, few dolomitic ooids and some quartz and dolomite cement Thin section photo, crossed nicols BAC1-1-964.96 Klettgau Fm. (Seebi Mb.)

Selected photos of microfacies from Klettgau Fm.

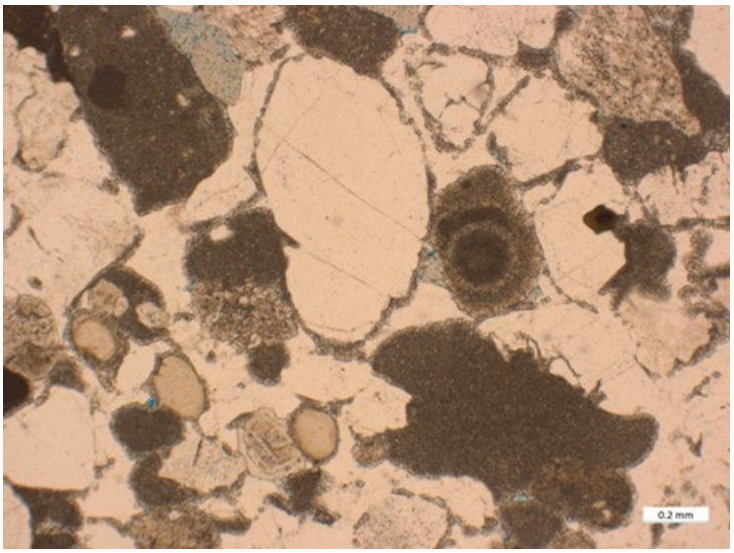	**Fig. B-7:** Sandstone (coarse-grained, dolomitic): Same sample as above (Fig. B-6), showing quartz-grains with small dolomite cement rims and quartz cement around. One of the ooids is located right of the centre Thin section photo BAC1-1-964.96 Klettgau Fm. (Seebi Mb.)
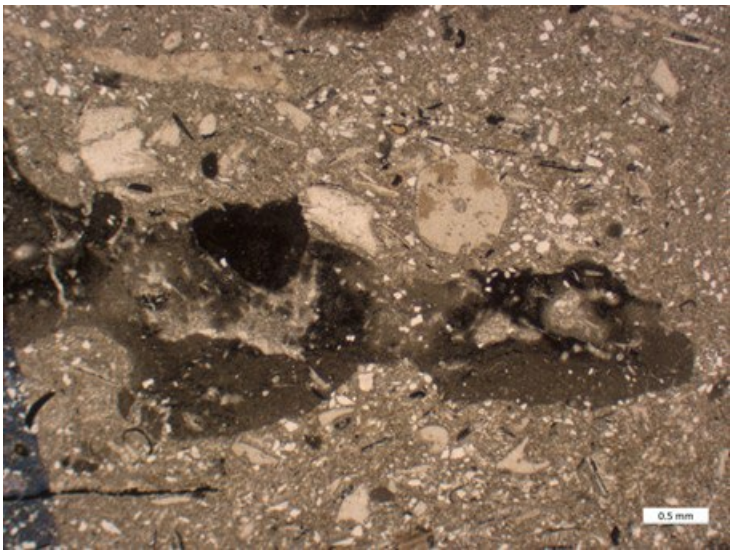	**Fig. B-8:** "Hiatus bed" (bioclastic limestone with nodules): Micritic, erratically formed, nodules, together with bioclastic components and fine quartz-sand in a marly matrix with "stellate cement" Thin section photo BAC1-1-861.65 Opalinus Clay
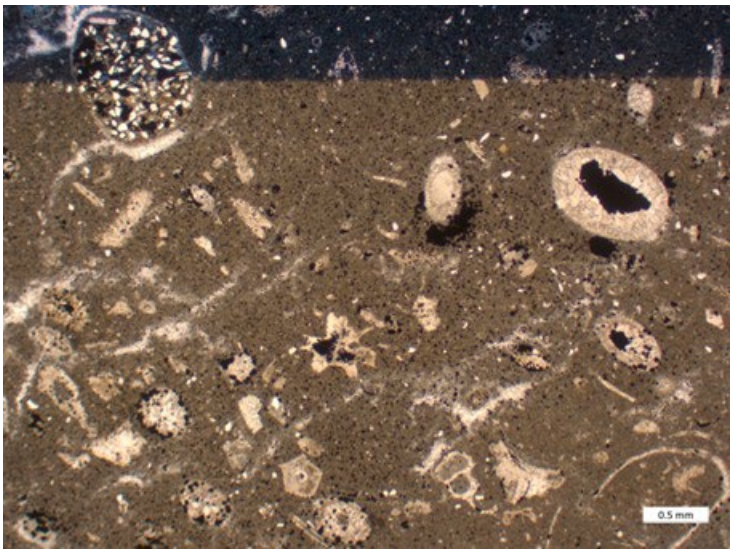	**Fig. B-9:** Nodular limestone (iron-oolitic): "hiatus bed", resp. hardground with numerous bivalve and echinoderm bioclasts, calcitic iron-ooids (with relicts of iron mineral layers), a siltstone intraclast and pyrite are the components, beside other intraclasts Thin section photo BAC1-1-825.52 Opalinus Clay

Selected photos of microfacies from Klettgau Fm. and Opalinus Clay

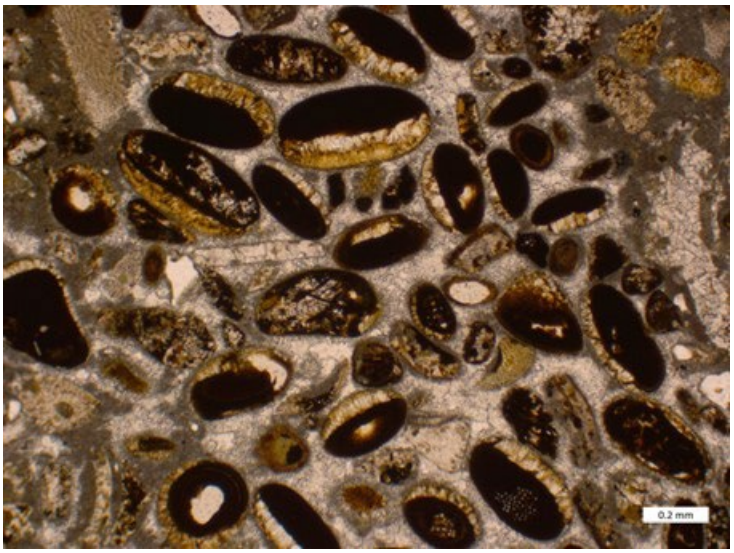	**Fig. B-10:** Iron-oolite horizon as part of a bioclastic limestone (iron-oolitic): Iron-ooids, partly replaced by calcite, and few bioclasts, sedimented with micrite matrix, but also cemented by calcite Thin section photo BAC1-1-811.57 Opalinus Clay
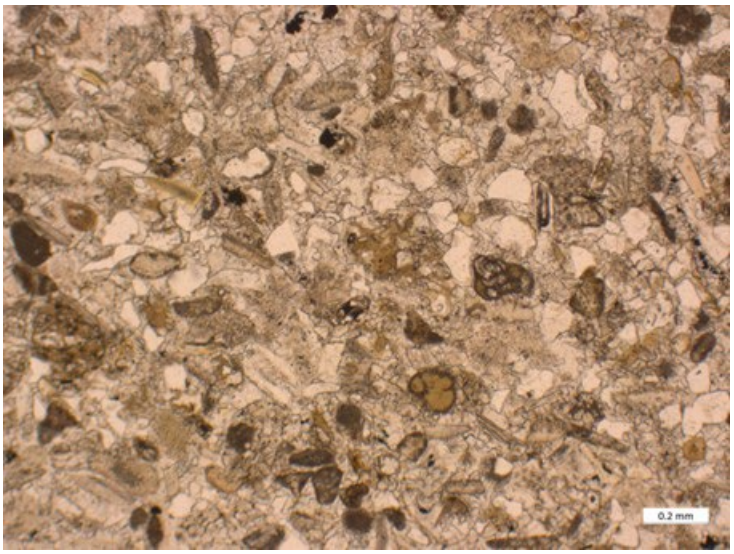	**Fig. B-11:** Bioclastic limestone (sandy): biogenic components of bivalves, echinoderms and foraminifera, together with pellets, micrite matrix and calcite cement Thin section photo BAC1-1-806.84 «Murchisonae-Oolith Fm.»
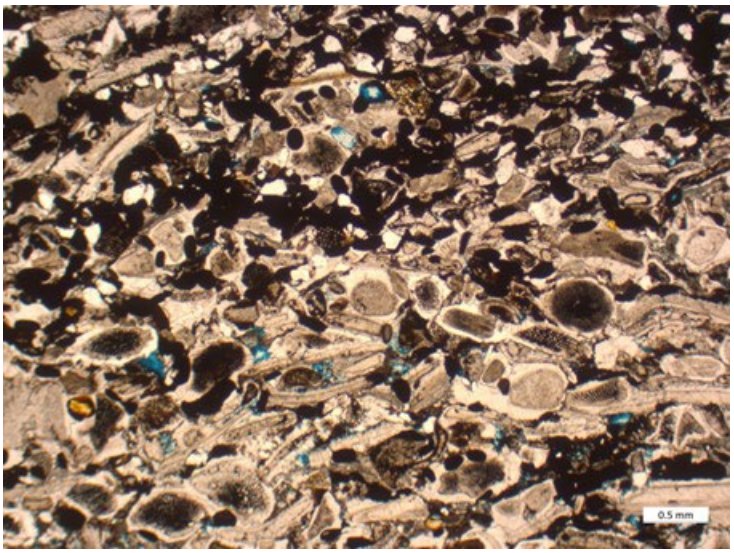	**Fig. B-12:** Bioclastic limestone (limonitic and iron-oolitic): dominated by limonitic echinoderm elements and limonitic bivalves, further components are iron-ooids; cemented by calcite (e.g. white rims around echinoderms) Thin section photo BAC1-1-799.00 «Murchisonae-Oolith Fm.»

Selected photos of microfacies from Opalinus Clay and «Murchisonae-Oolith Fm.»

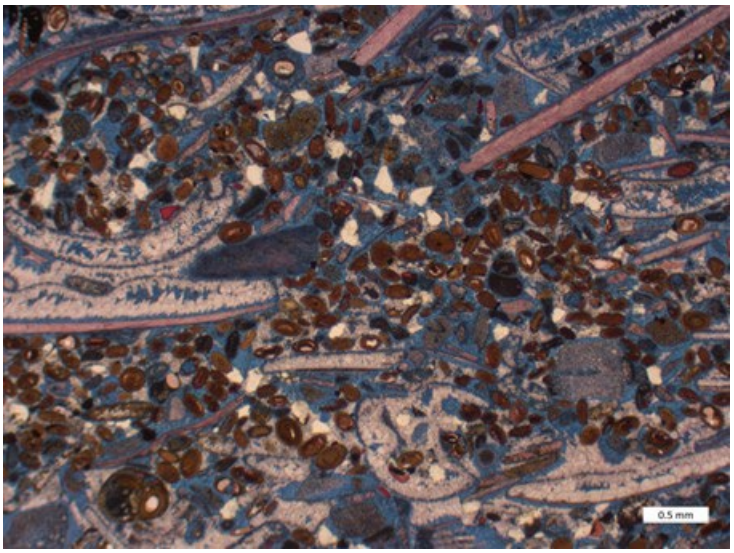	**Fig. B-13:** Bioclastic limestone (iron-oolitic): bioclasts and small iron-ooids with different calcite cement generations Thin section photo: stained for calcite = red (some early diagenetic calcite crystals not coloured), iron-calcite = blue BAC1-1-797.34 «Murchisonae-Oolith Fm.»
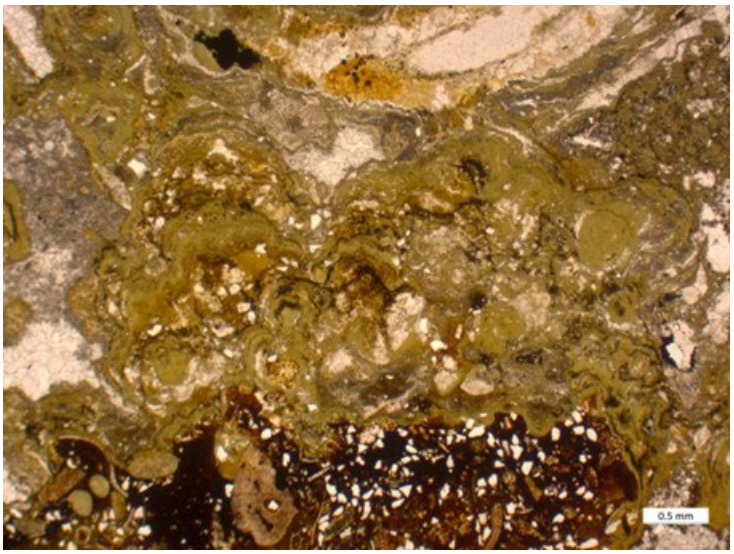	**Fig. B-14:** Hardground, composed of different horizons: a green-ish, wavy layered, chamositic iron-stromatolite and a brown, limonitic, sandy horizon (underneath) Thin section photo BAC1-1-793.63 «Murchisonae-Oolith Fm.»
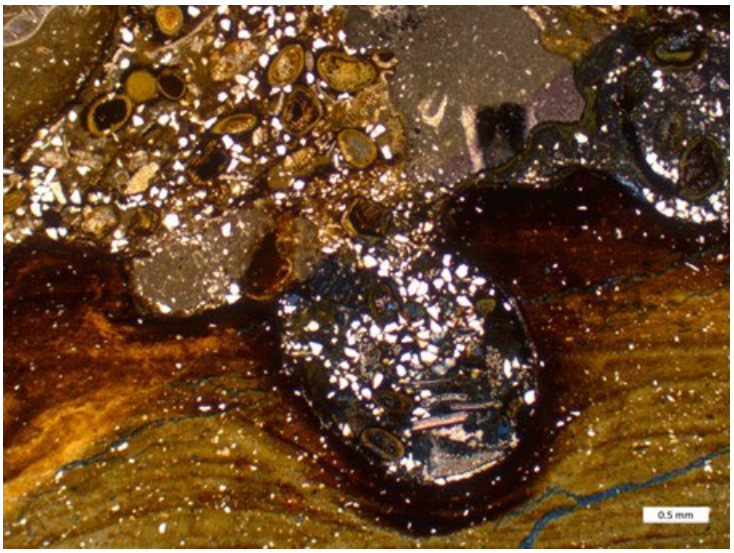	**Fig. B-15:** Hardground (same as above, Fig. B-14): Horizon with bored iron-stromatolitic intraclast and above an iron-oolitic, bioclastic, sandy horizon Thin section photo BAC1-1-793.63 «Murchisonae-Oolith Fm.»

Selected photos of microfacies from «Murchisonae-Oolith Fm.»

	**Fig. B-16:** Limestone (iron-oolitic): Calcitic iron-ooids, in which limonitic calcite replaces the primary chamosite or goethite, whereof a small rest is preserved Thin section photo BAC1-1-790.85 «Humphriesioolith Fm.»
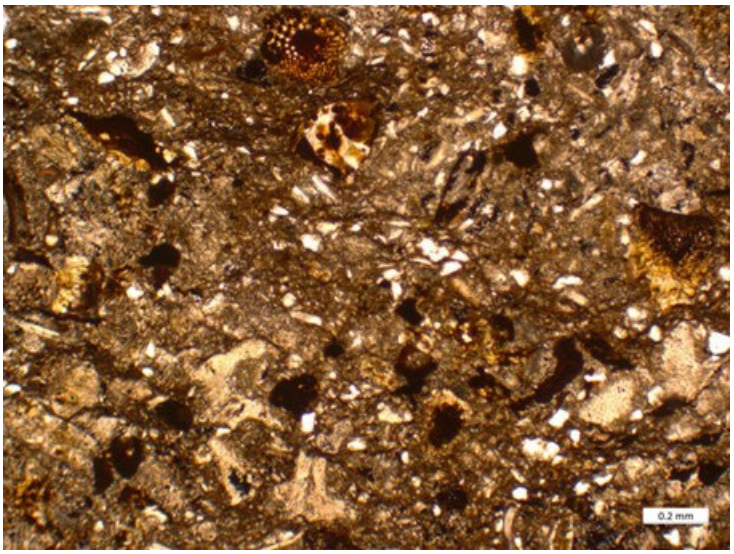	**Fig. B-17:** Bioclastic calcareous marl (limonitic): Limonite rich bed in the lower part of «Parkinsoni-Württem-bergica-Schichten» Thin section photo BAC1-1-781.44 «Parkinsoni-Württem-bergica-Schichten»
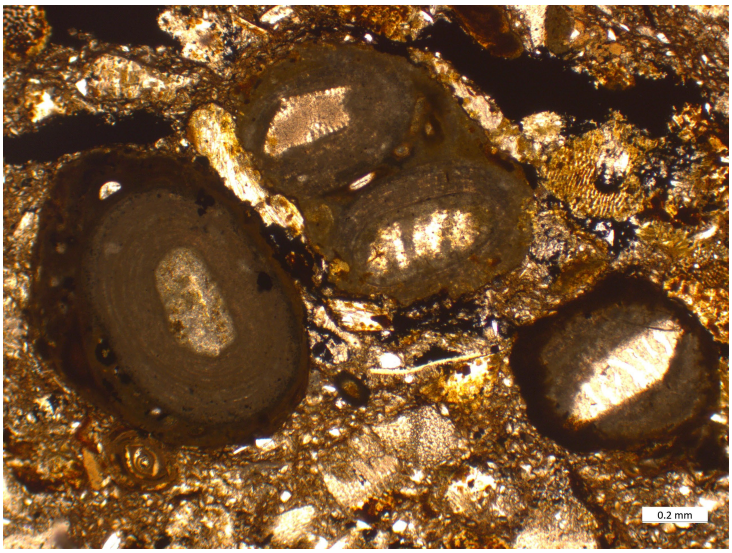	**Fig. B-18:** Bioclastic calcareous marl (limonitic): Same sample as above (Fig. B-17), few "normal" calcite ooids, similar to those of the Hauptrogenstein (e.g. BOZ1-1-476.00), the two on the right with presumed coral fragments as nuclei Thin section photo BAC1-1-781.44 «Parkinsoni-Württem-bergica-Schichten»

Selected photos of microfacies from «Humphriesioolith Fm.» and «Parkinsoni-Württem.-Sch.»

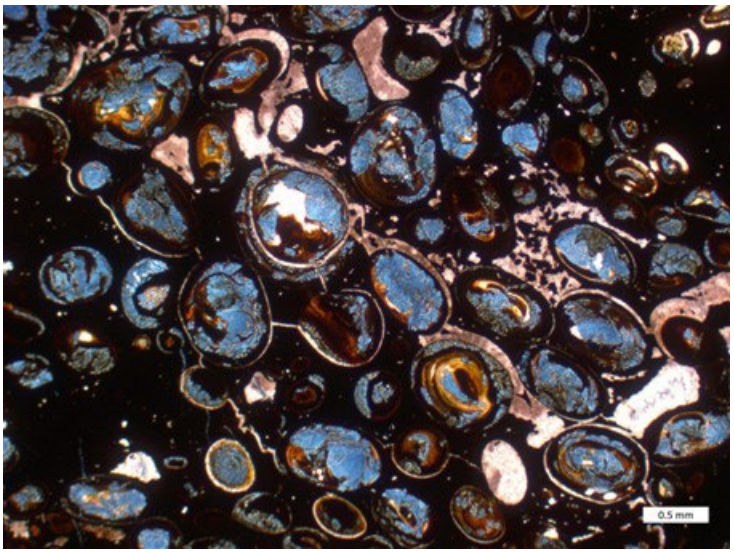	**Fig. B-19:** Iron-oolite: Composed of calcitic iron-ooids and totally limonitic matrix: calcite replaces the iron-minerals of the ooids, and the matrix around the ooids is full of limonite Thin section photo, TS stained for calcite = red, iron-calcite = bluish BAC1-1-737.20 Wutach Fm.
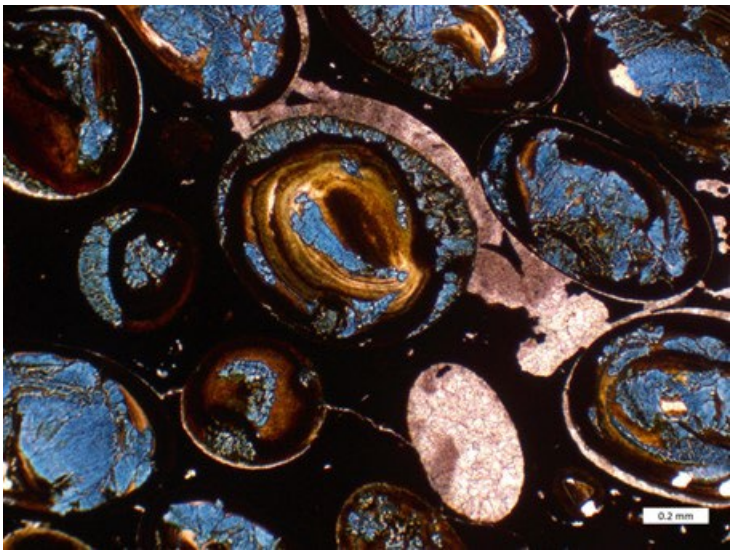	**Fig. B-20:** Iron-oolite: Detail of Fig. B-19, partial replacement of the chamosite cortices by calcite Thin section photo, TS stained for calcite = red, iron-calcite = bluish BAC1-1-737.20 Wutach Fm.
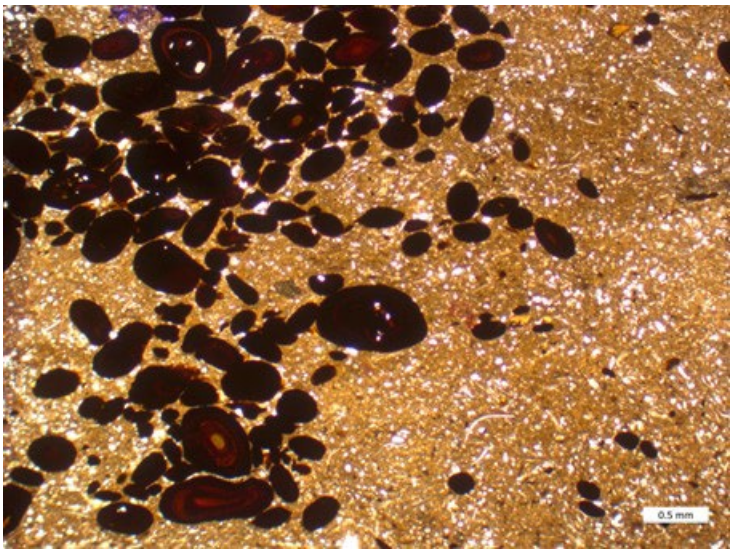	**Fig. B-21:** Limestone (iron-oolitic): Iron-ooids and micritic matrix with small white bioclasts and dolomitic crystals Thin section photo BAC1-1-737.14 Wutach Fm.

Selected photos of microfacies from Wutach Fm.

Appendix C: Plates of ammonites

Plate I BAC1-1 (917.97 – 915.06 m)

Fig. 1: *Pseudogrammoceras* sp., depth: 917.97 m, Staffelegg Fm. (Gross Wolf Mb.), Thouarsense Zone, probably Fallaciosum Subzone.

Fig. 2: *Pleydellia leura* (Buckman, 1890) (1) and *Cotteswoldia* ex gr. *lotharingica* (Branco, 1879) or *pseudolotharingica* (Maubeuge, 1950) (2), depth: 915.09 m, Staffelegg Fm. (Gross Wolf Mb.). Aalensis Zone, Torulosum Subzone.

Fig. 3: *Pleydellia* ex gr. *buckmani* (Maubeuge, 1947), depth: 915.06 m, Staffelegg Fm. (Gross Wolf Mb.), Aalensis Zone, Torulosum Subzone.

All figures are illustrated in individual scales; black bars indicate 1 cm.

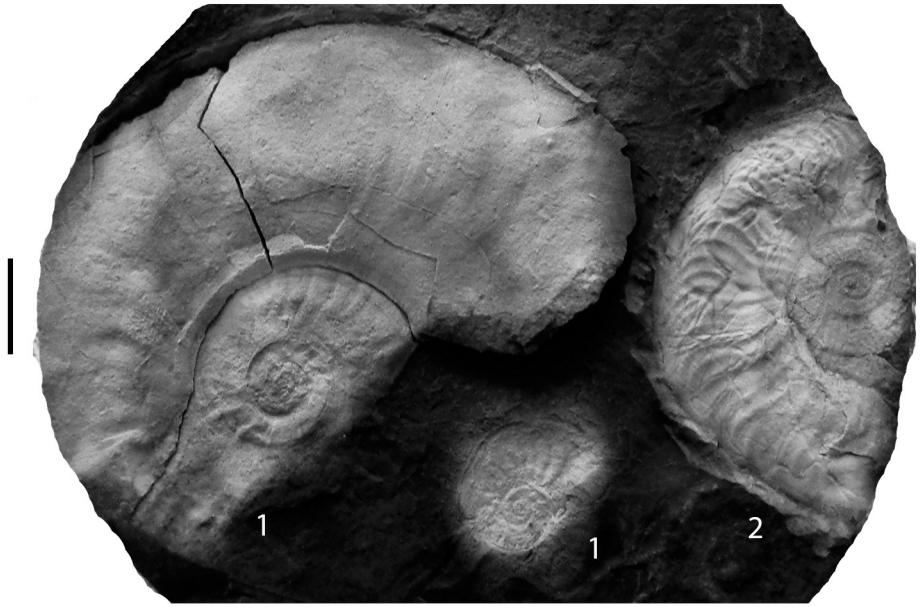

2

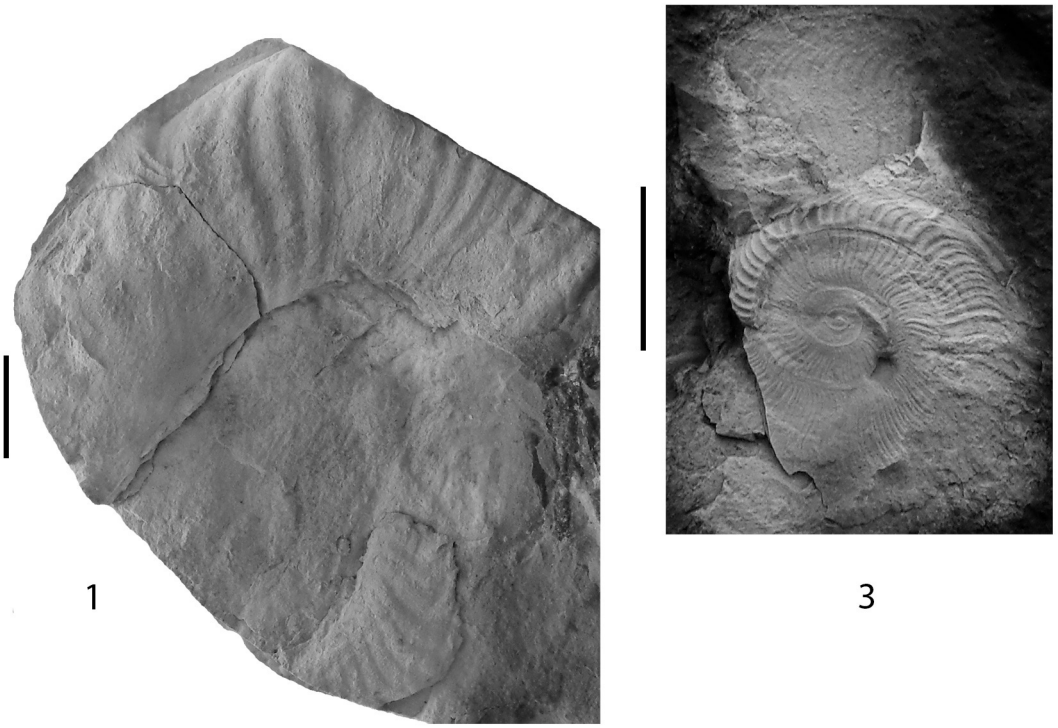

Plate I: BAC1-1 (917.97 – 915.06 m)

Plate II BAC1-1 (905.41 – 840.75 m)

Fig. 1: *Leioceras* ex gr. *subglabrum* (Buckman, 1902), Macroconch, depth: 905.41 m, Opalinus Clay, Opalinum Zone, Opalinum Subzone.

Fig. 2: *Leioceras* ex gr. *opalinum* (Reinecke, 1818), depth: 901.82 m, Opalinus Clay, Opalinum Zone, Opalinum Subzone.

Fig. 3: *Leioceras* ex gr. *opalinum* (Reinecke, 1818), depth: 901.63 m, Opalinus Clay, Opalinum Zone, Opalinum Subzone.

Fig. 4: *Leioceras* ex gr. *subglabrum* (Buckman, 1902), depth: 900.90 m, Opalinus Clay, Opalinum Zone, Opalinum Subzone.

Fig. 5: *Leioceras* sp., depth: 840.75 m, Opalinus Clay, Opalinum Zone, Opalinum Subzone.

All figures are illustrated in individual scales; black bars indicate 1 cm.

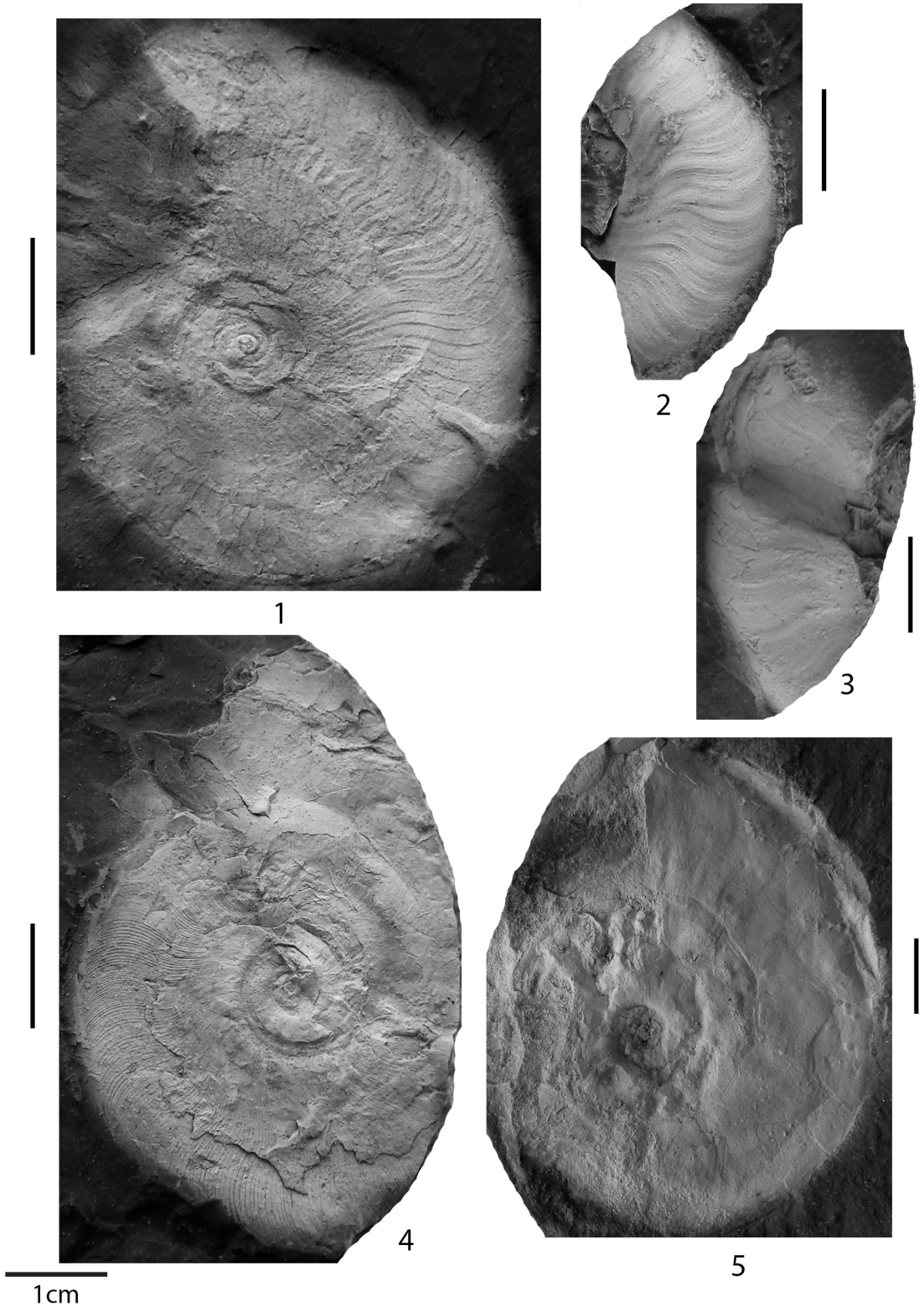

Plate II: BAC1-1 (905.41 – 840.75 m)

Plate III BAC1-1 (811.90 – 793.26 m)

Fig. 1: *Leioceras* ex gr. *goetzendorfense* (Dorn, 1935), smooth morph, depth: 811.90 m, Opalinus Clay, Opalinum Zone, Bifidatum Subzone.

Fig. 2: *Leioceras* ex gr. *goetzendorfense* (Dorn, 1935), smooth morph, depth: 811.52 m, Opalinus Clay, Opalinum Zone, Bifidatum Subzone.

Figs. 3a, 3b: *Leioceras* ex gr. *goetzendorfense* (Dorn, 1935), smooth morph, depth: 811.50 m, Opalinus Clay, Opalinum Zone, Bifidatum Subzone. Fig. 3a : lateral view, Fig. 3b : cross section.

Fig. 4: *Leioceras* sp., depth: 810.64 m, Opalinus Clay, probably Early Aalenian.

Fig. 5: *Hyperlioceras* sp., depth: 793.26 m, «Murchisonae-Oolith Fm.», Concavum or Discites Zone, probably Early Bajocian.

All figures are illustrated in individual scales; black bars indicate 1 cm.

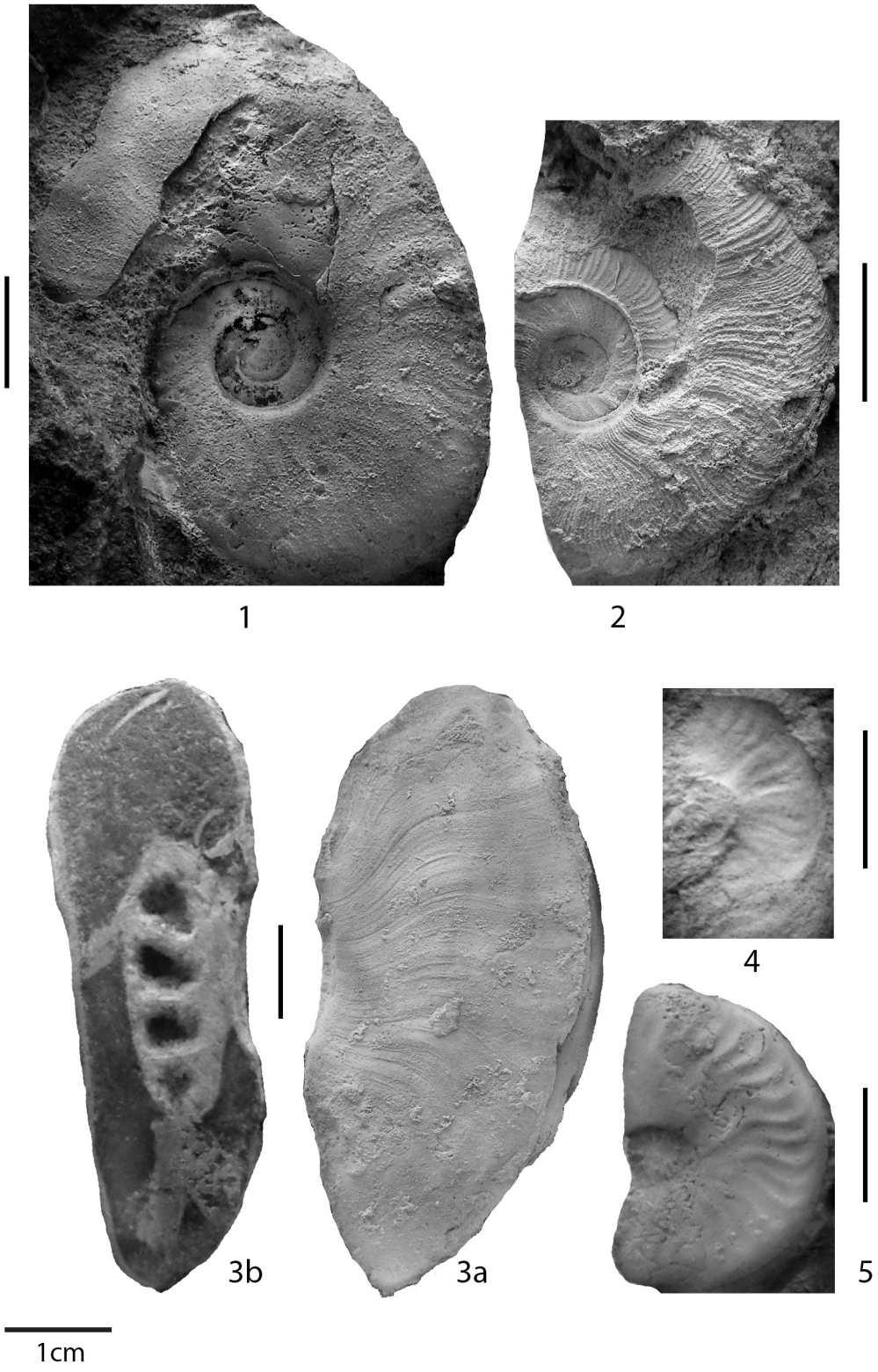

Plate III: BAC1-1 (811.90 – 793.26 m)

Plate IV BAC1-1 (741.00 – 736.84 m)

Figs. 1a, 1b: *Oxycerites* ex gr. *limosus* (Buckman, 1925), depth: 741.00 m, Variansmergel Fm., Zigzag Zone. Fig. 1a: lateral view, Fig. 1b: cross section.

Figs. 2a, 2b: *Parkinsonia* (*Oraniceras*) ex gr. *wuerttembergica* (Oppel, 1857), depth: 740.56 m, Variansmergel Fm., Zigzag Zone. Fig. 2a: lateral view, Fig. 2b: cross section.

Figs. 3a, 3b: *Oecotraustes* sp., depth: 737.53 m, Wutach Fm., Bathonian. Fig. 3a: lateral view, Fig. 3b: cross section.

Fig. 4: *Euaspidoceras* sp.? or *Peltoceras* sp.? (1), Hecticoceratidae indet. (2), depth: 736.84 m. Wildegg Fm., Late Callovian or Early Oxfordian.

All figures are illustrated in individual scales; black bars indicate 1 cm.

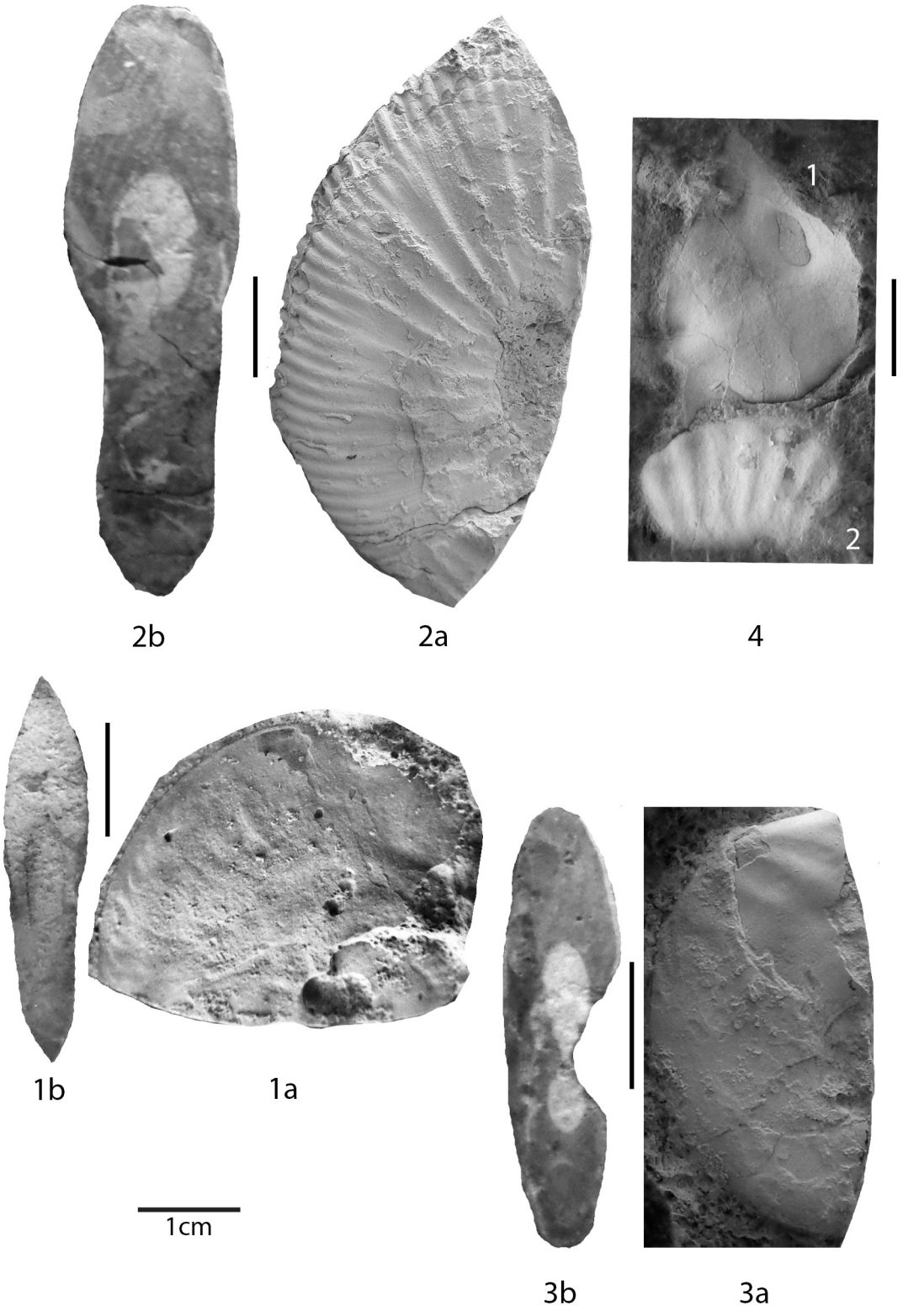

Plate IV: BAC1-1 (741.00 – 736.84 m)

Appendix D: Palynostratigraphy

Appendix D1: Range Chart: Quantitative stratigraphic distribution of Middle Jurassic palynomorphs in the Bachs-1-1 borehole

Appendix D2: Depth/Age plot: Bachs-1-1 borehole

Note: The appendices are only included in the digital version of this report (PDF) and can be found under the paper clip symbol.

Appendix E: Chemostratigraphy

Appendix E1: List of all geochemical samples and results mainly drilled from specific calcareous beds in the Opalinus Clay and its confining units

Data are discussed in Section 3.4 and partly illustrated in Fig. 3-4 (part of the data points lie outside the presented scale for the $\delta^{13}C_{carb}$): HB: drilled from a "hiatus bed" (for definition of HB see Section 2.1), CC: drilled from a calcareous concretion, SC: drilled from a sideritic concretion or nodule, SN: drilled from a septarian nodule, TS: drilled directly from thin section sample (see microfacies description in Section 3.1).

Depth [m]	**Description of sample**		**TS**	**$\delta^{13}C_{carb}$** [‰ VPDB]	**$\delta^{18}O_{carb}$** [‰ VPDB]	**Carbonate** [wt.-%]
582.88	Calcite crystal of a druse			2.36	-9.95	95.3
811.50	bioclastic limestones (iron-oolitic)			-2.28	-3.88	69.3
811.84	bioclastic limestones (iron-oolitic)		×	-2.05	-3.52	71.3
811.93	Base of greenish iron-oolite			-1.04	-7.11	59.9
811.94	Calcareous concretion	CC		-0.60	-2.45	72.8
815.07	Bioclastic calcareous marl	HB	×	-2.33	-4.04	63.5
825.52	"Hiatus bed" with calcitic iron-ooids	CC	×	-0.47	-2.17	80.9
825.57	Calcareous conc. & calcitic Fe-ooids	CC	×	-12.46	-2.94	75.4
826.30	Calcareous concretion	CC		-21.48	-2.26	86.2
827.56	Septarian nodule	SN		-24.20	-1.38	87.4
827.77	Septarian nodule with calcite vein	SN		-25.02	-1.23	84.7
827.81	Septarian nodule with calcite vein	SN		-23.47	-1.31	88.2
829.02	Sideritic and pyritic concretion	SC		-4.41	-1.70	62.0
829.17	Sideritic conc. & calcitic Fe-ooids	HB	×	-6.86	-2.42	82.6
829.24	Calcareous concretion	CC		-4.66	-3.53	84.2
829.28	Calcareous concretion	CC		-17.89	-1.58	89.5
832.88	Bioclastic calcareous marl	HB		-3.20	-3.09	58.3
834.50	Bioclastic calcareous marl	HB		-6.80	-5.35	60.2
861.65	Nodular, bioclastic limestone (argill.)	HB	×	-16.79	-5.26	78.2
861.72	Calcareous concretion	CC		-24.52	-2.77	73.3
900.40	Calcareous concretion	CC		-0.28	-0.91	39.5
901.06	Septarian nodule	SN	×	-21.38	-2.38	74.3
901.50	Septarian nodule	SN		-27.41	-1.22	80.3
901.87	Septarian nodule	SN		-32.13	-1.22	85.4
920.50	«Monotisbank»? (Rietheim Mb.)			-0.12	-6.85	74.9
924.03	«Homog. Kalkbank» (Rietheim Mb.)			-0.95	-3.10	87.8
924.50	«Unterer Stein» (Rietheim Mb.)			-2.09	-2.95	97.1